PREDICTING STRENGTH OF WOOD BEAMS WITH TENSION END NOTCHES

by

Greg C. Foliente

Thesis submitted to the Faculty of the

Virginia Polytechnic Institute and State University

in partial fulfillment of the requirements for the degree of

Master of Science

in

Wood Science and Forest Products

APPROVED:

Thomas E. McLain, Chairman

Joseph R. Loferski

Siegfried M. Holzer

November 1989

Blacksburg, Virginia

PREDICTING STRENGTH OF WOOD BEAMS WITH TENSION END NOTCHES

by

Greg C. Foliente

Thomas E. McLain, Chairman

Wood Science and Forest Products

(ABSTRACT)

An equation for predicting the strength of wood beams with tension end notches (TEN) was derived using a critical fillet hoop stress (CFHS) theory. The equation is a simplified description of the results of hundreds of finite element (FE) analyses of TEN beams with varied geometries (total of 690 configurations). It accounts for the effects of loading type and beam and notch geometry variables, such as beam height, fractional notch depth, radius and notch location. The effect of span-to-depth ratio is implicitly incorporated in the formulation of the model. Notched beam strength is represented by a material parameter, K, which was found to be related to specific gravity. A simple equation for predicting K from specific gravity was derived from experimental results.

The CFHS equation is applicable to both filleted and sharp-cornered notches. An effective radius, R_e, which models the effect of a sharp-cornered notch, was determined and confirmed for two wood materials. A method of determining R_e for other materials was established. The CFHS equation was compared with other models and notch equations currently recommended in design codes and significant differences were noted. Chief among them is the sensitivity of notched beam strength to notch location (or the ratio M/V). This is not currently considered by "notch factor"-based design equations.

Stiffness of TEN wood beams was experimentally found to be influenced by fractional notch depth and notch location, M/V. The effect of end notching on beam stiffness has not been seriously addressed before and theoretical analysis does not predict the reduction.

Acknowledgements

I would like to acknowledge the many individuals (faculty, staff, fellow graduate students and friends) who provided me support and encouragement in this pursuit. They made this task not just a bearable but an unexpectedly enjoyable experience for me. My major advisor, Dr. Thomas E. McLain, patiently guided me through the rigors of this research, in particular, and graduate life, in general. His ideas and technical support are dearly acknowledged. I thank other members of my committee, Drs. Joseph Loferski and Siegfried Holzer, for their suggestions in this work. The helping hand extended to me by Dr. Frank Woeste in various areas of graduate work is appreciated. Very special thanks is accorded to Dr. Panickos Palettas who kindly and patiently helped me in all the statistical work, a very crucial part of this study.

My deep gratitude to Dr. Barry Zalph, a co-worker and friend, for his untiring assistance and guidance in many aspects of this research. His dissertation work laid the path that gave direction to the present work. I acknowledge the assistance provided by who entertained my most urgent statistical questions and needs. The

cheerful help provided by ,
in various stages of the experimental work is appreciated.

Many friends in the US and in the Philippines stood by me through moral support and prayers in my most trying times. My heartfelt thanks to who helped me in any way she can. The faithful and abiding love of my parents, , and brothers, , is preciously held. Finally, I would like to acknowledge the upholding hand of my Father

Table of Contents

List of Illustrations

List of Tables

1. Introduction

1.1 General

Wood is one of the earliest and most popular structural materials known to man. But rapid technological developments and advances in other materials (e.g. concrete, steel, aluminum, plastics and other composites) have seriously affected the position of wood in the engineering market place. Wood is often taken for granted and research on improving structural use of wood has not received adequate attention. In the last decade, greater understanding of wood properties has improved timber design technology to some extent. Some obvious needs, however, remain to be addressed.

In the United States, Peterson (1983) observed that only modest improvements in residential building methods were made in the last 50 years or so. Many years ago, Huddleston (undated) made a similar remark in Australia. Present day designers and engineers may feel the same disappointment if they encounter work on notches in wood beams. Current design codes and standards in many parts of the world provide very limited guidance on notch effects. Most recommendations are based on results from limited tests performed by Scholten (1935) more than 50 years ago.

Wood beams are notched in construction to bring top surfaces (e.g. floors, roofs) to desired levels, allow for necessary clearance and/or fit support or framing connection conditions. Notches are cut in pallet stringers for access by forklift, hand trucks or by robot pickers in automated storage and retrieval systems (McLain 1988). In most of these cases, notching is planned. But, there are also cases where notches occur unintentionally. Sometimes, unplanned but practical, on-site modifications during construction lead to notching -- a common example is accomodating piping installations and ductwork (Breyer 1988; Mettem 1986).

Whatever is gained in convenience and practicality is given up in strength of the notched member. This is well known and recognized (Scholten 1935; Stieda 1964) but not completely understood nor quantified. Beam strength is severely decreased over that expected due to effective net section reduction because of stress concentrations at the notch root. Because of the complex interaction of stresses involved and limited practical research findings, most building codes, standards and design guides recommend avoiding notches (USDA 1987; NFPA 1986; AITC 1985; Mettem 1986; CSA 1989). Some design formulae are given subject to many restrictions (e.g. geometric). In most cases, engineers and designers who find specific need(s) for notches in wood beams are left on their own in making important design decisions (Breyer 1988).

1.2 Research Basis and Significance

A fundamental problem for analysts is the lack of any practical means of estimating the magnitude of complex stresses at a notch root in an orthotropic wood beam; this is coupled with an ignorance of the critical stress level that initiates failure of the beam. Gerhardt (1984a,b) successfully modeled stresses in pallet stringers with filleted tension interior notches using a hybrid finite element (FE) model. He found that failure was initiated when a critical hoop stress is reached on the notch fillet. He proposed a simple equation to predict this critical hoop stress from geometric and material property parameters. Later investigation by Abou-Ghaida and Gopu (1984) confirmed Gerhardt's work for tension interior notches and supported the hoop stress criterion advanced by the latter. Zalph (1989) tested the general applicability of the theory for a wide range of notch geometric cases on the interior tension face of full-size wood beams using eight experimental materials. He successfully developed a closed-form equation that predicts the flexure strength of these notched beams.

The critical hoop stress criterion, originally developed for interior notched beams, i.e. pallet stringers, has not been extended to the end-notch case; Abou-Ghaida and Gopu (1984) found that Gerhardt's (1984a) equation seriously underestimates the hoop stress in end-notched beams. This research addresses the reformulation of Gerhardt's (1984a) equation for applicability to the tension end notch (TEN) case. Quantifying the effect of end notches in wood beams in terms of strength and stiffness will enhance design confidence and increase reliability and safety in use, decreasing risk of economic loss or human injury.

Improving design options for engineers and designers using wood as a structural material will improve its competitive standing in the construction market. To do so, timber design technology will have to keep pace with the needs dictated by modern concepts and conditions.

1.3 Objectives

The overall objective is to develop accurate and practical design recommendations for TEN wood beams. Specific sub-objectives are to:

- develop a theoretical closed-form prediction equation for the maximum hoop stress in a TEN wood beam considering notch, beam, loading and material variables,
- experimentally assess the validity of the critical hoop stress theory to modeling the failure phenomenon in TEN wood beams,
- formulate a practical design equation for filleted and sharp-cornered TEN wood beams.

1.4 Overview

Gerhardt's (1984a) finite element (FE) program was used in an extensive numerical analysis of the effects of various variables that define a TEN wood beam on the maximum hoop stress, e.g. beam height, fractional notch depth, fillet radius, notch length and location and material elastic properties. The FE formulation assumes plane stress conditions and a material that is linear elastic, orthotropic and free of slope-of-grain. A closed-form equation sensitive to a wide range of the identified variables was developed. Prediction accuracy and simplicity of form were key considerations in the selection of this equation.

Based on the theoretical results, an experimental program was designed to test the hypotheses that the critical hoop stress theory is valid in predicting failure of TEN wood beams and that the critical hoop stress is a practically obtainable material parameter independent of notch, beam and loading geometries. Two materials, representing anatomically different hardwood and softwood species groups, were mechanically tested in full-size bending. The experimental study was conducted without an explicit consideration in the design of the effects of loading rate and duration, moisture content, temperature and other service and environmental factors on the strength of TEN beams.

Experimental and theoretical results were combined to determine the critical hoop stress levels in the failure process of TEN wood beams. Standard material properties (specific gravity, block shear strength and perpendicular-to-grain tensile strength) were used to predict these critical hoop stress levels. A simple equation involving specific gravity was derived to predict the critical strength of a notched beam material. An effective radius was determined to model sharp-cornered notches for two materials. As a side study, the effect of TEN on beam stiffness was evaluated using deflection data from beam tests before and after notching of selected beams.

The derived expression for predicting the strength of TEN wood beams was compared with other models and notch equations currently recommended in design codes. Application scope and limitations related to its proper use were identified.

2.0 Literature Review

2.1 General

Wood beams are notched in different ways, usually to suit different needs. The simplest and most common are sharp-cornered notches. Filleted notches are commonly found in pallet stringers. Tapered and beveled notches are used to minimize the stress concentrations occurring at the notch root. Nomenclature for TEN wood beams are shown in Fig. 2.1.

The term "stress concentration factor" (SCF) is usually used to describe the weakening effect of notches in various materials. Richards (1974) defines SCF as "the ratio of the maximum stress at the notch to the stress in a parallel-sided beam with the same depth as the net depth of the notched beam".

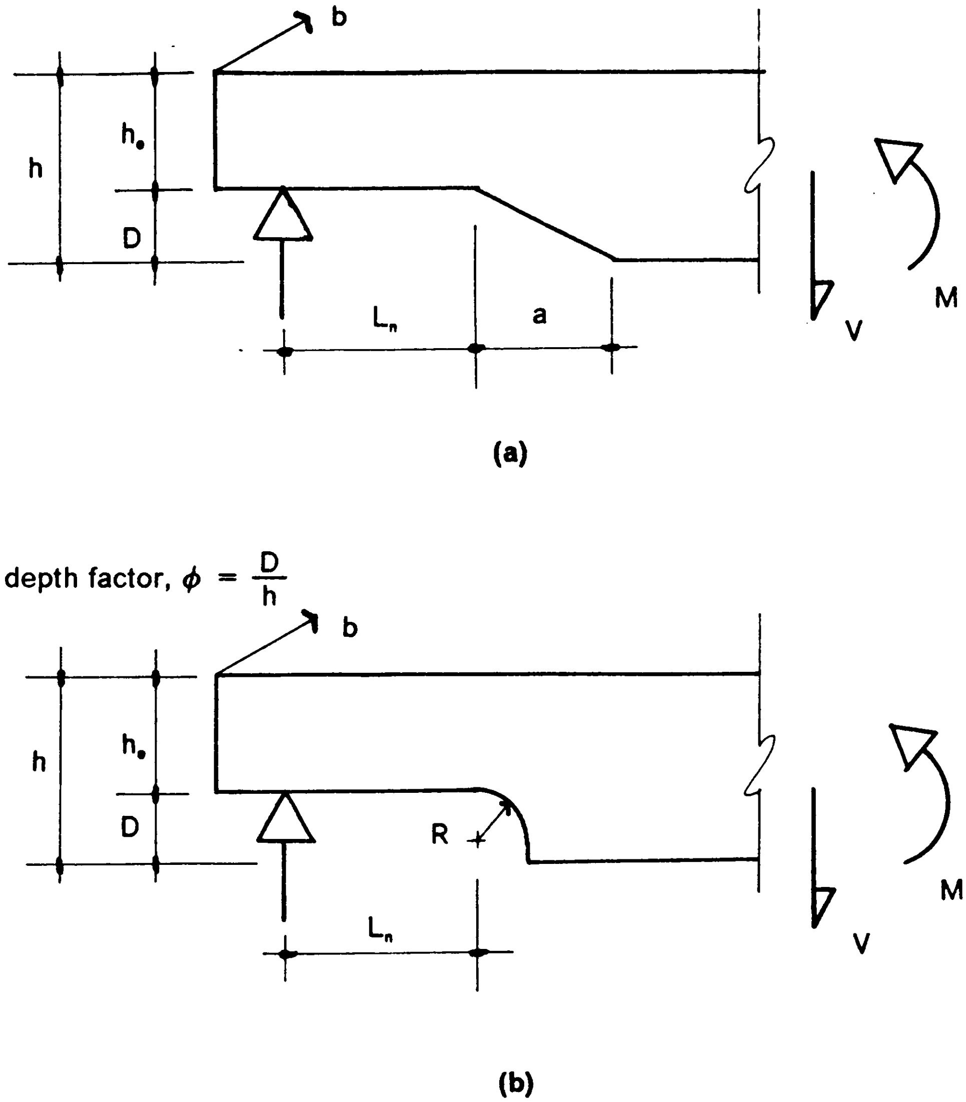

Figure 2.1. Nomenclature for tension end notches: (a) tapered, (b) filleted.

2.2 Notch effects on wood beams

Most work on notch effects has assumed material isotropy. This is not surprising considering the relative ease of analysis associated with uniformity of properties in all directions. Well documented results have been compiled in reference guides. Most of these findings do not, however, apply to wood because of its anisotropic nature. This anisotropy causes a clearly different stress distribution at discontinuities than that observed in isotropic materials and requires a modified analytical approach.

2.2.1 Geometry

Scholten (1935) found that end-notched wood beams, governed in strength by horizontal shear, are weaker than prismatic beams with depth equal to the net depth of the notched beam. Stieda (1964) cites similar results of Kollmann's tests on wood beams governed in strength by flexure. These results point to stress concentrations at the notch root that contribute to strength reduction above that caused by effective cross-section reduction. Failure was observed to be caused by the combined action of shear parallel and tension perpendicular to grain at the reentrant corners of the notch (Scholten 1935; Stieda 1964). Murphy (1986) discovered this effect to be particularly severe for large glued-laminated (glulam) beams with tension interior notches. Gustafsson (1988) confirmed the same beam height effect on end-notched dimension lumber. Scholten (1935) also found that these stress concentrations are relieved to some extent by tapering the notch (as in Fig. 2.1a). Gerhardt (1984a) and Zalph (1989) found similar stress relief for filleted interior notches (as in Fig. 2.1b).

Later work of Stieda (1966) on interior notches showed that the stress concentrations are a function of notch geometry, beam geometry, and some material properties. Gerhardt (1984a) and Zalph (1989) confirmed the influences of these factors and added the influence of loading conditions. Notch depth was observed to strongly influence the beam's strength capacity, i.e. deeper notches produce larger SCF's (Stieda 1966; Gerhardt 1984a; Zalph 1989). Stieda (1966) and Murphy (1978) observed notch length effect on beam strength from small clear specimen tests. They found that beams with wide notches are stronger than those with narrow slit notches. However, Zalph's (1989) limited full-size bending tests of two lumber species did not show this effect. For TEN beams, Abou-Ghaida and Gopu (1984) analytically determined a strong notch length influence on strength.

2.2.2 Other factors

Stieda (1966) observed that notch failure in kiln-dried material occurs at a lower percentage of clear wood strength than that for green material. He tested notched beams of Western hemlock (***Tsuga heterophylla***) and Western balsam fir (***Abies grandis***). For dry small clear specimens, crack initiation at the notch often triggered a sudden cross-grain failure that led to collapse. For green material, crack initiation allowed only a small load reduction and the notched beam continued to support load again after a gradual peeling of the bottom part of the beam, i.e. acting as a prismatic beam with net depth, h_e. Zalph (1989), however, observed opposite failure trends on full-size tests. He found that dry notched beams of Southern yellow pine (***Pinus*** spp.), yellow poplar (***Liriodendron tulipifera***), red oak (***Quercus*** spp.), spruce (***Picea*** spp.) and Douglas fir (***Pseudotsuga menziesii*** (Mirb.) Franco) sustained extended crack growth after crack initiation while green beams of Southern yellow pine, yellow poplar and hard maple (*Acer* spp.) failed at or right after crack initiation. The moisture content (MC) effect still needs to be established. The effect of temperature on notched beam strength has not been investigated in the literature.

Stieda (1966) also reports that based on Kollmann's experiment, notches have a large effect on a beam's impact strength. For extended loading, limited tests showed smaller strength reduction for beams with tension interior notches than unnotched beams (Leicester 1974; Madsen 1975). The duration-of-load (DOL) study by Krebs et al. (1984) on dry notched spruce beams, however, gave results compatible with the "Madison curve" (Wood 1951). Wet notched beams were found to have significantly shorter times to failure than dry materials (Krebs et al. 1984). It is also evident that there is currently no consensus on the influence of rate of loading and DOL on the strength of notched beams.

Based on limited tests of mixed Australian species, Leicester (1974) suspected that the overall effects of variation in slope of grain, density, DOL and moisture content on strength of notched wood beams are different than their effects on unnotched beam strength. No other experimental work, however, has confirmed these tendencies. He later suggested additional investigations on these topics (Leicester 1985). In the absence of established data, the effects of environmental, service and loading factors when taken into account in the calculation of notched beam strength were assumed to be the same with those for unnotched members in the different codes reviewed next.

2.3 Current Design Guidance

Building codes and standards provide guidance to engineers and designers in solving common problems. They offer recommendations based on known results of investigations and/or field experience. A review of different codes and standards in selected parts of the world provides some hints for the basis of notched beam design guidance.

2.3.1 North American design standards

The United States has a number of similar timber design guides. Most codes are based entirely or in part on the *National Design Specification* (NDS) *for Wood Construction*, prepared by the National Forest Products Association (NFPA 1986). The American Institute of Timber Construction (AITC), an industrial association of manufacturers and fabricators, publishes the *Timber Construction Manual* (TCM) (AITC 1985). The US Department of Agriculture (USDA) compiles recommendations of the Forest Products Laboratory (FPL) and other research institutions in the *Wood Handbook* (USDA 1987).

The TCM (AITC 1985) gives an empirical equation for shear stress in a square-cornered end notch

$$f_v = \frac{3V_r}{2bh_e}\left(\frac{h}{h_e}\right) \qquad [2.1a]$$

where f_v = horizontal shear stress,

V_r = shear force at support,

b = beam width,

h = beam height,

h_e = net beam height at notch = (h-D),

D = notch depth.

In calculating V_r, TCM allows that loads within distance h_e from the face of the support may be neglected. It limits the ratio of notch depth to beam depth (D/h or ϕ in Fig. 2.1) to 1:10 and does not recommend notching at supports of large glulam beams. The given formula is recommended only for "smaller wood members" (AITC 1985), without further specification. The gross shear strength can be alternatively expressed in terms of the ratio of notch depth to beam height, ϕ

$$\frac{3V_r}{2bh} = f_v\ (1-\phi)^2. \qquad [2.1b]$$

The NDS (NFPA 1986) states that end notches do not directly affect the flexural strength of the beam and gives equation [2.1a] as a formula to check shear capacity. Use restrictions, however, differ with those of TCM. NDS (NFPA 1986) states :

> Where members are notched at the ends, the notch depth shall not exceed one-fourth the beam depth. The tension side of the sawn lumber bending members of 4 inch or greater nominal thickness shall not be notched, except at ends of members.

The 1955 edition of the *Wood Handbook* (22) acknowledges that equation [2.1a] is based on Scholten's (1935) work. The 1974 edition (USDA 1974) is surprisingly silent on this. The latest edition (USDA 1987) presents a new general formula based on Murphy's (1979) fracture mechanics approach. The equation is described as a "conservative criterion for crack initiation" (USDA 1987) and is given as:

$$\sqrt{h}\left[A\left(\frac{6M}{bh^2}\right) + B\left(\frac{3V}{2bh}\right)\right] = 1 \qquad [2.2]$$

where M = bending moment,

V = vertical shear force,

b,h = same as in Eq. [2.1a],

A,B = coefficients (for values, refer to Fig. 2.2).

The values of A and B are species-dependent (USDA 1987) and are derived from conservative estimates of critical stress intensity factors for Modes I and II fracture (Murphy 1978). This equation in its present form, however, cannot be directly used in design without some modification.

The *Wood Handbook* (USDA 1987) agrees with TCM (AITC 1985) in recommending avoiding notches in large beams because of a disproportionate reduction in strength but gives no specific guidance on the matter. NDS (NFPC 1986) and TCM (AITC 1985) echo Scholten's (1935) findings in recommending gradually tapered notches to reduce stress concentrations. However, there are no answers to the important questions of "How much?" and "What is the effect?".

Another recommendation is to provide mechanical reinforcement such as full threaded lag bolts to a square-cornered notch to resist the tendency to split (AITC 1985; Breyer 1988). But some caution is necessary in using reinforcements. Reeves (1973) found that for tension interior notches in pallet stringers, nail reinforcing (countersunk) caused considerable checking of the stringer adjacent to the base. And while nail reinforcing increased the immediate flexural strength of green stringers, the advantages were eventually lost when the stringers seasoned.

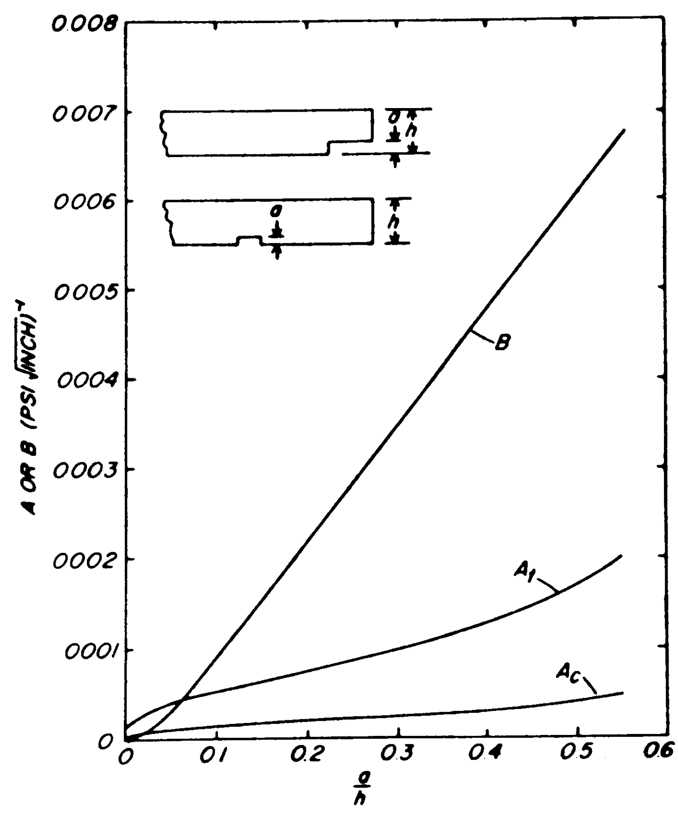

Figure 2.2. Coefficients (A and B) for equation [2.2]: From *Wood Handbook* (USDA 1987).

The Canadian Standard limit states design format CAN3-086.1-M89 (CSA 1989) does not recommend notching of wood beams. When it cannot be avoided, the following equation for sawn lumber is given

$$\frac{3V_r}{2bh} = 0.90\,(f_v \zeta)\; K_{Zv}\; (1-\phi)^2 \qquad [2.3]$$

where V_r = shear resistance,

f_v = specified material shear strength,

ζ = adjustment factor for DOL, system, service condition and treatment,

K_{Zv} = size factor in shear.

This equation is recommended only for cases where $\phi \leq 0.25$. A closer look will reveal that equation [2.3] is just a sophisticated adjustment of equation [2.1b], which is Scholten's (1935) equation. Values for K_{Zv} are tabulated in the Canadian code for visually stress-graded lumber. This size factor is dropped for glulam beams with volume, $V < 2.0\ m^3$. The design equation becomes complicated for $V > 2.0\ m^3$.

2.3.2 European design standards

European countries have their own independent design standards but these are not discussed individually here. Rather the focus is on the code draft of the Common Unified Rules for Timber Structures for the European Communities (EUROCODE 5) issued by the Commission of the European Communities (CEC). The latest code draft is based on studies within Working Commission W18 (Timber Structures) of the International Council for Building Research Studies and Documentation (CIB), particularly on the 1983 CIB Structural Timber Design Code (Crubile et al. 1988). EUROCODE 5 serves as an alternative set of design rules for CEC member countries.

For sharp-cornered rectangular TEN, the gross shear strength is evaluated as

$$\frac{3V_r}{2bh} \leq f_v \left[(1-\phi)(1-2\phi) \right] \qquad [2.4]$$

for beam volume, $V \leq 0.10\ m^3$, and

$$\frac{3V_r}{2bh} \leq f_{vv} \left[(1-\phi)(1-2\phi) \right] \left(\frac{0.10\ m^3}{V} \right)^{0.20} \left(\frac{1}{1-2(h/L)} \right) \qquad [2.5]$$

where f_{vv} = material shear strength adjusted with appropriate modification factors,

L = beam span,

for glulam beams with volume, $V > 0.10\ m^3$ (Crubile et al. 1988). Note the addition of volume effect and span-to-depth ratio for large glulam beams.

The earlier draft of EUROCODE 5 (Crubile et al. 1985) recommended a design equation which was essentially equation [2.1b] for $V \leq 0.10\ m^3$. Most European national codes use the same equation, e.g. United Kingdom, Norway and Sweden (Mettem 1986; Larsen 1975). The earlier report for CIB-W18 (Mohler 1978) recommended the form

$$\frac{3V_r}{2bh} \leq f_v \left[(1-\phi)(1-2.8\phi) \right]. \qquad [2.6]$$

Based on these developments, it would seem that equation [2.4] is a compromise between the earlier drafts of EUROCODE 5 and CIB-W18. No explanation nor reference literature for the changes were provided.

Certain provisions are given for the design of tapered TEN's in various European country codes although different treatment of the tapering effect is oftentimes confusing.

2.3.3 Pacific design standards

Only two countries, Japan and Australia, are considered in this review.

The Architecture Institute of Japan (1974), providing guidance and commentary on the Japanese Timber Code, presents this equation (using the nomenclature given in Fig. 2.1)

$$\alpha \frac{V_r}{bh} \leq f_v \,(1 - \phi)^2 \qquad [2.7]$$

where α = coefficient, for rectangular notch— 3/2

for circular notch——— 4/3.

The above equation is recommended for cases where $\phi < 0.50$. It differs with equation [2.1b] only with the guidance on circular notches. The code recognizes the stress relief caused by the fillet but does not provide application and limitation details. The basis of the 12.5 percent shear strength increase provided by the fillet is not stated. The Japanese code is silent on tapered end notches.

The Australian Timber Engineering Code AS1720.1-1988 (SAA 1988) provides a general interaction equation for rectangular and tapered notches on the beam tension face in the form:

$$f_b + 4 f_s \leq g_{40} F_{sj} \qquad [2.8]$$

where f_b = nominal maximum bending stress = $\frac{6M}{bh_e^2}$,

f_s = nominal maximum shear stress = $\frac{3V_r}{2bh_e}$,

F_{sj} = permissible shear stress for joint details calculated by adjusting the basic working stress for joint details for DOL, seasoning, temperature and lateral stability,

g_{40} = notch angle constant to account for tapered notches (see Table 2.1).

It is further recommended that "defects shall not be permitted within 150 mm of the notch roots of critical beams, i.e. non-load-sharing beams". Equation [2.8] was developed by using the theory of linear elastic fracture mechanics (LEFM) and test data of some Australian species (Leicester 1974; Barrett 1981; Leicester and Poynter 1979). It can be noted from Table 2.1 that the effects of beam height, h, and notch depth, D, do not interact in equation [2.8] but are applied separately depending on the ϕ-value. Over a large range of ϕ ($\phi > 0.10$), D does not appear in the expression except through its effect on the net section.

2.4 Experimental and Theoretical Development

Based on the review of current design guidance for TEN wood beams, it is evident that there are basically two methods of estimating strength, namely by "notch factor" and by linear elastic fracture mechanics (LEFM). The development and evo-

Table 2.1. Angle factor g_{40} versus notch slope (from SAA 1988).

Notch slope a/D	g_{40}	
	$\phi > 0.10$	$\phi < 0.10$
0	$9.0/h^{0.45}$	$3.2/D^{0.45}$
2	$9.0/h^{0.33}$	$4.2/D^{0.33}$
4	$9.0/h^{0.24}$	$5.2/D^{0.25}$

Note: D and h are to be stated in millimeters.

lution of these two approaches leading to present recommendations are now traced and other related works reviewed.

2.4.1 Traditional methods of analysis

2.4.1.1 "Notch Factor"

All design equations using a "notch factor" can be traced to Scholten's (1935) experimental work. The resulting empirical equation is strictly applicable only to the case covered by the experiment-- sharp-cornered end notches on beams with unsupported span to depth ratio of 12 or less. No theoretical analysis was presented. This leaves room for speculation as to the extent of effects of notch geometry, notch location and/or material properties on the beam strength.

Current code recommendations using the "notch factor" approach assume different forms as shown in equations [2.1], [2.3], [2.4], [2.5], [2.6] and [2.7]. Design methods for unnotched wood members have improved in recent years because of increased understanding of the behavior of wood material and wood structural systems. The Canadian design equation for shear resistance of prismatic beams (CSA 1989), for example, now incorporates modification factors for treatment, system and size. New developments such as these were also applied to the basic "notch factor" equation (Scholten 1935), where the stress concentration at the notch root is crudely approximated by the ratio h/h_e. For tapered notches, the stress relief was accounted for by a "notch factor" adjustment consisting of different combinations of the geometric variables a, D and h (see Fig.2.1 for nomenclature). The strength adjustment form may have evolved from a combination of local experience and some logical interpolation, resulting in the differences observed in various codes (Larsen 1975; Crubile et al. 1988). It should be remembered, however, that no matter how elegantly well adjusted, a notch factor equation based on Scholten's equation is also subject to its many limitations.

2.4.1.2 Orthotropic elasticity approach

Stresses around the notch have been experimentally studied and calculated in different ways. In stress analysis of wood beams, the longitudinal, radial and tangential axes of the wood are considered as three orthonormal axes of elastic symmetry (Stieda 1966; Goodman and Bodig 1970). Orthotropic elastic theory was the basis for early theoretical work in analyzing stresses in wood. Green and Taylor (1939) numerically calculated fundamental stress functions of generalized plane stress systems of anisotropic plates. This foundational work started a series of papers (Green and Taylor 1942, 1945a, b) investigating stress systems on this type of materials with discontinuities, e.g. circular holes, elliptical, square and triangular holes, using elastic constants from spruce and oak. They forwarded approximate failure prediction models but acknowledged incomplete understanding of failure action under complex stresses.

Reviewing other works, Richards (1974) states:

> Because of the increased complexity of the problem, notches of other than hyperbolic or semicircular shapes have not received much theoretical attention for the orthotropic case, nor has there been adequate theoretical treatment of a beam or tension specimen of orthotropic material with a notch on only one edge.

Stieda (1964) experimentally investigated stresses around a notch by the photostress method. In this and later work (Stieda 1966), he also used closed form orthotropic elastic solutions and estimated SCF's from tests on different wood species. He found a general stress distribution pattern around a hole on the neutral axis similar to that calculated by Green and Taylor. He also concluded that there is a limiting radius below which a constant SCF is reached and that the SCF approach gives better results when applied to beam shear strength than to its bending strength.

Woeste (1972) compared Stieda's (1966) experimentally observed stresses in the vicinity of a notch with predicted stresses using the Rizzo-Shippy Integral Formula (Rizzo and Shippy 1970) for plane orthotropic elasticity problems (computer program EL1a). The predicted stresses differ from those observed by Stieda (1966) by 23 to 37 percent. The Rizzo-Shippy formulation is a unified method of approximate solution based on Betti-Somigliana methods of integration differing from FE and finite difference procedures in that "approximations take place only on the boundaries of the domains" (Woeste 1972). Using the same method in the determination of stress concentrations around holes and notches in glulam wood beams, Woeste (1972) observed differences ranging from 3.6 to 63.6 percent between the experimental and the predicted results. The use of this method thus depends on the level of accuracy desired in stress prediction of notched wood beams.

Goodman and Bodig (1970) state that there is disparity between the actual behavior of wood and that predicted by idealized orthotropic elastic behavior because of the nonhomogeneous, layered structure of wood and influence of its shear moduli and Poisson's ratios. They proposed an adjustment to orthotropic elasticity theory for wood which was also mentioned by Palka and Holmes (1973). Goodman and Bodig (1970), at the time of their investigation, expressed optimism that accurate modeling could be achieved through the use of FE methods. However, without rapid sophisticated analysis techniques, direct use of stresses and SCF's at the vicinity of notch is impractical for design. Hooley and Hibbert (1967) and Stieda (1966) express the need for establishing the stress-strain relationship beyond the elastic limit as well as failure criteria under combined stresses in wood.

The use of a "notch factor" to guide designers and engineers seems a simple expedient until a more rational method is developed for predicting strength of notched wood beams.

2.4.1.3 Fracture mechanics approach

Fracture mechanics is a branch of study which deals with the "failure phenomena of materials by crack extension" (Wu 1967). Material crack growth due to an inherent or induced flaw which leads to fracture is of concern. Notches in wood, as pointed out earlier, create discontinuities. Leicester (1969) showed the applicability of linear fracture mechanics to notched wood beams.

The LEFM theory assumes that the stress level in the material indefinitely increases in the vicinity of the crack tip (Patton-Mallory and Cramer 1987). While this can not be completely true for any material, stress calculations according to the theory are valid outside the region around the crack tip and gives acceptably small errors (Porter 1964) for seasoned wood. LEFM criteria are the basis for equation [2.8] resulting from research developments in Australia, the earliest code adoption using this theory (Leicester 1974; Barrett 1981).

Fracture computations usually take one of two approaches: (i) a stress-intensity factor (SIF), K, criterion or (ii) a strain energy release rate, G, criterion. The former is most often used by researchers in wood fracture. Unlike with isotropic materials, there is no closed-form solution available for the computation of K in anisotropic materials (Patton-Mallory and Cramer 1987). Hence, most workers have used FE modeling to estimate K in notched wood beams (e.g. Walsh 1972; Mall et al. 1983; Lum and Foschi 1988).

Murphy (1978) used a transformed theoretical SIF approach and an experimental program to establish a relationship between failure loads of small clear rectangular-notched beams and that of slit-notched beams. This work forms the basis of equation [2.2] adopted by the *Wood Handbook* (USDA 1987). See Appendix A. Work by Mall et al. (1983) failed to confirm the linear mixed mode criterion used by Murphy (1979) and Leicester (1974). The latter's work formed the initial basis for the recommendations in the Australian Code (1988). For eastern red spruce (***Picea rubens***), Mall et al. (1983) accepted the nonlinear criterion proposed by Wu (1967) for balsa (***Ochroma lagopus*** Sw.). In a later work, Murphy (1986) successfully used Wu's mixed mode criterion to conservatively predict strength of large Douglas fir glulam beams with slits and rectangular notches.

These developments reflect a lack of understanding in a fracture mechanics mixed mode criterion for wood. If Wu's criterion is accepted as a general trend for a wide range of species, then equations [2.2] and [2.8] may not be the most efficient for design of notched wood beams. Further, there are other inherent problems in applying fracture mechanics to wood design problem. McLain (1988) states, "While fracture mechanics has great potential for some applications ... the analyses use some fundamental assumptions which cannot be justified for wood in many failure modes". The measurement of Mode I and Mode II fracture toughness values K_{IC} and K_{IIC}, respectively, alone is not in order yet. (See Fig. 2.3 for displacement modes). A comprehensive review by Patton-Mallory and Cramer (1987) shows that the fracture toughness is dependent on moisture content (MC), specific gravity (SG), specimen geometry and size, strain rate, type of test and temperature. However, a standardized test procedure for measuring fracture toughness has not been developed. This results in an apparent large variability in critical SIF values within species and between test methods. The Australians avoided this problem by relating fracture toughness to readily obtainable properties of wood, such as density, shear block strength and bending strength (Leicester 1974, 1985; Leicester and Poynter 1979). This explains the reason why equation [2.8] from the Australian Code (1988) is devoid of any fracture parameters. Equation [2.8] neglects the stress relief due to filleted notches because, according to Leicester (1985), drilled holes or fillets at notch roots do "not appear to have a significant effect on fracture strength". Theoretical and experimental investigations of Abou-Ghaida and Gopu (1984), Gerhardt (1984a) and Zalph (1989) have shown, however, a fillet effect on notched beam strength of some materials.

Gustafsson (1988) theoretically derived a closed-form expression for the strength of notched wood beams using fracture mechanics energy balance consideration (G-criterion). The equation is applicable to predicting the strength of beams with notches, cutouts or cracks anywhere along the tension face and is given as

$$f_b \sqrt{\frac{5(\alpha - \alpha^4)}{E_x}} + f_s \sqrt{\frac{8(\alpha - \alpha^2)}{G_{xy}}} \leq \sqrt{\frac{30\, G_c}{h}} \qquad [2.9]$$

where f_b, f_s = as defined in equation [2.8],

$\alpha = (1 - \phi)$,

G_c = material dependent fracture energy for splitting along the grain.

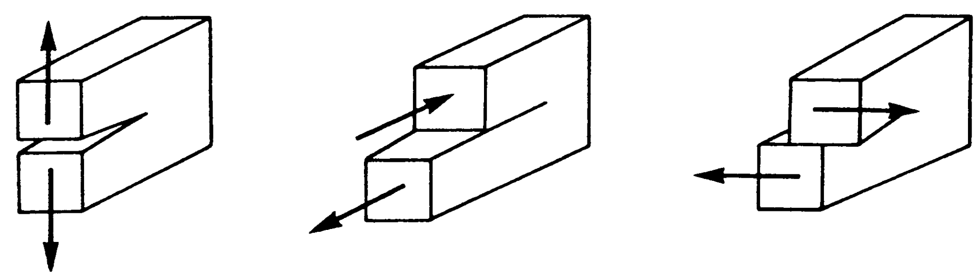

Figure 2.3. Displacement mode for cracks

Considering gross bending and shear stresses and using the nomenclature in the present work, it can be alternatively expressed as

$$\left(\frac{6M}{bh^2}\right)\sqrt{\frac{1}{(1-\phi)^3}-1} + \left(\frac{6V}{bh}\right)\sqrt{\frac{\phi}{10(1-\phi)}\;\frac{E_x}{G_{xy}}} \le \sqrt{\frac{6G_cE_x}{h}} \quad . \qquad [2.10]$$

Similar to the SIF approach (K-criterion), the strain energy release rate approach requires a failure criterion. Unfortunately, there is no established mixed mode criterion for this approach (Masuda 1988). The difficulty in mixed mode problems is that energy contributions corresponding to each fracture mode are cross-influenced and so, are hard to separate (Sih et al. 1965). The material dependent fracture energy, G_c in equation [2.10] is actually caused by the combined action of shear stress and tension stress perpendicular to grain. Gustafsson (1988) assumed that "the actual mixed mode fracture energy is equal to the fracture energy in pure tensile splitting perpendicular to grain, $G_c = G_{f,y}$" . He also provided a modified equation for small ordinary beams to account for the non-zero length of the fracture region. Equation [2.10] was derived consistent with the linear fracture assumption of zero or negligible size fracture region (Gustafsson 1988), which may be appropriate for large beams. To account for initial cracks and knots at the notch root, he proposed an effective width (b′) adjustment on beam geometry and elastic parameters in his equation.

Gustafsson (1988) found good agreement between his theoretical equation and experimental results of 21 notched beams of ***Pinus sylvestris*** L.. He also compared strength predicted by equation [2.9] with experimental results from eight other sources. Strength was conservatively predicted in five of these sources. It was not clear, though, how he computed or estimated G_{xy} and G_c from these sources.

2.4.2 Hoop stress criterion

Gerhardt's (1984a) work on pallet stringers led him to the problem of filleted notches. Principles of LEFM could not be applied because of the assumption of a sharp crack that can not be justifiably assumed for filleted notches. No publications were found on the analysis of filleted notches by LEFM although the recently proposed "finite small area theory" (Masuda 1988) shows some promise. It is a unified theory of LEFM and von Mises's criterion supposedly applicable for notched problems with or without cracks, e.g. filleted notches. Theoretical refinements, however, are still being worked out (Masuda 1988).

Gerhardt (1983, 1984a,b) developed a special hybrid finite element for the notched region and modeled other parts of the stringer with cubic isoparametric plane elements patterned after Taylor (1977). The hybrid FE enabled him to model exactly the shape and stress-free conditions of the discontinuity while maintaining the assumed stress and displacement fields and satisfying all governing elasticity equations. The hybrid element can be used to "calculate stresses or stress intensity factors at ... other geometric discontinuities in plane-loaded anisotropic materials" (Gerhardt 1984b).

An extensive experimental program of mechanical tests of 600 full-size, green red oak beams with various notch geometries and loading conditions was conducted by Gerhardt (1984a). His experimental results of notched beam strength and stiffness verified the theoretical trends earlier established. A most significant finding is that the maximum hoop stress ($\sigma_{h,max}$) along the fillet surface governs failure and that $\sigma_{h,max}$ can be directly computed by the hybrid fillet element.

Fillet hoop stress, $\sigma_{h,\theta}$, is the "non-zero principal stress acting on the free surface of a filleted notch corner at an angle θ from the horizontal" (Zalph 1989). See Fig. 2.4. While the stress distribution along the fillet is very complicated, $\sigma_{h,\theta}$ can be resolved into simple stress components:

(i) along the grain (σ_x),

(ii) perpendicular to grain (σ_y), and

(iii) shear (τ_{xy}).

However, the locations of maximum stress components σ_y and τ_{xy} along the fillet are distinct (Gerhardt 1984a). Generally, the location of maximum hoop stress ($\sigma_{h,max}$) is even different from those of the stress components σ_y and τ_{xy}. The locations and magnitude of these stresses are affected by elastic property ratios, loading conditions, notch depth and fillet radii. Derivation of a generalized beam strength prediction based on these complexities is currently impractical. Some elastic property data are not available (McLain 1988). Combining available stress distribution information with an interaction equation such as proposed by Norris (1962) will lead to very complex equations. Accuracy of this method may even be questionable because Norris (1962) recommends further experimental verification of his proposed interaction equation, i.e. need for "tests imposing combined tensile stress in two directions and shear".

Without explicit consideration of actual stress component interaction in the critical fillet region and investigating hoop stress alone, Gerhardt (1984a) found that $\sigma_{h,max}$ generally occurred at θ = 82 to 90 degrees and can be expressed for all loading conditions as

$$\sigma_{h,max} = \left(\frac{6M}{bh^2}\right) f_1(\phi) + \left(\frac{6V}{bh}\right) f_2(\phi) \qquad [2.11]$$

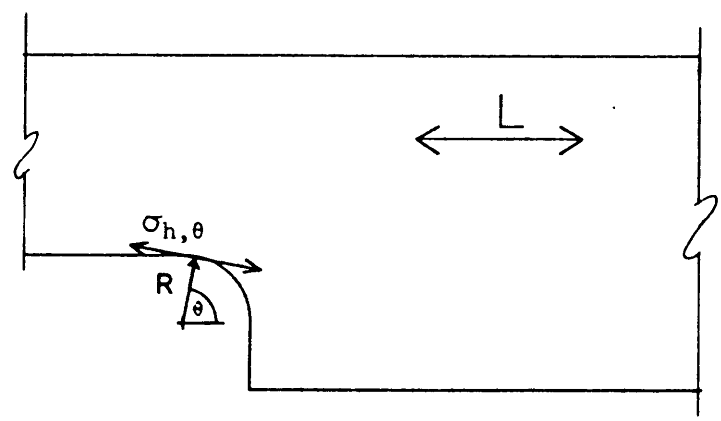

Figure 2.4. Fillet hoop stress in notched wood beam

where M, V = resultant bending moment and shear, respectively at point where $\sigma_{h,max}$ occurs,

$f_1(\phi), f_2(\phi)$ = dimensionless functions of ϕ.

This equation resembles the forms of equations [2.2], [2.8] and [2.10], which were developed by LEFM theory (Murphy 1978; Leicester 1974; Gustafsson 1988), but has a relative advantage in that it neatly avoids the unresolved combined stress failure criterion.

Using his experimental results, Gerhardt (1984a) simplified the combined bending and shear equation to

$$\frac{6M}{bh^2} = \frac{K_{crit}}{\frac{1}{-1.26\phi + 1} + h\left(\frac{V}{M}\right)(1.13\phi + 0.30)} \qquad [2.12]$$

where K_{crit} = $B\ \sigma_{h,max}$ = critical material property,

B = coefficient dependent on assumed elastic properties

for the range $0.267 < \phi < 0.667$. The K_{crit} value for any species can be experimentally determined at one notch depth and is hypothesized as a material property, independent of notch geometry and loading conditions. However, like other properties of wood, K_{crit} may be influenced by anatomical, environmental and other factors (Zalph 1989).

Mechanical tests failed to show any practical influence of fillet radius on hoop stress in the range $0.50 < r < 1.0$ inch. There was significant difference between the response of beams with filleted notches and that of unfilleted notches (i.e. $r = 0$) (Gerhardt 1984a). Recent work (Zalph 1989) supports the principle of a limiting radius at which stress no longer increases as radius approaches zero (Stieda 1966). This is important because it supports the validity of using the hoop stress criterion in the analysis of sharp-cornered notches.

Abou-Ghaida and Gopu (1984) investigating stress concentrations in notched wood beams used an orthotropic isoparametric FE model throughout the beam utilizing a very fine mesh layout in the notch region. They verified the accuracy of Gerhardt's FE model. The authors hailed it as "a significant improvement over the current procedure". However, they found that Gerhardt's (1984a) closed-form equation is not applicable to predict the strength of end-notched beams. Other significant findings include that

(i) notching (either tension or compression) influences the shear stress distribution *only* at beam sections less than 4 to 5 times the notch depth, D, from the corner of notch.

(ii) for end notches, the distance between the support and the notch corners (L_n in Fig. 2.1) significantly influences the stress concentrations at the fillet.

Zalph (1989) reformulated Gerhardt's (1984a) equation for general applicability to tension interior notches. A closed-form equation for this notch case was developed from theoretical analyses of 879 notch configurations. A total of 860 full-size notched beams comprising eight wood materials were experimentally tested (Zalph 1989). The beam depth was not studied experimentally. He observed that the proportional limit (PL) load did not have any consistent relationship with the crack initiation load and so, did not analyze PL load any further. The theoretical model (Gerhardt 1984a) used is strictly valid only before crack initiation (Zalph 1989), but was also found to estimate failure loads with reasonable accuracy; Gerhardt (1984a) used ultimate moments while Zalph (1989) used the level of first major drop in load ($\geq$ 2 percent).

Previous work (Stieda 1966; Murphy 1978) considered PL load as the crack initiation or initial failure load for dry material.

The simple prediction equation developed by Zalph (1989) requires a single material parameter, κ, which was found to be significantly independent of notch, beam and loading geometries and related to perpendicular-to-grain tensile strength and specific gravity of a wood species.

3. Finite Element Modeling

3.1 Overview

This research focuses on the hypothesis that a crack-initiated mode of failure in a tension end-notched (TEN) wood beam is a result of the maximum hoop stress at the notch root exceeding some critical stress level . This is an extension of Gerhardt's (1984a) critical hoop stress theory. It is further hypothesized that (Gerhardt 1984a)

$$\sigma_{h,max} = \left(\frac{6M}{bh^2}\right) f_1 + \left(\frac{6V}{bh}\right) f_2 \qquad [3.1]$$

where $\sigma_{h,max}$ = maximum hoop stress at critical notch root,

f_1 = moment term apparent stress concentration factor,

f_2 = shear term apparent stress concentration factor.

This may be normalized and rearranged to yield

$$ShCF = \frac{\sigma_{h,max}}{\left(\frac{6V}{bh}\right)} = f_1 \left(\frac{M}{V}\right) \frac{1}{h} + f_2 \qquad [3.2]$$

where ShCF = normalized hoop stress or "***Sh*ear Concentration *F*actor**". Calculation of ShCF provides a way to estimate the TEN influence on a beam's load capacity.

The moment and shear functions, f_1 and f_2, are expected to contain terms related to some or all of the following: beam span (L), depth (h), notch depth (D), fillet radius (R), notch length (L_n), loading condition (M/V), and material properties.

Finite element (FE) analysis was used to develop a set of theoretical f_1 and f_2 terms for a wide range of beam, loading and notch geometries. FE modeling allows analyses of a wide number of different cases with much less time and expense than would be needed for an experimental program covering the same range of variables. A deterministic FE model also provides results that may be approximated using simplified closed-form equations. However, these benefits hold ***only if*** the underlying theory used in the FE formulation is valid for the physical problem on hand. It is, therefore, one of the objectives of this work to validate the applicability of Gerhardt's (1984a) critical hoop stress theory to modeling the failure phenomenon in wood beams with tension end notch (TEN).

3.2 Finite Element Model

An end-notched wood beam is characterized by its span (L), beam width (b) and depth (h), notch depth (D), fillet radius (R), notch length (L_n), loading condition (M/V) and elastic parameters. See Fig 3.1. Gerhardt's (1983, 1984a and b) FE program (slightly modified by Zalph 1989) was used to model beams with different combinations of these parameters. All analyses were run on an IBM 3090 using the VS

FORTRAN 2.0 compiler. A single output file-- containing the hoop stresses, $\sigma_{h,\theta}$, given at 1° increments from 0° to 90° with respect to the horizontal axis, the maximum hoop stress, $\sigma_{h,max}$, its angle of occurrence, θ_{max}, the maximum displacement and its node location-- was received from the program. All other output files were suppressed after initial verification that the program was running correctly.

3.2.1 Element Characteristics

The end-notched wood beam was modeled using cubic isoparametric quadrilateral plane elements except at the notch root which was modeled with a planar hybrid fillet element. See Fig. 3.1. Note the exploitation of symmetry. Characteristic details of these elements were published by Gerhardt (1983, 1984a and b). User input guidelines and a users guide to the program for calculating $\sigma_{h,\theta}$ are described by Zalph (1989).

The cubic isoparametric quadrilateral element was used to model the beam parts other than the notch region because of convenience. A mesh generator for TEN beams (Zalph 1989) incorporating this element was already in place. The interested reader is referred to Zalph (1989) for further details.

3.2.2 Assumptions of the Model

In this work, the following basic assumptions were made for general applicability of results: (a) plane stress loading, (b) orthotropic linear elastic material, with (c) principal material axes aligned with beam axes (i.e., no slope-of-grain). The FE model was formulated using standard assumptions for linear elasticity.

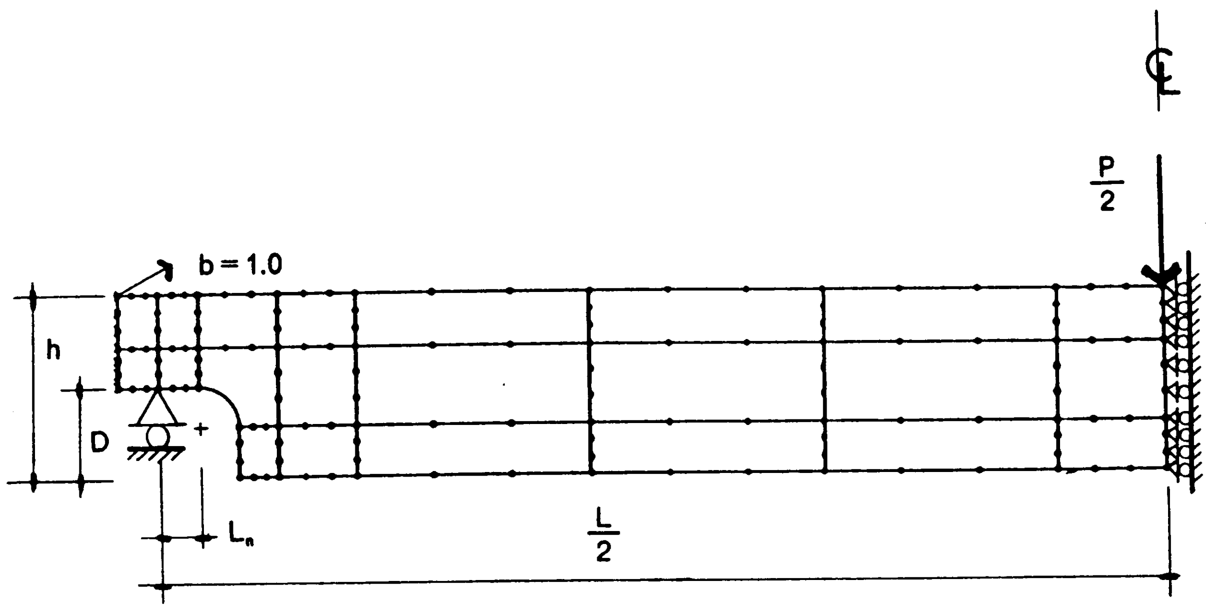

Figure 3.1. FE model of wood beam with TEN.

3.3 Material Properties

3.3.1 Influence of Elastic Properties on ShCF

The f_1 and f_2 terms in equation [3.2] are expected to be related to the orthotropic elastic constants assumed in the FE analysis. For study purposes, it was most convenient to express the effect of these constants separately from other variables as

$$\begin{aligned} f_1 &= \mu_1 \; F_1 \\ f_2 &= \mu_2 \; F_2 \end{aligned} \qquad [3.3]$$

where μ_1, μ_2 = material parameters which are solely functions of the designated elastic properties

F_1, F_2 = beam and notch geometry functions independent of material properties.

This division of material and geometric influences on maximum hoop stress is central to simplification of any closed form equation for ShCF and must be tested. Note that this assumption precludes any explicit interaction between geometry and material properties.

Elastic properties may be described by the Young's moduli, E, shear moduli, G, and Poisson's ratios, ν. For orthotropic materials (where x corresponds to the longitudinal axis and y to a transverse axis -- radial and tangential properties assumed equal), the ratios E_x/E_y and E_x/G_{xy} have been shown to influence beam displacements and stresses using Gerhardt's (1984a) model. Changing orthotropy ratios changes the resulting ratios of longitudinal to transverse tensile stress and tensile to shear stress, thus, affecting the location and magnitude of the maximum hoop stress, $\sigma_{h,max}$ (Gerhardt 1984a).

A preliminary study was made on the effect of the orthotropy ratios on normalized hoop stress or ShCF. Ten different combinations of E_x/E_y and E_x/G_{xy} were used in FE analysis of a single end-notched beam geometry. Scatter plot of ShCF against (E_x/G_{xy})/(E_x/E_y) shows that for a certain E_x/E_y value, variability is most affected by (E_x/G_{xy})/(E_x/E_y), which can be simply stated as E_y/G_{xy}. This indicates that when selecting levels of E_x/E_y and E_x/G_{xy}, the E_y/G_{xy} ratio must be considered. This is especially important for the shear-dominated end-notched beams where the shear-term factor f_2 is more sensitive to the elastic properties than the moment-term factor f_1 (Gerhardt 1984a, Zalph 1989). This is a distinction between this study and that of Zalph (1989).

3.3.2 Selection of Material Property Sets

The regression equations provided by Bodig and Goodman (1973) for predicting elastic parameters yield a good ballpark range for the elastic properties of most commercially important species. These regressions were determined using available elastic properties of species grown all over the world and from an extensive testing program of a wide range of material densities and species in North America. Using these equations for hardwood and softwood species with a density range of 0.30 to 0.75 g/cm^3, material elastic property (EP) sets A, B, and C were selected (Table 3.1). The EP sets have E_y/G_{xy} ratios of 0.846, 1.00 and 1.286, respectively. Set B was designated as a base set by Zalph (1989) and represents a set of midrange properties. To extend the E_y/G_{xy} ratio for the base E_x/E_y = 17 set and cover other possible materials, EP sets D and E with E_y/G_{xy} ratios of 0.647 and 1.588, respectively,

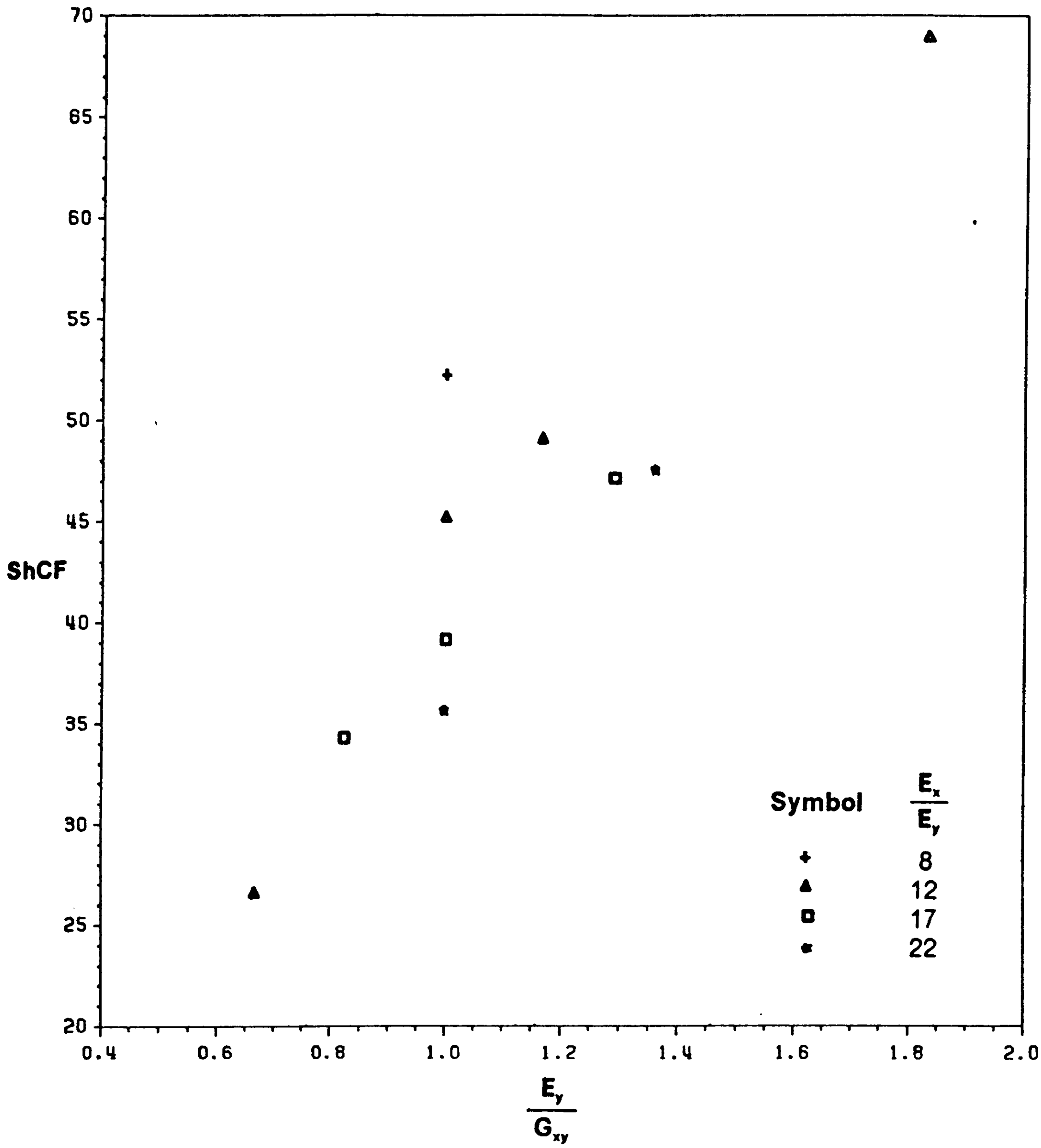

Figure 3.2. **Scatter plot of normalized hoop stress against a combination of elastic property ratios**

were added. The actual chosen value of E_x for an EP set in Table 3.1 did not affect the normalized hoop stress across EP sets.

The Poisson's ratio, ν_{xy}, was set at 0.40, the average value for combined hardwood and softwood data from Bodig and Goodman's (1973) study. Gerhardt (1984a) found that ν_{xy} had a negligible influence on calculated stresses and displacements.

3.4 Geometry Variables for FE Analysis

3.4.1 Effective Radius

Linear elasticity theory predicts for a sharp notched beam (i.e., R = 0) that $\sigma_{h,max} = \infty$. This is not practically possible. It has already been established that there is an effective limit radius at which the notch stress concentration factor becomes constant (Stieda 1966) or the hoop stress ceases to increase (Zalph 1989). These findings justify the use of Gerhardt's hybrid fillet element to model the notch root of a sharp cornered notch. It is significant because most, if not all , practical cases of wood beams with TEN are sharp cornered. Finding an effective radius, R_e, generally applicable to all species would tremendously simplify both the FE analysis and the experimental work.

Preliminary experimental bending tests were performed on a total of 47 pairs of end-notched beams of various species (Fig.3.3). Table 3.2 presents summary results of the tests. Paired t-tests (also called "matched samples t-test" or "dependent samples t-test") were performed on average shear strengths (computed by equation

Table 3.1. Elastic property (EP) sets considered in the FE analysis of TEN wood beams.Poisson's ratio was constant at 0.40.

EP Set	Designation	Orthotropy Ratios			E_x (x 10^6 psi)
		$\frac{E_x}{G_{xy}}$	$\frac{E_x}{E_y}$	$\frac{E_y}{G_{xy}}$	
A	G11-E13	11	13	0.846	1.3
B	G17-E17	17	17	1.000	1.7
C	G27-E21	27	21	1.286	1.7
D	G11-E17	11	17	0.647	1.7
E	G27-E17	27	17	1.588	1.7

[2.1]) for $R = 0$ (case A) and $R = 0.25$ in. (case B). From these results, it seems that $R_e < 0.25$ in. for dry D. fir and Y. poplar and $R_e \geq 0.25$ in. for dry red oak. Zalph (1989) reported for interior-notched beams that $R_e < 0.25$ in. for dry Southern yellow pine (SYP), dry red oak, dry fir and green Y. poplar (average $R_e = 0.21$ in. for the four species, $V/M = 0$). His findings on dry red oak contradict the preliminary test results of beams with TEN. Note, however, that Zalph's work was with interior notches where the moment term is dominant and shear may be less important than with the TEN case.

There are several ways to establish an effective radius, R_e. One is to conduct an extensive experimental program for a wide range of notch geometries and species. A graphical relationship between breaking (crack initiation) load and radius could identify a limiting radius equivalent to that of a sharp notch. A conservative R_e value applicable to most commercially important species can be selected. This approach, however, is impractical considering the requirements of time, effort and money. Another possible method is to establish an equation that accurately predicts the FE-determined critical stress of filleted notched beams of widely varying geometry. Using this equation, a critical material parameter that signals crack initiation can be defined. With a broad, but limited test program of sharp-cornered TEN beams and counterpart filleted TEN beams (this time with fixed R), back-calculation will yield an effective R_e. This approach was selected for this work because of its practicality. It hinges, however, on the validity of the theoretical strength prediction equation, the confirmation of which is the main object of this work.

b = 1.50 in.
h = 3.50 in.
D = 1.1 in. (or $\phi = 0.30$)

L = 22 in.
strain rate : 0.10 in./min
specimen MC : 5 to 9%

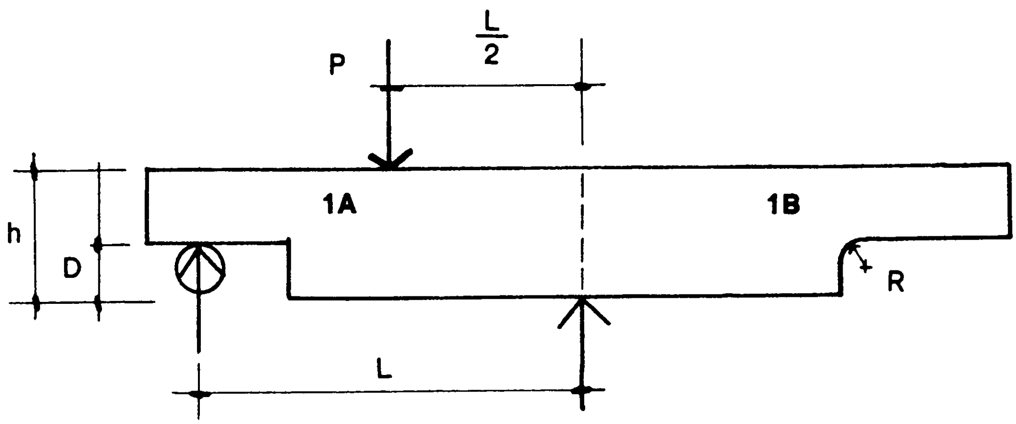

(a) For R = 0 (Case A)

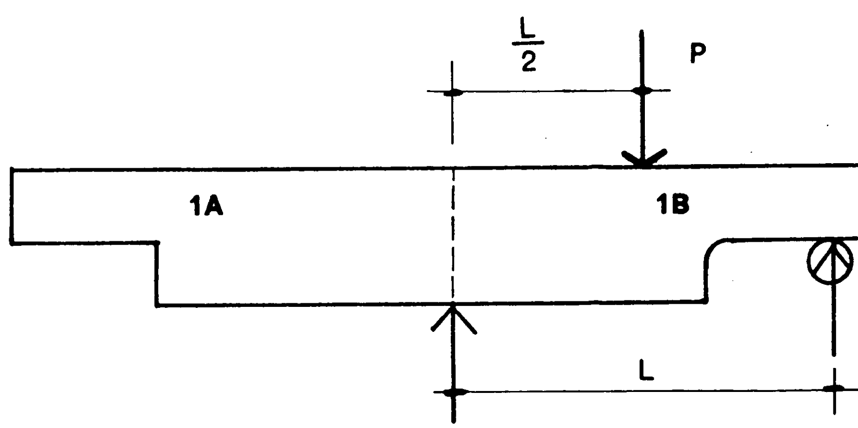

(b) For R = 0.25 in. (Case B)

Figure 3.3. Set up for preliminary mechanical tests of beams with TEN to determine the radius effect

Table 3.2. Summary of preliminary bending test results to determine the radius effect for beams with TEN (see Fig. 3.2 for set up).

Notch Length, M/V (in.)	Species	n	Mean Shear Strength, $\bar{f}_v$[1]		Paired t-test[2]
			Case A (R = 0)	Case B (R = 0.25 in.)	
1.00	D. fir	8	771	907	*
2.75	D. fir	9	616	994	*
	Y. poplar	10	834	1257	*
	R. oak	8	1093	1107	ns
7.0	D. fir	12	378	496	*

[1] Based on Scholten's (1935) equation $\bar{f}_v = \dfrac{3\bar{V}}{2b\,(h-D)} \; \dfrac{h}{(h-D)}$

[2] Ho : $\bar{f}_v(A) = \bar{f}_v(B)$
* - significant at 5% level
ns - non-significant

3.4.2 Loading Effect

Different loading types (e.g., center-point, uniform, etc.) that yield the same ratio of applied shear (V) to applied moment (M) at the location of the notch root are assumed to generate the same $\sigma_{h,max}$ in equation [3.1]. In other words, any effect due to loading type is accounted for solely by the ratio M/V. For this work, M/V was chosen rather than Zalph's V/M since it does not become undefined at the support and because M/V = notch length, L_n, for concentrated loading. Appendix B gives other expressions describing M/V by some notch and beam dimensions for selected loading types.

At the support, moment is zero ($M=0$) and only shear is present. This a common case in construction. Figure 3.4a shows, however, that the distance between notch root and the concentrated reaction at the support, L_n, rarely becomes truly zero. This is a fortunate observation because Gerhardt's FE formulation cannot handle a theoretical case of $L_n = 0$. Placing a support at the node on one end of the hybrid fillet element creates a complex interaction between compressive stresses at the support and the (tensile) hoop stress along the fillet arc (Fig. 3.4b). The program is also unreliable if there is a very small distance between these points (e.g., $L_n = 0.20$ in.). In actual case, for a notch flush with the face of the support, L_n or M/V would assume a value a little less than half of the support width when the beam is loaded (Fig.3.4a). The L_n value in this situation will depend on the beam's span-to-depth ratio. Considering a 2 in.-wide support, $L_n = M/V = 1.0$ in. would be appropriate to model a nominally pure shear case.

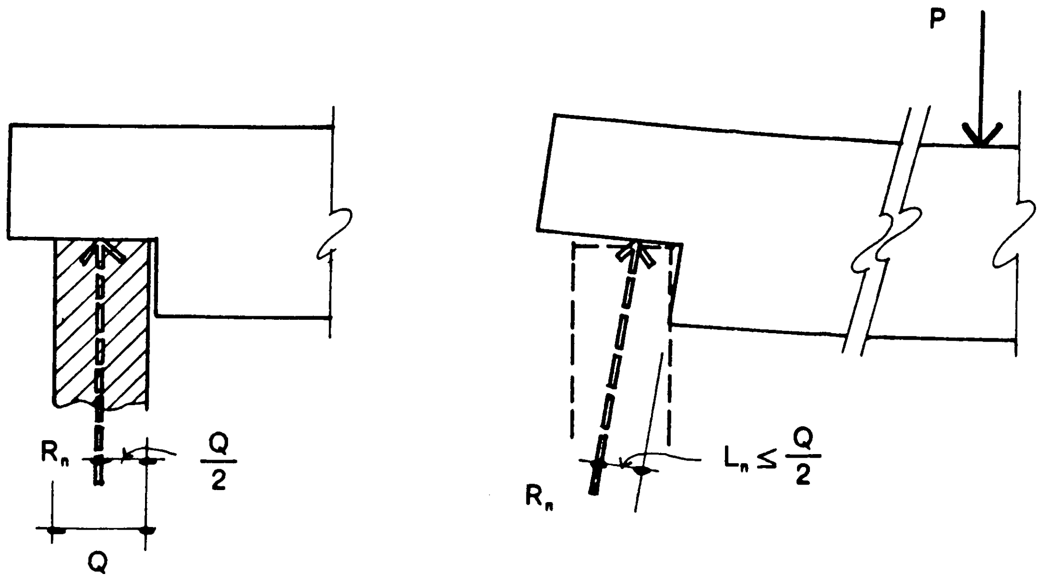

(a) In construction

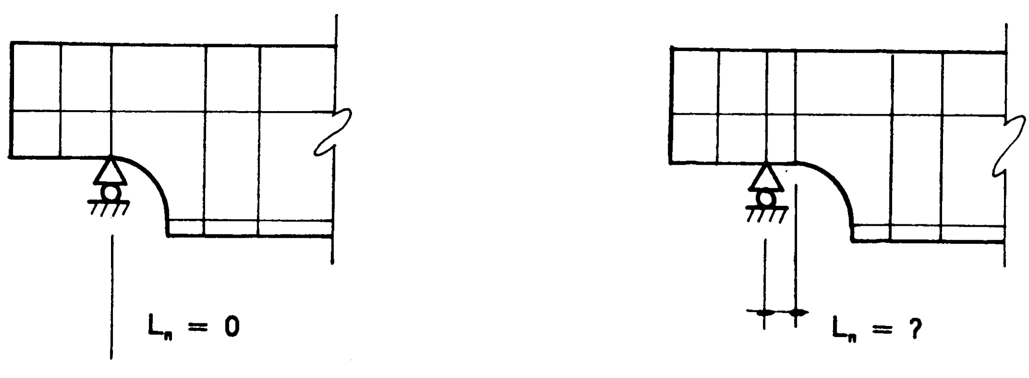

(b) FE model

Figure 3.4. Practical and theoretical illustration of an almost pure shear case beam with TEN

Zalph (1989) reconfirmed Gerhardt's (1984a) finding that, for interior-notched wood beams, $\sigma_{h,max}$ is linearly related to M and V. Zalph (1989) normalized a FE-based $\sigma_{h,max}$ by the gross-section nominal bending stress and found it to be linearly related to V/M. This was a key basis of his final formulation . A similar approach would work for TEN if the same relationship extends to very high V/M ratios (i.e., notch root is near the support, equivalent to low M/V ratio in this work). To explore this, FE-based ShCF's were computed for beams using a single material EP set (G11-E13) and two geometries (h = 3.5 in., ϕ = 0.314, R = 0.1875 and 0.50 in.). Seven different levels of M/V in the range 0.50 to 11.0 in. were employed. The results shown in Fig 3.5 indicate that $\sigma_{h,max}$ is a linear function of M/V and that the approach using equation [3.2] is not contradicted. But the anomalous behavior of ShCF at M/V = 0.50 in. for the beam with R = 0.50 in. is evident and the reliability of ShCF calculation for this case may be questionable. Although this behavior is less evident for the beam with R = 0.1875 in. (and possibly for the sharp-cornered TEN case with R_s if this trend is consistent), M/V = 1.0 in. was chosen to model a TEN at the support. Complete data are in Appendix C.

3.4.3 Beam Size Effect

Theoretical analysis by linear elastic fracture mechanics and experimental data show an effect of beam height, h, on the strength of notched wood beams (Leicester 1969; Murphy 1986; Gustafsson 1988). Similar results should be found with the critical hoop stress theory. Using Leicester (1969) and Gustafsson's (1988) fracture strength-size relationships for beams of different heights, then

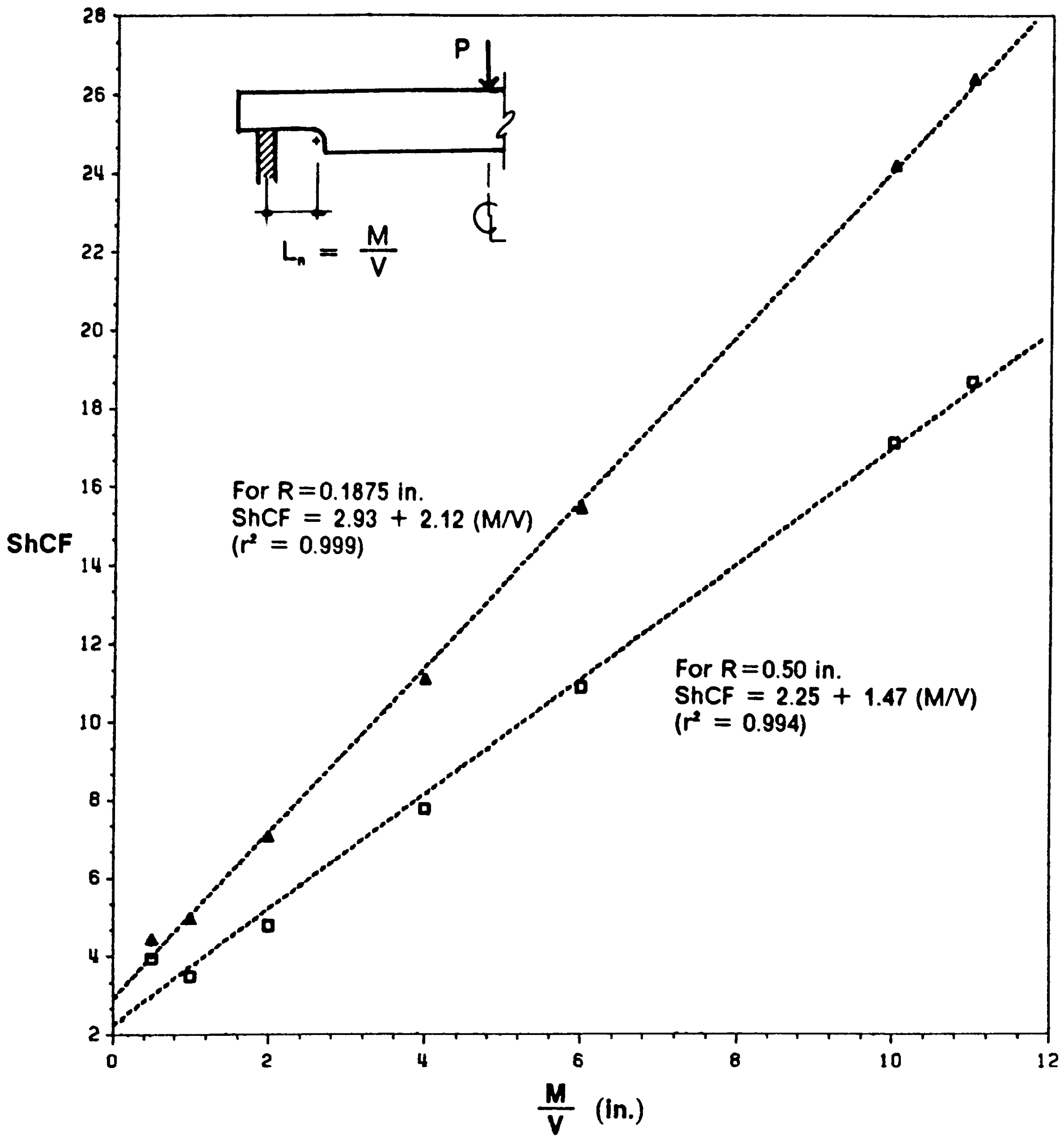

Figure 3.5. Relationship between normalized hoop stress, ShCF, and M/V.

$$\left(\frac{S_1}{S_2} \right) = \left(\frac{h_1}{h_2} \right)^{\lambda} \qquad [3.4]$$

where S_1, S_2 = hoop stresses corresponding to beam heights h_1, h_2,

λ = exponent accounting for the beam height effect on stress.

Computed hoop stresses for beams with the material set G11-E13 and geometry: R = 0.163 in., L_n or M/V = 0.50 in., h = 2.0 and 9.50 in. and 3 levels of ϕ (or ratio D/h) were substituted in equation [3.4]. These yielded λ-values of 0.532, 0.393 and 0.321 for ϕ-values of 0.10, 0.314 and 0.50, respectively. Complete data are in Appendix C. Leicester (1969) found λ to range from 0.33 to 0.50. While Gustafsson (1988) proposed λ = 0.50 for simplicity, he acknowledged that a more accurate prediction is achieved using a little more complex relationship than equation [3.4]. Zalph (1989) showed that the height effect for the moment term factor, f_1, is different from that for the shear term factor, f_2. Keeping the height effect in these separate terms provides a more accurate treatment of the beam size effect than applying a single factor to a combined expression of the moment and shear terms. Note that this height effect is not related to brittle failure-related size or volume effects.

On beam width, Leicester and Poynter (1979) reported that, "some pilot studies failed to reveal any measurable effect of thickness (or width) on fracture stress". Equation [2.5], recommended in EUROCODE 5 (1988) for shear calculation in notched wood beams, reflects a volume effect for a glulam beam more than 0.10 m^3 in volume. If beam length and depth are kept constant, this would suggest a width effect on notched beam strength. Hirai and Sawada (1980) found a beam width effect on maximum nominal bending stresses of notched ***Picea glehnii*** dimension lumber for shallow notches, $\phi \leq 0.20$. The width influence was not found with deeper notches. They provided possible explanations for this effect based on fracture mechanics and statistical strength theory. This effect, however, is not considered in this work because of the planar FE formulation of the critical hoop stress theory.

3.4.4 Span-to-depth Ratio

It is generally assumed that notched beams fail in shear at the notch. Other modes of failure may dominate, however, depending on the beam span-to-depth (L/h) ratio. McLain (1989) evaluated the current NDS bending design criteria for three materials (Southern pine lumber, S-P-F lumber and Southern pine glulam) with L/h ranging from 10 to 26. He used equation [2.1a] as the shear criterion and found that it governs in design for L/h values less than or equal to 12 and 17 for notched glulam and lumber materials, respectively (small ϕ case). Either bending or deflection governs in design for higher L/h ratios. Additional details are given in Appendix D. The present shear criterion may not be accurate but does give an indication of the L/h ratios to consider for FE study. Zalph (1989) found in his FE analysis that, for L/h range of 6.7 to 12.6, changes in his actual factors f_1 and f_2 were negligible. For this reason, he did not include span or L/h ratio in his predictive equations for f_1 and f_2. On the basis of these results, L/h was not considered as a predictor variable for the FE analysis of wood beams with TEN. Span, L, was fixed at 42 in. for all h. However, this does not mean that L/h is unimportant for assessing beam strength and/or stiffness since failure at the notch may not govern design.

3.5 Experimental Design of FE Analyses

Beam geometry in the FE analysis was described by variable height, h, a fixed span, L, and a unit width. Notch geometry was defined by variable fillet radius, R and variable notch factor ϕ (ratio D/h). Notch length, L_n, identifies the location of the notch root. For center-point loading, L_n is equivalent to the applied moment to shear ratio (M/V). This loading type was selected for convenience. In practice, the FE mesh generator set the concentrated load P such that 6V/bh was equal to unity; hence, ShCF is numerically equal to the $\sigma_{h,max}$ determined by the FE program.

The use of M/V to define loading geometry allows omission of L_n in the notch geometry description. Combinations of elastic parameters selected in section 3.2.2 and given in Table 3.1 are categorical variables used to describe material effects. Although the study did not include span-to-depth, L/h, as a predictor variable, it covered cases for L/h ranging from 3.91 to 12.00.

A full factorial experiment was performed using the variables given in Table 3.3. With each material set, six geometric cases were not analyzed because $R > D$. This gave a total of 138 ShCF values per material set and a grand total of 690 notched beams analyzed numerically. These results are tabulated in Appendix E.

Table 3.3. **Experimental design of FE study**

Variable	Levels	No. of Levels
h (in.)	3.50, 4.71, 7.125, 10.75	4
ϕ	0.10, 0.35, 0.52, 0.60	4
R (in.)	0.1875, 0.344, 0.50	3
M/V (in.)	1.0, 6.5, 12.0	3
material	A, B, C, D, E (see Table 3.1)	5

beam width, b = 1.0 in.
notch length, L_n = M/V
loading : center-point

beam span, L = 42 in.
beam length = 48 in.

3.6 Derivation of Closed-form Equations

3.6.1 Approach

It is not practical to use Gerhardt's (1983, 1984a and b) FE program as a design or analysis aid to determine the critical hoop stress of a specific notched wood beam geometry. A closed-form equation which considers all relevant variables is a good alternative if it has reasonable accuracy for a range of practical cases.

Equation [3.2] is used to derive a closed-form expression for ShCF. Rearranging into a general linear form

$$\text{ShCF} = A + B\left(\frac{M}{V}\right) \qquad [3.5]$$

where $A =$ intercept $= f_2$ [EP set, ϕ, R, h]

$B =$ slope $= \left(\frac{1}{h}\right) f_1$ [EP set, ϕ, R, h] .

A linear regression analysis using ShCF and M/V as dependent and independent variables, respectively, was made for all combinations of ϕ, R and h for each material set. Forty six values of A and B were obtained for each EP set (4Hx4ϕx3R - 2 = 46; there were two geometric cases where R > D at this stage). The shear term factor, f_2, is equal to A while the moment term factor is computed as $f_1 = B\ h$.

Results of all linear regression analyses of ShCF by M/V using equation [3.5] confirmed the preliminary linearity results described in section 3.4.2 and shown in Fig. 3.4. The worst fit had a coefficient of determination, $r^2 = 0.988$; about 80 percent of all linear relations between ShCF and M/V in all EP sets had $r^2 > 0.999$. The analyses considered cases from a shear-dominated case close to the support (M/V = 1.00 in.) to a moment-dominated case (M/V = 12.0 in.).

The relationships between the stress concentration factors (f_1 and f_2) determined from equation [3.5] and the notch and geometric variables were graphically examined for two EP sets, A and B. Typical plots are shown in Figs. 3.6 and 3.7. In all plots, the parallel nature of the lines for the two EP sets substantiates the initial assumption that material invariant functions F_1 and F_2 can be derived. Material factors μ_1 and μ_2, that account for the observed difference between material sets, were calibrated relative to a baseline EP set, selected as G17-E17 (set B), where μ_1 and μ_2 are unity and $f_1, f_2 = F_1, F_2$. Geometric functions F_1 and F_2 were statistically fitted by least squares method using the beam and notch geometric variables as predictors. With closed-form expressions for geometric factors (F_1, F_2) and numerical values of material factors (μ_1, μ_2), then maximum hoop stress or ShCF may be estimated.

Substitution of equation [3.3] into equation [3.2] gives

$$\frac{\sigma_{h,max}}{\left(\frac{6V}{bh}\right)} = \mu_1 \, F_1 \left(\frac{M}{V}\right) \frac{1}{h} + \mu_2 \, F_2 \ . \qquad [3.6]$$

Rearranging terms,

$$\frac{\sigma_{h,max}}{\mu_1} = \left(\frac{6V}{bh}\right)\left[\, F_1 \left(\frac{M}{V}\right) \frac{1}{h} + \frac{\mu_2}{\mu_1} \, F_2 \right] . \qquad [3.7]$$

Let $K = \frac{\sigma_{h,max}}{\mu_1}$ and $\mu = \frac{\mu_2}{\mu_1}$,

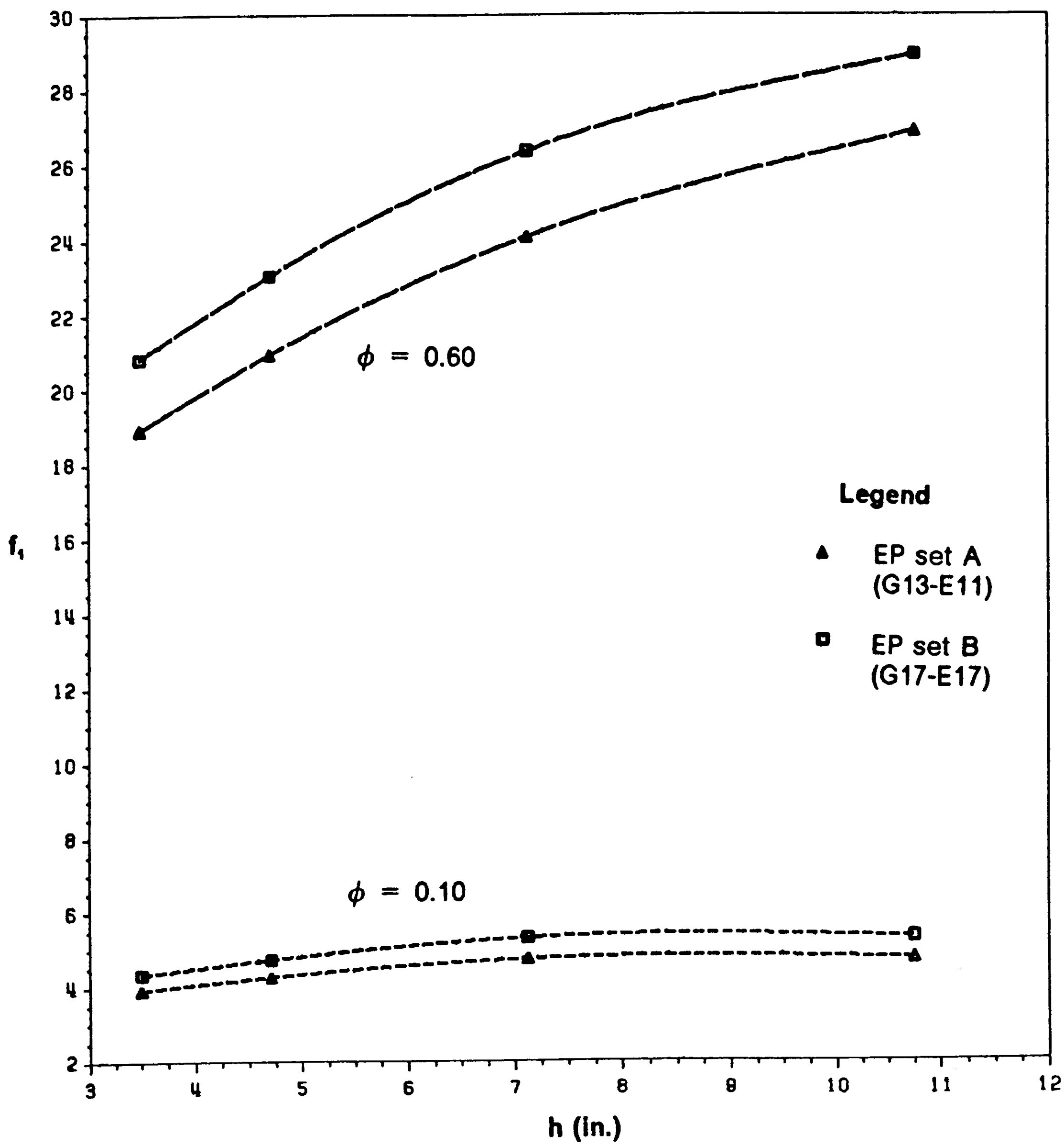

Figure 3.6. Influence of beam height on moment term factor for EP sets A and B

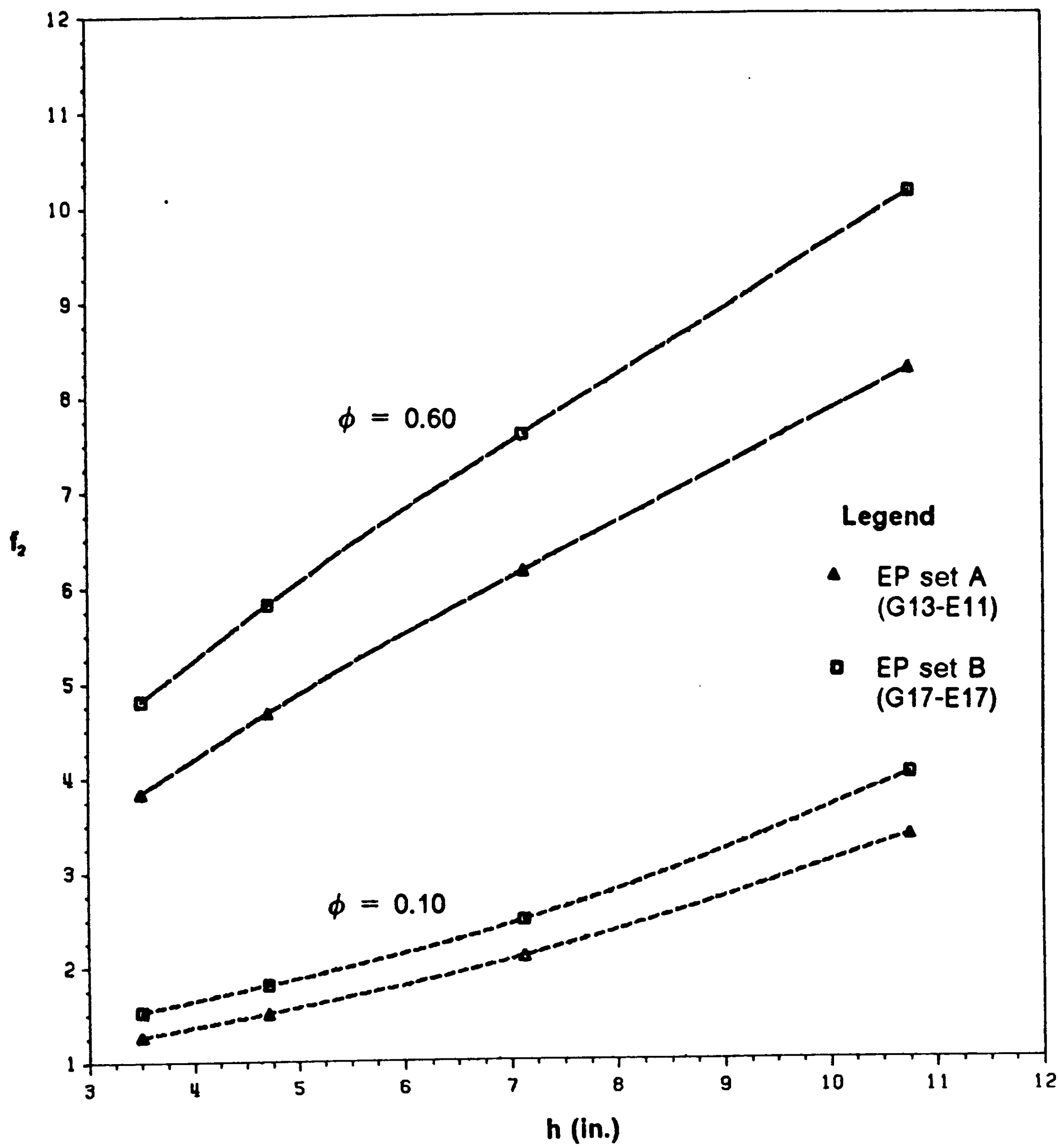

Figure 3.7. Influence of beam height on shear term factor for EP sets A and B

$$\frac{6V}{bh} = \frac{K}{\left[F_1 \left(\frac{M}{V} \right) \frac{1}{h} + \mu F_2 \right]} \qquad [3.8]$$

which is now in a form convenient for prediction of a critical shear value for a notched beam. This form assumes that μ is a single constant for all EP sets. K is an experimentally determined material constant for a species. A similar approach worked well for interior-notched wood beam (Zalph 1989). The validity of this approach for TEN is assessed in this work.

3.6.2 Forms of F1 and F2

Form A. From a host of functional forms, Zalph (1989) obtained the following best-fit functions for interior-notched beams

$$F_1 = \frac{1}{C_0 + C_1 \phi + C_2 \left(\frac{R}{D} \right)} \qquad [3.9]$$

$$F_2 = C_0 \, \phi^{C_1} \left(\frac{R}{h} \right)^{C_2} h^{C_3} \qquad [3.10]$$

where C_0, C_1, C_2 and C_3 are coefficients derived from statistical fitting, independent of material property. This was a natural starting point for finding best-fit forms of F_1 and F_2 for wood beams with TEN. Two reasons are obvious. First, both works used Gerhardt's (1984a) critical hoop stress theory. Second, both works share the same underlying assumptions in deriving a closed-form prediction equation.

Form B. Linear models and nonlinear models that are intrinsically linear, by suitable transformation of variables, were also fitted with the TEN data. These are shown in Table 3.4. In performing these, some functions that did not work for Zalph (1989) were tried once again, but this time using TEN data.

Form C. Strictly nonlinear models presented in Table 3.5 were also explored.

Zalph (1989) used a Central Composite Design (CCD) in his FE study. In many cases, a CCD experiment is very efficient, time- and effort-wise. A limitation, however, is its applicability to second order interactions only (i.e., it does not discern effects like D*R/h, D*R*h, etc.) (Myers 1976).

The full factorial design used here is capable of discerning higher-order effects. Third order effects such as R*D/h and R*h/d may be expressed as second order interactions R*ϕ and R/ϕ in a response surface experimental study originally designed with variable ϕ (ϕ=D/h). The levels of study variables for this work are given in Table 3.3. With Form B, the variable X_j (j= 1,k) could take any one of these original and combination variables. Four different sets of nine variables (k=9) each were fitted to each equation given in Table 3.4. The capability of the full factorial design to discern effects higher than second order was also useful in fitting Form C equations (Table 3.5) with TEN data.

3.6.3 Regression Fitting and Evaluation

All forms of F_1 and F_2 given in the previous section were fitted to the TEN data of the baseline EP set G17-E17 (with 46 values of f_1 and f_2 from regression of equation [3.5];

Table 3.4. **General forms of linear and nonlinear models (Form B) fitted with tension end-notched wood beam data.**

Form B Models
$F_i = C_0 + C_1 X_1 + C_2 X_2 + \ldots + C_k X_k$
$F_i = \dfrac{1}{C_0 + C_1 X_1 + C_2 X_2 + \ldots + C_k X_k}$
$F_i = C_0 X_1^{C_1} X_2^{C_2} X_3^{C_3} X_4^{C_4}$
$F_i = \exp (C_0 + C_1 X_1 + C_2 X_2 + \ldots + C_k X_k)$ **or** $C_0 \exp (C_1 X_1 + C_2 X_2 + \ldots + C_k X_k)$

where X_j = predictor variables ($j = 1,k$)

Table 3.5. Strictly nonlinear models (Form C) fitted with tension end-notched wood beam data.

Form C Models
• For i = 1,2 $F_i = C_0 + C_1 R^{C_2} + C_3 D^{C_4} h^{C_5}$ $F_i = \left(C_0 + C_1 R^{C_2} + C_3 D^{C_4} \right) h^{C_5}$
• For F_2 only $F_2 = C_0 + C_1 \phi^{C_2} + C_3 (\frac{R}{h})^{C_4}$ $F_2 = C_0 D^{C_1} R^{C_2} h^{C_3} + C_4 \phi$ $F_2 = C_0 D^{C_1} R^{C_2} h^{C_3} + C_4 \phi^2$ $F_2 = C_0 D^{C_1} R^{C_2} h^{C_3} + C_4 \phi^{C_5}$ $F_2 = C_0 \phi^2 R^{C_1} + C_2 D^{C_3} h^{C_4}$ $F_2 = C_0 \phi^{C_1} R^{C_2} + C_3 D^{C_4} h^{C_5}$ $F_2 = \left(C_0 D^{C_1} R^{C_2} + C_3 D^{C_4} \right) h^{C_5}$ $F_2 = C_0 \phi^{C_1} R^{C_2} h^{(C_3 + C_4 \phi)}$ $F_2 = C_0 \phi^{C_1} R^{C_2} h^{C_3 \phi}$

recall that for this EP set $f_1,f_2 = F_1,F_2$). Forms B (Table 3.4) are linearizable by transformation of either the predictor variables (X_j) or the response variables (F_i). As such, any linear regression procedure in the Statistical Analysis System (SAS) software (SAS Institute 1985) is applicable for least squares analysis using these forms. Using PROC RSQUARE (with Cp-statistics), the 10 best subsets for 1-variable model were obtained for each functional form, 10 best subsets for 2-variable model, 10 best subsets for 3-variable model, and so on. Several practical and promising models were selected for further examination. These selected models were analyzed using the SAS procedure PROC GLM (SAS Institute 1985) and their residual plots were visually evaluated.

Forms A and C were fitted to TEN data using the iterative Marquardt algorithm in procedure PROC NLIN (SAS Institute 1985). The residuals were plotted and visually evaluated.

Residuals are the differences between actual data and the values predicted by a regression equation. It could be thought of as "the observed errors if the model is correct" (Draper and Smith 1981). Assumptions on these errors are: (a) independence, (b) zero mean, (c) constant variance, and (d) normal distribution. Denial of any of these assumptions is an indication of incorrect fit. These assumptions were checked using the following residual plots:

- overall plot - this is a frequency plot of all the residuals and was used to visually evaluate the residual mean and distribution.

- plot of residual vs. predicted value - was used to evaluate if the variance was constant over the range of predicted values and if there is error in analysis or inadequacy of model.

- plots of residual vs. independent variables - were used to determine if the variance was constant over the range of an independent variable or if there is error in the fitted model.

Most models failed the residual evaluation process. For those that did not fail, relative prediction error was computed for every observation as FERR = (actual - predicted)/(actual) x 100%. The mean FERR was calculated and the overall FERR distribution was plotted for visual evaluation. The results of this evaluation process were given greater importance over other criteria because the functions will be primarily used for prediction purposes.

3.6.4 Best fits for F1 and F2

Two functions for the moment term factor, F_1, were further considered. Function coefficients were calculated using three methods: (i) regular least-squares estimates of transformed variables, (ii) weighted least-squares estimates (i.e. weighted on ϕ) of transformed variables, and (iii) non-linear approximation of coefficients of untransformed variables using the Marquardt algorithm in PROC NLIN (SAS Institute 1985). The mean and standard deviation of FERR were calculated and compared between estimation methods. The set of coefficients that gave the best prediction for each equation was adopted.

The form of Zalph's (1989) F_1 was found to be one of the two best fit moment term functions. With coefficients obtained from the NLIN procedure, it is expressed as

$$F_1 = \frac{1}{0.159 - 0.213\,\phi + 0.187\,(\frac{R}{D})}. \qquad [3.11]$$

Equation [3.11] yields an FERR mean of 1% on the overprediction side and a standard deviation of 8.2%. Maximum overprediction of actual values is 25.3% and maximum underprediction is 11.8%.

The other F_1 function is an extension of equation [3.11]. With coefficients obtained from weighted least-squares estimates, it is given as

$$F_1 = \frac{1}{0.161 - 0.218\phi + 0.105\,(\frac{R}{D}) + 0.015\,(\frac{R}{\phi})}. \qquad [3.12]$$

Mean FERR is 0.2% and standard deviation is 5.2%. This equation overpredicts the actual values by as much as 11.5% and underpredicts by a maximum of 11.7%.

At this stage, a comparison of equations [3.11] and [3.12] shows that the additional term R/ϕ in the denominator of the latter provided a tighter distribution of FERR about zero than the former. The maximum underprediction errors in both equations, however, are essentially the same.

For the shear term factor, the best fit function was

$$F_2 = C_0\,\phi^{C_1}\,R^{C_2}\,h^{(C_3 + C_4\phi)}. \qquad [3.13]$$

An h-ϕ dependence was observed in Fig. 3.7 which shows that the relationship between F_2 and h varies with different levels of ϕ. Recall also that, in the initial investigation of the height effect on hoop stress, the λ-values in equation [3.4] were dependent on ϕ-values (see section 3.4.3). With coefficients estimated by PROC NLIN from all the geometric data, equation [3.13] overpredicted the actual values by over 13% in 2 cases. This occured for the cases where ϕ = 0.10, R = 0.1875 in. and h = 4.71 and 7.125 in. (overprediction of 13.4 and 15.2%, respectively). Underprediction by over 11% occured in 2 cases where ϕ = 0.10, h = 10.75 in. and R = 0.344 and 0.50 in. (underprediction of 11.3 and 11.4%, respectively). FERR's for all other geometry cases, however, fall within the tight range of $\pm$5.9% of mean zero. Based on this, the FERR distribution was judged to be excellent.

The FE study covered cases of ϕ = 0.10, 0.35, 0.52 and 0.60. The data were, therefore, weighted heavily for cases of $\phi > 0.35$. The fitted F_2 model revealed this effect as evidenced by the occurrence of maximum overprediction and underprediction errors in cases where $\phi = 0.50$. Since very deep notches may not be of greatest practical importance, the data for $\phi = 0.60$ were excluded to allow estimation of coefficients on the remaining data set. Recalculating FERR for ***all*** data (including $\phi = 0.60$) using these modified coefficients, it was found that the maximum range of overprediction and underprediction errors was reduced by about 1% at both ends. With these adjusted coefficients, the geometric shear term factor is, thus, proposed as

$$F_2 = 1.464\ \phi^{0.712}\ R^{-0.418}\ h^{(0.847 - 0.316\phi)}. \qquad [3.14]$$

3.6.5 Delineating material effects

The material factors μ_1 and μ_2 for different EP sets were computed from actual values of f_1 and f_2 resulting from the regression of equation [3.5]. The material factor was generally expressed as

$$\mu_{ij} = \frac{f_{ij}}{f_{i,B}} \quad \text{or} \quad f_{ij} = \mu_{ij}\, f_{i,B} \qquad [3.15]$$

where i = 1,2 (designations corresponding to moment-term and shear-term, respectively),

j = material EP sets A, C, D, E,

B = baseline EP set (G17-E17) where μ_1 , μ_2 = 1.0.

For each EP set, μ_i was determined using the REG procedure in SAS (SAS Institute 1985) for a linear regression with no intercept. It has the form

$$Y = a X \qquad [3.16]$$

where a is the slope of the line equivalent to μ_i in equation [3.15]. Factors μ_1 and μ_2 were obtained from 46 pairs of f_1 and f_2. Figure 3.8 shows a typical regression fit where the slope is the material factor μ_1 for EP set A (G11-E13). The ratio $\mu = \frac{\mu_2}{\mu_1}$ was computed for each EP set and tabulated in Table 3.6. Results show that μ is not constant across EP sets but is predicted resonably well by a linear expression involving the orthotropy ratio E_x/G_{xy} . Because E_x/G_{xy} is not always known and applicability to all EP sets is desired, μ is conservatively set as 1.12. Since μ is a multiplier to the shear term (see equation [3.8]), its effect would be minimal or negligible for moment-dominated cases, but would provide additional safety in some materials for shear-dominated cases, e.g. notch root at or close to the support.

Table 3.6. Material factors calibrated from the baseline EP set G17-E17 (from 46 observations).

EP Set	Orthotropy Ratios			Material Factor			Predicted μ_p [1]
	$\frac{E_x}{G_{xy}}$	$\frac{E_x}{E_y}$	$\frac{E_y}{G_{xy}}$	μ_1	μ_2	$\mu = \frac{\mu_2}{\mu_1}$	
A	11	13	0.846	0.915	0.818	0.894	0.894
B	17	17	1.000	1.000	1.000	1.000	1.006
C	27	21	1.286	1.112	1.246	1.121	1.118
D	11	17	0.647	0.930	0.939	1.010	1.006
E	27	17	1.588	1.110	1.150	1.036	1.006

Note: [1] From $\mu_p = 0.530 + 0.028\,(E_x/G_{xy})$; (coeff. of determination, $r^2 = 0.971$)

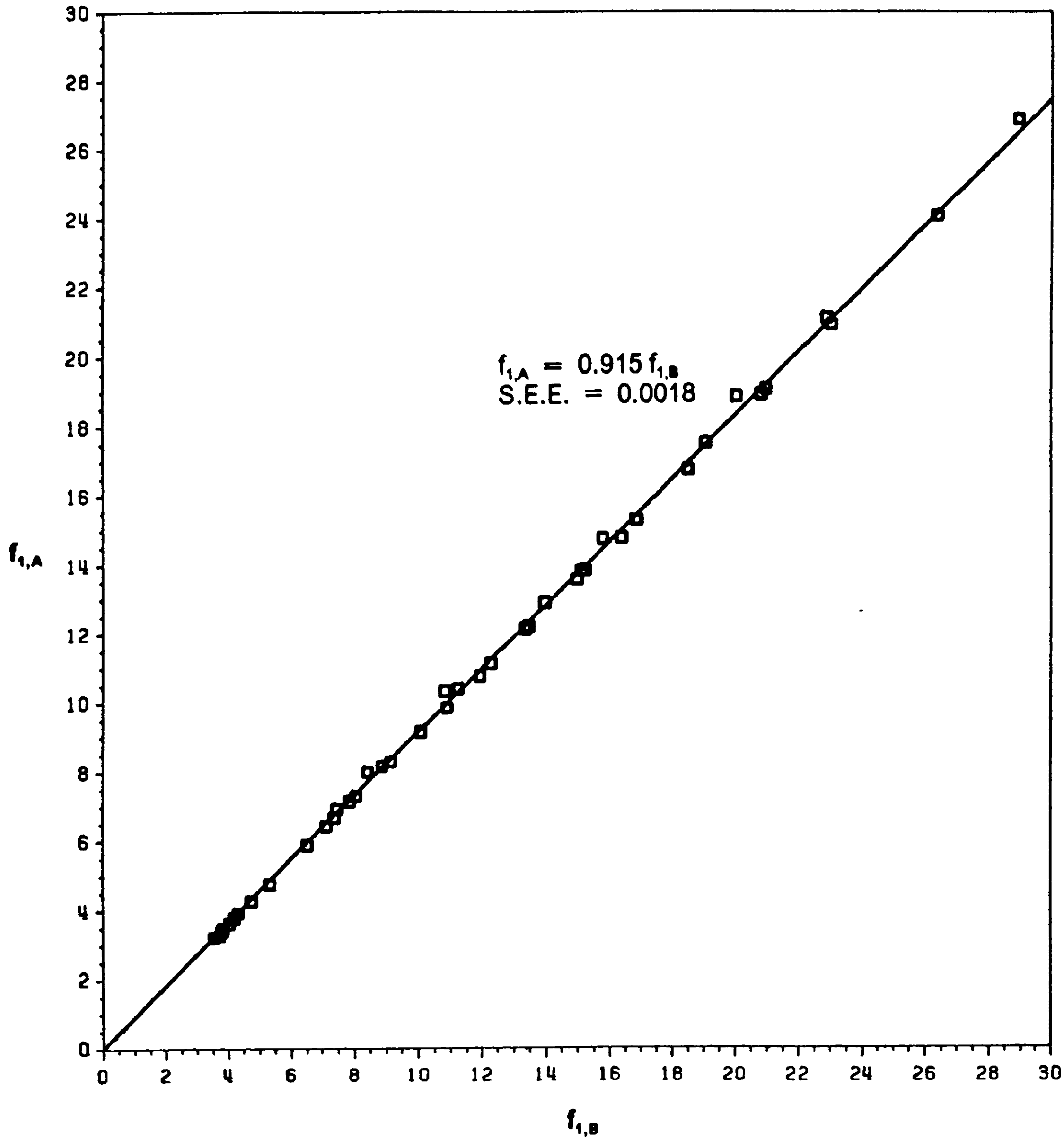

Figure 3.8. **Resulting regression line for EP set A (G11-E13) in determining μ_1 using equation 3.17.**

3.7 Evaluation of Closed-form Equations

3.7.1 Prediction accuracy

The FE-based expressions for f_1 and f_2 are substituted into equation [3.2]. Because two alternative models for F_1 were considered, there were two alternative prediction equations for ShCF:

$$\frac{\sigma_{h,max}}{\left(\frac{6V}{bh}\right)} = \mu_1 \left[\frac{1}{0.159 - 0.213\phi + 0.187(\frac{R}{D})} \right] \left(\frac{M}{V}\right)\left(\frac{1}{h}\right) + \mu_2 \; 1.464\, \phi^{0.712}\, R^{-0.418}\, h^{(0.847-0.316\phi)} \qquad [3.17]$$

and

$$\frac{\sigma_{h,max}}{\left(\frac{6V}{bh}\right)} = \mu_1 \left[\frac{1}{0.161 - 0.218\phi + 0.105(\frac{R}{D}) + 0.015(\frac{R}{\phi})} \right] \left(\frac{M}{V}\right)\left(\frac{1}{h}\right) + \mu_2 \; 1.464\, \phi^{0.712}\, R^{-0.418}\, h^{(0.847-0.316\phi)} \qquad [3.18]$$

where μ_1 and μ_2 for different EP sets are those given in Table 3.6. These two equations were used to compute predicted ShCF's for all geometries considered in the FE study. The predicted values were compared to actual ShCF's obtained from FE analysis (138 comparisons per EP set). Relative prediction error was computed as ShCFERR = (actual - predicted) / (actual) x 100%. Results are tabulated in Table 3.7.

Table 3.7. Comparative ShCF prediction errors between equations [3.17] and [3.18].

EP Set	Equation	Relative Prediction Error, ShCFERR (%)			
		Mean[1]	Std. Deviation	Maximum Overprediction	Maximum Underprediction
A	3.17	0.67	4.84	12.75	13.92
	3.18	0.32	4.26	8.69	13.27
B	3.17	0.66	4.79	15.18	11.91
	3.18	0.30	3.66	8.38	11.22
C	3.17	0.58	5.26	17.02	12.48
	3.18	0.23	3.65	10.72	8.10
D	3.17	0.54	5.29	15.60	14.83
	3.18	0.17	4.51	8.81	16.36
E	3.17	0.40	5.62	18.86	12.23
	3.18	0.06	4.18	17.86	7.85

Note: [1] Positive sign means on the side of underprediction

Note that the right hand side of equations [3.17] and [3.18] are statistical estimates and, therefore, actually include an error term (omitted in the given expressions) earlier identified as residuals. A standard method of evaluating the accuracy of statistical fits is to investigate these residuals. In this study, however, it is more helpful to look at the prediction error, ShCFERR, more closely in the same manner as residuals were evaluated in section 3.6.3.

An overall ShCFERR plot was obtained and visually examined for each EP set using both equations. ShCFERR's were also plotted against the predicted values and the different geometric variables. The overall ShCFERR plot for equation [3.18] was judged slightly superior to that for equation [3.17] in that the mean is closer to zero and the standard deviation is smaller for the former. The plots of ShCFERR against predicted values in the two equations showed different scatter trends but similar variance. (Note that observations for an equation were generally consistent across EP sets in all these plots.) Relevant observations for plots of ShCFERR against geometric variables were:

- against ϕ - in both equations, largest ShCFERR variance occured for shallow notches, i.e., $\phi = 0.10$,

- against D (an interaction term, $D=\phi h$) - in both equations, scatter plot of ShCFERR's did not show systematic trend nor unequal variance over the range of D,

- against h - ShCFERR's for equation [3.17] revealed a slight curvilinear trend against h, thus, underpredicting most cases for h= 3.50 in.; ShCFERR's for equation [3.18] did not show systematic trend nor highly unequal variance.

- aganst R - for cases where R = 0.50 in., ShCFERR's for equation [3.17] have slightly larger variance than those from equation [3.18]; the opposite, however, was true for R = 0.1875 in. cases,

- against M/V - in both equations, the smallest variance was for cases nearest the support, i.e., M/V = 1.0 in., although for EP set D, ShCFERR means were on the side of underprediction.

At this point, reasonable accuracy could be claimed for both equations. Prediction confidence for shear-dominated cases was enhanced by the low ShCFERR variance for M/V = 1.0 in. cases in both equations. Equation [3.18] generally provided better prediction accuracy. For sharp-cornered TEN wood beams (i.e., $R \simeq 0$ which is theoretically $R = R_{*}$), however, equation [3.17] showed better potential because of low ShCFERR variance for smaller R-values. Considering the practical applicabilty to these notch cases and the simplicity of the latter prediction form, equation [3.17] was judged the best selection overall.

3.7.2 Applicability

It is helpful to note the notch geometries for which the closed-form expression was derived so that the scope and limitations of its possible applications can be defined. Theoretical analyses covered TEN beams with L/h from 3.91 to 12.0. Short and deep beams, known to be critical in shear, were therefore considered in the formulation. The percentage of cases for which this is true can be computed by setting the moment and shear terms in equation [3.1] to have equal contributions to $\sigma_{h,max}$. In equation form

$$f_1 \left(\frac{6M}{bh^2} \right) = f_2 \left(\frac{6V}{bh} \right) \qquad [3.19]$$

Substituting values for M and V for center-point loading, it yields

$$f_1 \left[\frac{6\left(L_{n(eq)} \frac{P}{2}\right)}{bh^2} \right] = f_2 \left[\frac{6\left(\frac{P}{2}\right)}{bh} \right] \qquad [3.20]$$

Solving for the notch distance from the support for which the M-term and the V-term are equal,

$$L_{n(eq)} = \left(\frac{f_2}{f_1} \right) h \qquad [3.21]$$

This was computed for each geometry and then compared to its actual L_n. If actual $L_n > L_{n(eq)}$, then M-term dominates; otherwise, V-term dominates. It was found that V-term actually dominated in 34% of all cases studied (234 out of 690) and M-term dominated for the remaining 66%. This indicates that the closed-form expression for calculating $\sigma_{h,max}$ for TEN beams would possibly be applicable also for notches anywhere on the tension side except where V is zero.

3.8 Summary of Key Findings

A total of 690 TEN wood beam cases were analyzed using Gerhardt's (1984b) FE program. The five material elastic property sets in this study covered a wide range of commercially important species in the world. Practical ranges of notch length, L_n, or notch location, M/V, fractional notch depth, ϕ, beam height, h, and fillet radius, R, were used to calculate normalized hoop stresses in TEN wood beams. With the exception of beam width, b, and slope-of-grain, all relevant variables that geometrically define a TEN wood beam were considered in this study.

A simplified closed-form equation for predicting maximum hoop stress, $\sigma_{h,max}$, in TEN wood beams was derived. Values predicted by the equation showed good accuracy with the actual FE $\sigma_{h,max}$ for a wide range of practical cases. It is now possible to determine the critical hoop stress of a specific notched wood beam geometry without resorting to the use of Gerhardt's (1984b) FE program.

4. Experimental Procedure

4.1 Overview

The objective of the experimental plan was to test the critical fillet hoop stress (CFHS) theory for predicting the strength of wood beams with a practical range of TEN configurations. Specifically, the hypotheses were that

- geometric and material effects are separable, i.e. the material strength parameter, K, is geometry-independent,
- the material strength parameter, K, is related to other standard material properties such as specific gravity, block shear strength and/or perpendicular-to-grain tensile strength, and
- sharp-cornered notches can be practically modeled as filleted with an effective radius, R_e.

The major effort was to determine K-values for filleted TEN beams of two species to test the geometry-independence of K. Small clear shear and tension perpendicular-to-grain specimens were taken from almost every filleted TEN beam. These clear strength properties, specific gravity (SG) and moisture content (MC) were determined. The physical and mechanical properties were used to predict K and test the second hypothesis. To determine an effective radius, R_e, a limited set of TEN geometries for filleted ($R = 0.25$ in.) and sharp-cornered ($R = 0$) cases were tested. Equation [3.17] developed in the previous chapter was used to calculate R_e.

A sub-study which evaluated the effect of TEN on the stiffness of wood beams was also conducted.

4.2 Materials

Two materials were selected to represent anatomically different softwood and hardwood species groups: Southern yellow pine (SYP) and yellow poplar (YP). Fig. 4.1 shows anatomical cross-sections of these species. Southern yellow pine was selected because of relative wide anatomical variability in the species group (Panshin and de Zeeuw 1980); this was reflected in high coefficient of variation (C.V.) of Zalph's (1989) material strength parameter, κ, for tension interior notched beams. Besides, it is widely available and is commonly used in the US construction industry. Yellow poplar, although not commonly used in the construction industry, gave Zalph (1989) the lowest C.V. for the κ-values in his study.

All SYP materials were purchased kiln-dried from the lumber yard of TimberTruss in Salem, Virginia. Best boards with minimum defects were selected from bunks of No.

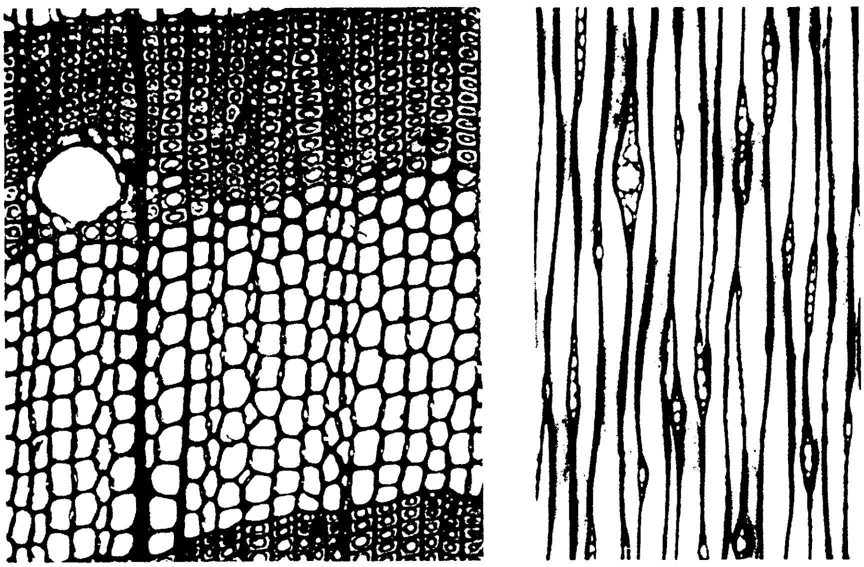

x—75×　　t—75×

(a)

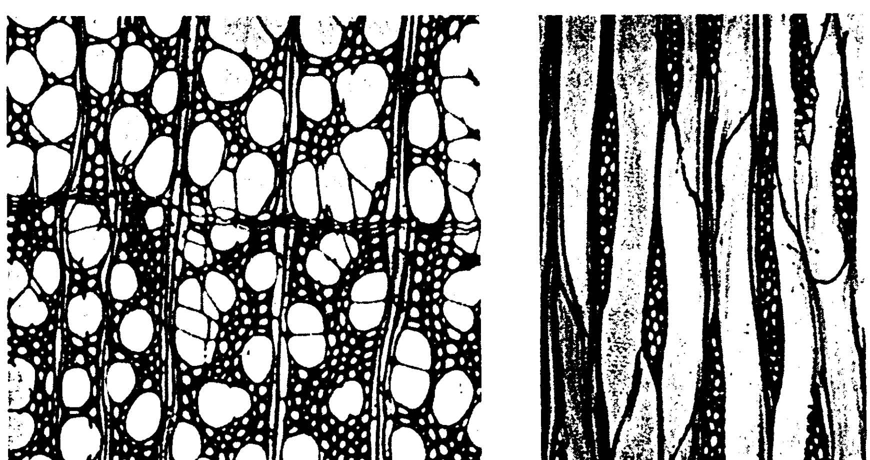

x—75×　　t—75×

(b)

Figure 4.1. Anatomical cross-sections of test materials (from Panshin and de Zeeuw 1980): (a) Southern yellow pine, (b) Yellow poplar

2 grade 2 x 8 in. x 10 ft. and 2 x 10 in. x 10 ft. lumber. Bending specimens measuring 1.5 x 3.5 x 48 in. and 1.5 x 9 x 48 in. were cut in Brooks Forest Products Center from the nominal 2 x 8 in. and 2 x 10 in. materials, respectively. Most of the boards in its final dimensions were free of defects. None had defects in the notch area.

Almost all of the YP materials were purchased kiln-dried from a mill in Natural Bridge, Virginia. A similar process of careful selection was employed to obtain nearly clear 2 x 10 in. x 8 ft. pieces. Full-size bending specimens measuring 1.5 x 3.5 x 47 in. and 1.5 x 3.5 x 47 in. were cut from the 2 x 10 in. boards. For the sharp-cornered TEN beam study, 15 pieces of 1.5 x 3.5 x 48 in. lumber were taken from the excess YP material of Zalph's (1989) study.

All boards, except those from Zalph, were end-coated with Anchorseal on both ends when cut to final dimensions to prevent the development of end checks. This was done even though the specimens were notched and tested within two weeks of being cut to final dimensions.

4.3 Filleted TEN Study

4.3.1 Experimental design

All variables considered in the FE study were also considered in this main study. The variables are: beam height, h, fractional notch depth, ϕ, radius, R, notch location, M/V, and material. A **randomized complete block design** was used with geometry variables contained in a block and each block representing a species group. The levels of the experimental variables are given in Table 4.1. Notch location, M/V, was measured from the center of a 2 in.-wide aluminum block support. Thus, a notch at the support has M/V = 1.0 in..

Originally, four replicates were prepared per cell. Two out of the sixteen cells per block, however, received from 6 to 9 additional samples per cell from the sharp-cornered TEN study. This increased the total number of bending tests performed on filleted TEN beams from 128 to 158 (2Rx2hx2ϕx2M/Vx2sp.x4 + 30 = 128 + 30 = 158).

Beam width, b, was kept constant at approximately 1.5 in.. Beam span, L, was maintained at 42 in.; this gave span-to-depth ratios of 12.0 and 4.7 for h of 3.5 and 9 in., respectively.

4.3.2 Specimen Preparation

Filleted notches were cut out using essentially the same notch machining techniques employed by Zalph (1989). An overview of the notching process on a 3.5in-deep beam is described. A work bed made of plywood and tempered hardboard with a top and right end stops for a 3.5in.-deep beam is clamped firmly to a workbench. A specimen is placed against the stops and marked for support location. A notch template (also made of plywood and tempered hardboard and shaped out to guide a router to cut R = 0.25 in. or 0.50 in. notch) is appropriately positioned on the top surface of the specimen and firmly clamped. A notch less than 1 in. in depth is cut by progressive passes of a 1.5 horsepower router using a two-flute carbide bit until the final dimensions are achieved. Notches deeper than 1 in. are first roughed out using a

Table 4.1. Experimental design of filleted TEN study : randomized complete block design

Variable	Levels	No. of Levels
h (in.)	3.50, 9.00	2
ϕ	0.20, 0.50	2
R (in.)	0.25, 0.50	2
M/V (in.)	1.0, 10.0	2

beam width, b = 1.5 in.
beam span, L = 42 in.

loading : center-point
L/h range : 4.67, 12.0

1.125in.-diameter carbide-tipped Forstner bit in a handheld drill. Two partly overlapping drilled holes are necessary to rough cut the notch for the $\phi = 0.50$ case. The notch is finished by the router guided by the notch template. A bandsaw was used to carefully cut remaining material between the top of the filleted notch and the end of the board. Fig. 4.2 shows a filleted notch cut in this manner.

A similar process was used to cut a 9in.-deep beam except that the rough cut was made using a bandsaw instead of a handheld drill.

4.4 Sharp-cornered TEN study

4.4.1 Experimental design

In this study, the notch location, M/V, and fractional notch depth, ϕ, were kept constant at 1.0 in. and 0.50, respectively. Most TEN cases in construction have M/V around 1.0 in.. Zalph (1989) did not find any conclusive evidence of ϕ-effect on the value of R_e.

Using SYP and YP materials, the following geometry variables were studied:

variable	**levels**
h (in.)	3.5, 9.0
R (in.)	0 , 0.25

The number of specimens per cell varied depending on the availability of materials. A total of 33 sharp-cornered TEN beams for SYP (18 for h=3.5 in. and 15 for h=9.0 in.) and 25 for YP (16 for h=3.5 in. and 9 for h=9.0 in.) were prepared. The filleted

Figure 4.2. Typical filleted notch

TEN counterparts (total of 44) were taken from two cells that correspond to the same geometry for each species in the filleted TEN study.

4.4.2 Specimen preparation

All filleted notches were cut as described in section 4.3.2. Fabrication of the sharp notch in beams with h=3.5 in. differed from that with h=9.0 in. specimens. All beams were marked for support and notch locations. A rough outline of the notch was sketched. For 3.5in.-deep beams, the bottom edge was also marked for notch location. This mark and the notch outline served as a guide to cut the material within the outline using a radial arm saw. The beam was then clamped to a template made from solid lumber with a plywood and tempered hardboard panel composite on top which was cut out to guide the router during machining. The specimen was positioned such that the edge of the beam where the notch would be cut is in full and firm contact with the template's composite top. A router bit aligned with the depth dimension of the beam was moved along the thickness dimension, acting as an end mill and providing a sharp-cornered notch. Theoretically, the radius of this notch is approximately equal to the radius of the carbide cutting tip. A typical notch cut is shown in Fig. 4.3.

For 9.0in.-deep beams, a guide-and-stop set-up on a bandsaw was used to cut a uniform sharp-cornered notch configuration for all beams (SYP and YP materials). In this case, the notch radius is approximately equal to the radius of the cutting tip of the band saw blade.

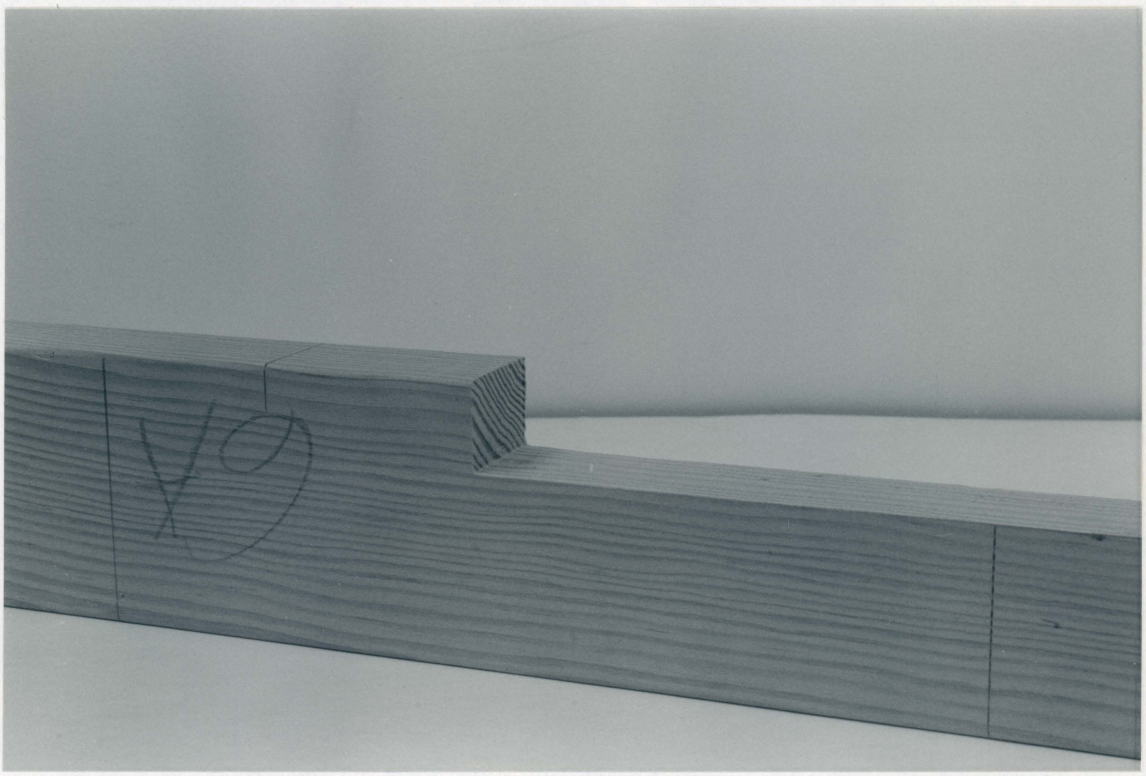

Figure 4.3. Typical sharp-cornered notch

4.5 Bending Tests

All bending tests were conducted using a servohydraulic testing machine by Material Test System (MTS) under deformation control. Beam span was 42 in.. In all cases, the load was applied continuously at the center-- the same loading configuration with the FE studies-- at a constant rate of motion of the crosshead of 0.10 in./min.. For 3.5in.-deep beams, a bearing block with contact radius of 8 in. was used. A bearing block with 22 in. contact radius was used for 9.0in.-deep beams. See Figs. 4.4 and 4.5. Notice in Fig. 4.5 that lateral support at the midspan was provided to restrict lateral deflection. The support was designed to allow vertical movement with minimum frictional restraint.

Load-deflection (P-Δ) curves were obtained for each test using an X-Y plotter. The Y-axis plotted load as sensed by the machine load cell and the X-axis recorded the deflection sensed by a linear variable differential transformer (LVDT). The LVDT was attached at midspan of a lightweight deflection yoke (shown in Figs. 4.4 and 4.5).

Support at the notched end was adjusted for each combination of h and ϕ so that all test beams were level before load application. A 2 in.-wide aluminum bearing block was placed at the supports to minimize compression. The blocks were attached to tubular steel supports which were free to roll, thus minimizing axial constraint.

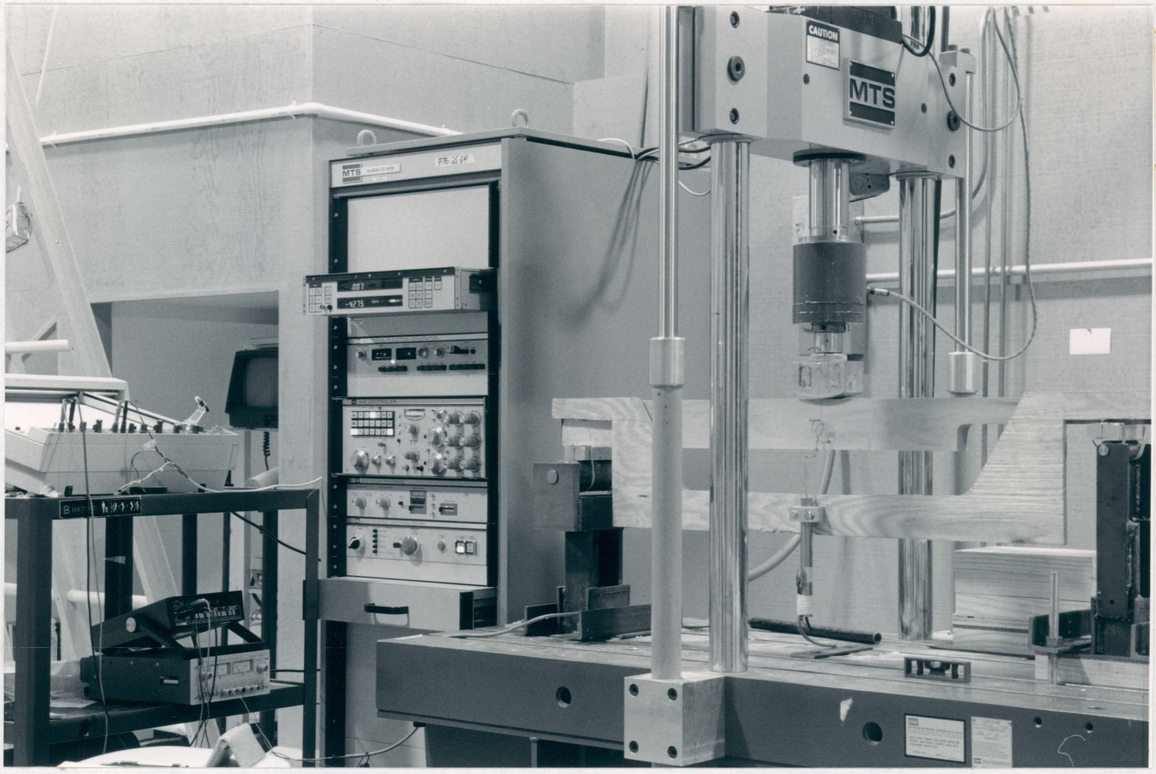

Figure 4.4. Test set-up for beam with h=3.5 in.

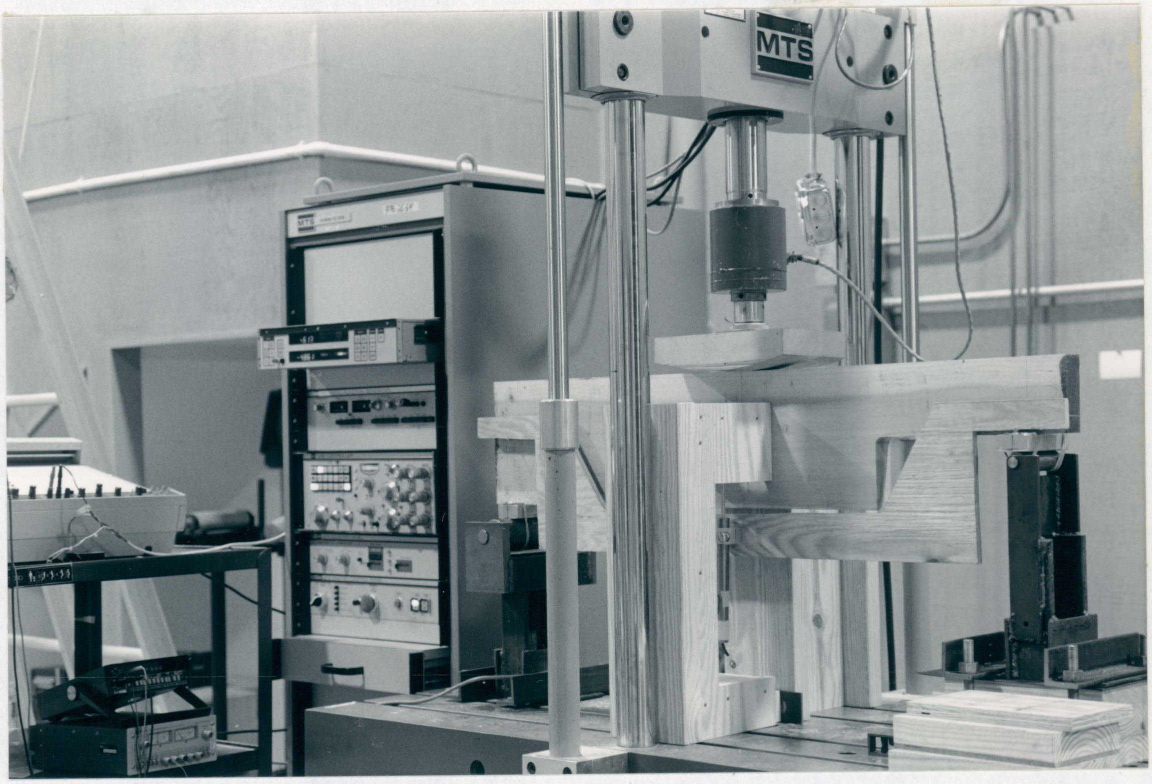

Figure 4.5. Test set-up for beam with h = 9.0 in.

4.6 Stiffness Determination Before Notching

Beam stiffness was measured and calculated for selected specimens before notching. Sixteen defect-free boards for the filleted TEN study were separated for each species. These boards were subjected to a flatwise, center-point bending load over a 42 in. span. Deflection rate was maintained at 0.50 in./min. on the MTS servohydraulic testing machine. From the P-Δ curve, stiffness (P/Δ) values were measured and recorded for each beam. The beams were properly labeled and distributed to the experimental block identified in the filleted TEN study (section 4.4.1). Experimental results of Gerhardt (1984a) showed that the stiffness of wood beams with tension interior notches was unaffected by notch fillet radius, R. The same was assumed to hold for TEN. Two beams were assigned for each cell with $R = 0.25$ in. and the following parameters:

variable	levels
h (in.)	3.5, 9.0
M/V(in.)	1.0, 10.0
ϕ	0.20, 0.50
species	SYP, YP

True modulus of elasticity ($E_{t,flat}$) was calculated from the P/Δ-values. Flatwise bending was used to measure $E_{t,flat}$ because subjecting a beam with low L/h ratio (e.g. 4.67 for beam with $h = 9.0$ in.) to edgewise bending may cause damage to the beams. This may influence the measurement of notch strength and affect the results of the main study. $E_{t,flat}$ was adjusted to an equivalent $E_{t,edge}$ as discussed in section 5.5.

4.7 Determination of Other Material Properties

4.7.1 Moisture content and specific gravity

An MC-SG specimen was cut from all tested beams that failed at the notch (61 samples per species). Samples were taken from the vicinity of the notch (area within a 3 in. radius from the notch root, see Fig 4.6). Knots, pitch pockets and other anatomical deviations were avoided.

Moisture content was calculated from green and oven-dry weights of the specimen. Specific gravity was calculated from oven-dry weight and volume measurements. Volume was measured by water immersion, Method B of ASTM D2395-83 (American Society for Testing and Materials 1988).

The SYP materials had an average MC and SG of 11.42% and 0.54, respectively; the YP materials averaged 7.72% and 0.50, respectively.

4.7.2 Block shear strength

Shear block samples were cut from test beams at one of three locations shown in Fig 4.6. Cracks, knots and other defects were avoided. A total of 49 samples for SYP and 51 for YP were obtained.

Block shear strength was determined according to the procedure given in ASTM D143 (American Society for Testing and Materials 1988) except for the specimen size and the ring orientation. Tests on samples with variable ring orientation and 2 x 1.5 in.

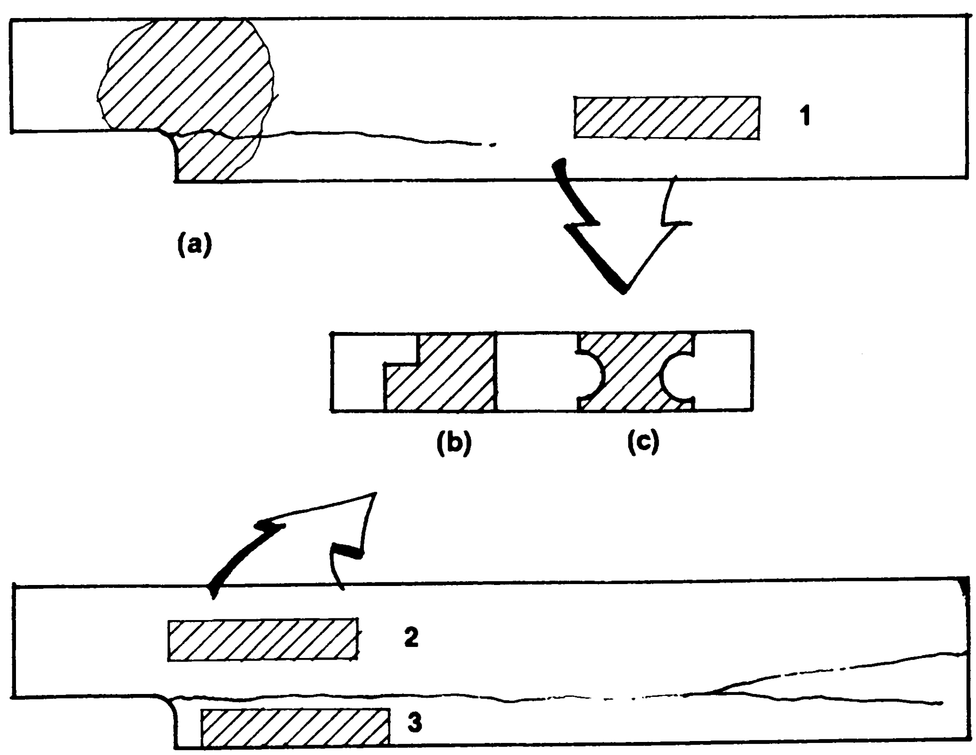

Figure 4.6. Sampling location(s) for determination of physical and mechanical properties: (a) moisture content-specific gravity, (b) shear block, and (c) tension perpendicular-to-grain

cross sections were conducted instead of the standard ring orientations and 2 x 2 in. cross sections stipulated by ASTM D143. These deviations were dictated by the nature and properties of full-size materials. Bendtsen and Porter (1978) evaluated the effect of size deviation and found no significant differences between standard and undersized samples. Block shear strength results reported herein were deemed acceptable for predicting K, neglecting the effect of variable ring orientation.

4.7.3 Perpendicular-to-grain tensile (TPERP) strength

Tension perpendicular-to-grain (TPERP) samples were taken from near the same location where the shear block samples were obtained (see Fig 4.6). The deviations of ring orientation and size from the standard samples were, therefore, carried over to the TPERP samples and were similar to those of the shear block samples. A total of 49 samples for SYP and 50 for YP were obtained.

Apart from the deviations just stated, the procedure given in ASTM D143 was used to obtain TPERP. Barrett (1974) and Barrett et al. (1975) found a strength-size relationship for TPERP but it is currently unquantified for SYP and YP. The obtained TPERP values were, therefore, used in the analyses of results of this study without applying any adjustment factor to these values to correct for the size effect, or any effect of ring orientation.

5. Results and Discussion

5.1 Notched Beam Strength

5.1.1 The material parameter, K

The material strength parameter, K, was calculated using

$$K_i = \left(\frac{6V_i}{bh}\right)\left[F_1 \left(\frac{M}{V}\right) \frac{1}{h} + \mu F_2 \right] \qquad [5.1]$$

where i = load level, PL for proportional limit

MAJ for major load drop (≥5%)

MAX for maximum load

μ = 1.12 (fixed value from Table 3.6)

$$F_1 = \frac{1}{0.159 - 0.213\phi + 0.187(\frac{R}{D})}$$

$$F_2 = 1.464\,\phi^{0.712}\,R^{-0.418}\,h^{(0.847-0.316\phi)}.$$

Individual calculated K-values from the main study (filleted TEN beams) are found in Appendix F. Summary statistics, classified by M/V, are given in Table 5.1.

Since the CFHS theory assumes linear elasticity, the theoretical model is strictly applicable only to notched beam behavior within the proportional limit (PL) range. If crack initiation (CI) occurs within this range, then the CI load is regarded as that causing the fillet hoop stress to exceed a critical stress level at the notch root. This is fundamental to the CFHS theory. Material behavior beyond either the PL or the CI may be unreliably modeled by the FE model since assumptions are not strictly met.

Zalph (1989) found no consistent relationship between PL and CI loads in his work on tension interior notches. He thus considered the load at CI for all his analysis and did not further analyze that at PL. Stieda (1966), however, associated PL load with CI or initial failure load noting that the two loads always coincided in experimental tests of small beams (1 x 1 x 16 in.) with three dry softwood materials. Murphy (1978) also considered PL load as "failure load because it corresponds to crack initiation that precedes visible opening". He tested dry Douglas fir 1 x 1 x 16 in. materials.

The actual notch root CI load is difficult to measure directly and accurately. Load at the first audible crack may be recorded but without a visible crack at the notch, crack initiation may have occurred elsewhere in the beam. In most TEN cases, the visible CI load was observed in the load-deflection (P-Δ) curve to coincide with the load at major drop (MAJ) which is the point where load drops by 5% or more. For a few

Table 5.1. Summary statistics of calculated K from experiment

Species[1]	M/V (in.)	Load Level	n	K Mean (psi)	K Std. Deviation	K C.V.[2] (%)
SYP	1.00	PL	38	5884	1418	24.09
		MAJ	39	10342	2516	24.33
		MAX	38	10984	2715	24.72
	10.00	PL	30	13895	4693	33.77
		MAJ	30	18316	5340	29.16
		MAX	30	22476	8091	36.00
YP	1.00	PL	34	7072	2061	29.14
		MAJ	34	11035	3033	27.49
		MAX	33	12084	3230	26.73
	10.00	PL	31	14417	4187	29.04
		MAJ	32	21830	3960	18.14
		MAX	31	27181	8843	32.53

[1] The average moisture content of SYP material was 11.42% and that of YP material was 7.72%.

[2] C.V.- coefficient of variation, C.V. = (std. deviation)/(mean) x 100%

beams, the MAJ load occurred at PL, but for most others, it occurred beyond PL. Figure 5.1 shows typical P-Δ curves for wood beams with TEN.

The definition of MAJ load and the experimental observations on its occurrence qualify it as the "true" failure load. In general, beam behavior after the MAJ load is unpredictable. For TEN cases with h=3.50 in., $P_{MAJ} = P_{max}$ for 81% of SYP and 92% of YP beams. For cases with h=9.0 in., this is true only for 38% of SYP and 31% of YP beams. Beams that continued to bear load after the major load drop acted as prismatic beams with effective depths either ≥ or ≤ to h_e at the notch (see Fig. 2.1). These effective depths were observed to be controlled in the failure process by slope of grain. K_{max} was dropped from subsequent analyses because commercial lumber has a high variation of grain angle and there is no assurance that a net section will remain after the MAJ load. These observations on the maximum load-carrying capacity of notched beams were consistent with those of Stieda (1966), Hirai and Sawada (1979) and Murphy (1986).

Failure load is therefore defined as P_{MAJ} and failure strength as K_{MAJ}. Table 5.1 shows lower coefficient of variation (C.V.) for K_{MAJ} than for K_{PL} in most cases. This suggests that the CFHS-based TEN equation predicts K_{MAJ} as well as it predicts K_{PL}. Zalph (1989) explained this as follows (he considered major load drop as ≥2%):

> For crack extension some small distance from the critical fillet, the applied loading and notch depth (or net section) are about the same as for uncracked fillet. It is reasonable to expect that the crack extension load in this region is roughly proportional to the crack initiation load. This is why the model can predict that first major (2%) drop in load...

Most of the variability in K_{MAJ} was due to the effect of widely varying ring angle orientation of notched beam specimens. Fig. 5.2 shows SYP shear block specimens with representative cross-sections from full-size notched bending specimens from which the block specimens were obtained.

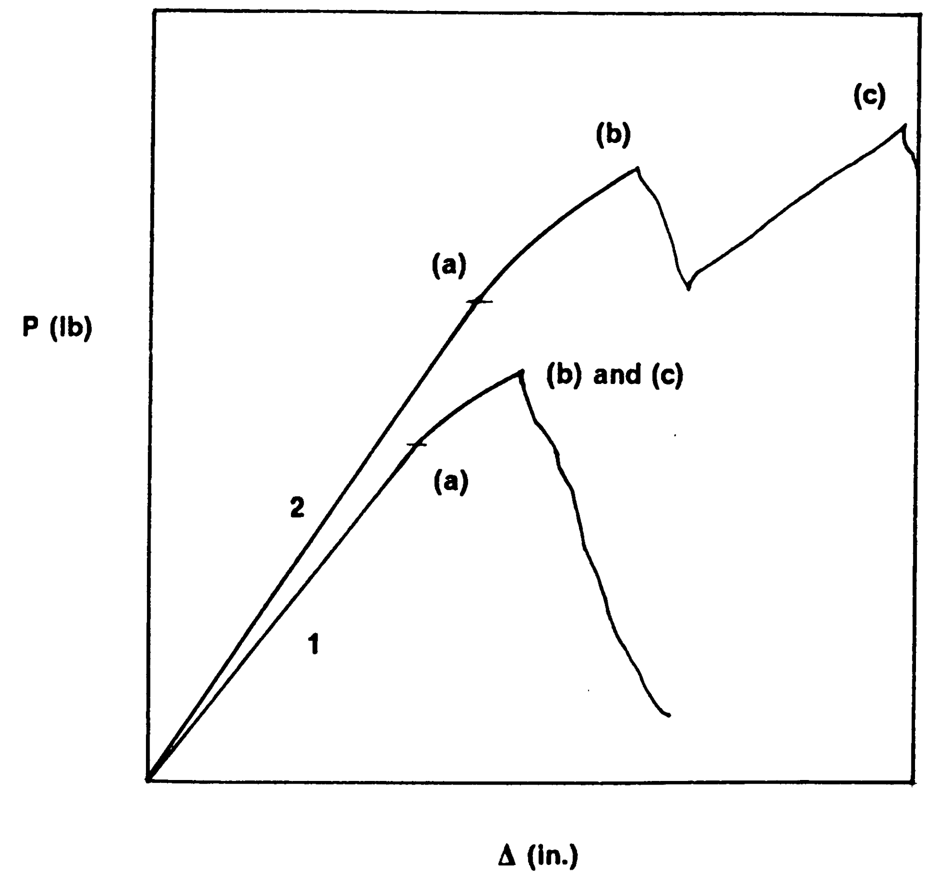

Figure 5.1. **Schematic diagram of typical load-deflection curves from tests of TEN wood beams-- 1 for most cases with h=3.5 in. and 2 for most cases with h=9.0 in.:** (a) proportional limit, (b) major drop, and (c) maximum load

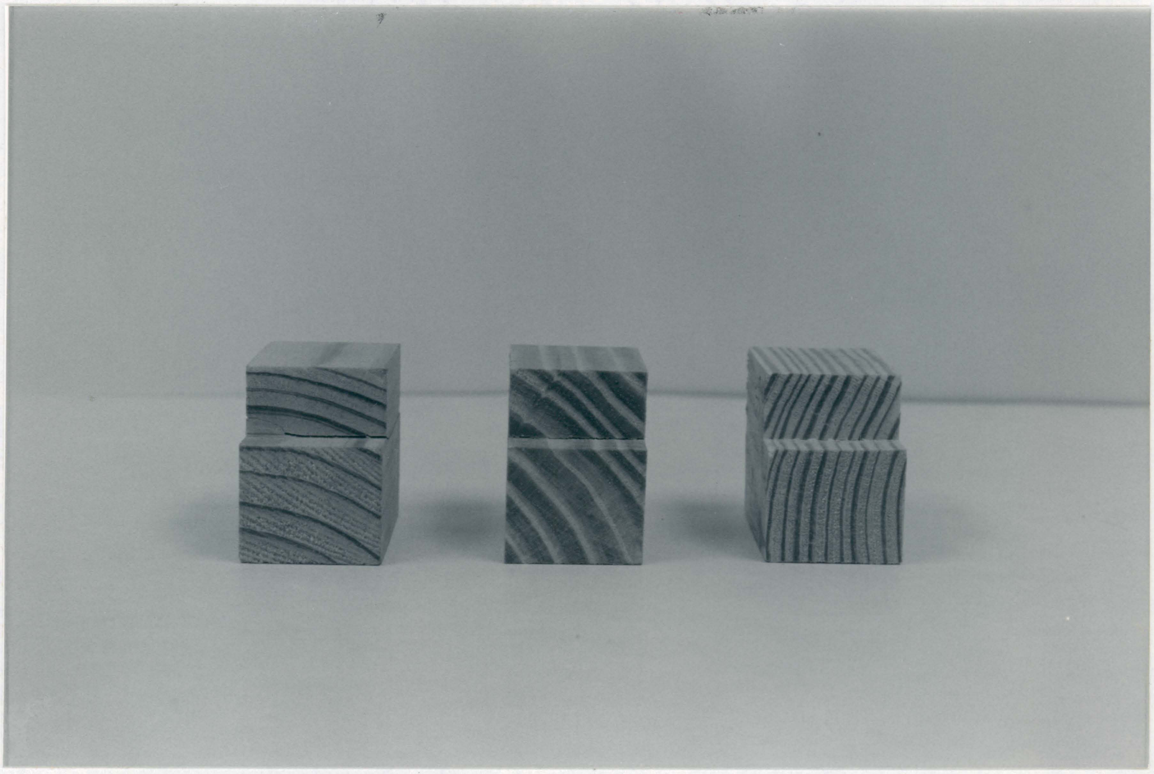

Figure 5.2. SYP shear block specimens with representative cross-sections from full-size TEN beams

5.1.2 Evaluation of geometry effect

The TEN equation based on CFHS theory assumes that geometric and material effects are separable, i.e. K is a purely material property and is geometry-independent.

There are several ways to test this hypothesis. One is the traditional approach of statistical hypothesis testing. In this case,

$$Ho : |\beta_1 - \beta_2| \geq \delta$$

$$H1 : |\beta_1 - \beta_2| < \delta \qquad [5.2]$$

where Ho = null hypothesis

H1 = alternative hypothesis, the condition that a researcher intends to show/prove

β_1, β_2 = true mean K's of notch geometries 1 and 2, respectively

δ = practical value within which notched beam strength differences are deemed acceptable; i.e. a realistic standard deviation for notched beam strength.

The alternative hypothesis, H1 states that the absolute difference between mean K's of different geometries is less than some value δ. There are 16 cells in the randomized complete block design experiment (filleted TEN study), each one representing a unique geometry combination. The statistical test may be administered by comparing all cells or by comparing between cell groups, i.e. collapsing data for M/V and R or MV and H or M/V and ϕ and so on. The null hypothesis, Ho, is rejected (Palettas 1989) when

$$C_1 < \frac{\overline{K}_1 - \overline{K}_2}{Q} < C_2 \qquad [5.3]$$

where $Q = \sqrt{\frac{S_1^2}{n_1} + \frac{S_2^2}{n_2}}$

$C_1 = t_{df,1-\alpha} - \frac{\delta}{Q}$

$C_2 = t_{df,\alpha} + \frac{\delta}{Q}$

$\overline{K}_1, \overline{K}_2$ = sample means

S_1, S_2 = sample standard deviations

n_1, n_2 = sample sizes

$t_{df,\alpha}$ = t-statistic corresponding to df and α

df = degree of freedom, $n_1 + n_2 - 2$

α = probability of Type I error

The power of a statistical procedure is the probability of rejecting Ho when it is false. The power of this procedure was estimated using actual experimental data, setting $\delta = 0.20\overline{K}$ and $\alpha = 5\%$, and assuming an actual difference between $\overline{K}$'s as 0.80δ or $0.16\overline{K}$. It was found that, even if cells are collapsed into two comparing groups to increase the sample sizes, the procedure has very low power because of high variances within groups. The available experimental results were not sufficient to make any conclusive statement because of low sample size and high variance.

Another way of investigating the geometry effect on K is through graphical representation of results; one method is to compare cumulative frequency distributions of cell groups. If there is no effect (i.e. geometry and material effects are separable), then the cumulative frequency distributions for K of different geometry sets should be on top of each other, essentially showing the same curve. In using a graphical method such as this, trends and differences are easily seen through a total data picture.

Figures 5.3, 5.4 and 5.5 show cumulative frequency distributions for K_{MAJ} of YP material classified by M/V and h, M/V and ϕ, and M/V and R, respectively. It is evident from these plots that the effect of geometry variables h, ϕ and R were very small compared to the effect of M/V, except for the noticeable difference between curves for R in M/V = 10.0 in. case in Fig. 5.4. This may be a real R-effect or just a manifestation of the sample's variability. The same general trends on h, ϕ, R and M/V effects were observed with the SYP material. When the K's are grouped only by M/V, as in Figs. 5.6 and 5.7, the differences are seen more clearly. Except for the M/V effect, the CFHS theory is apparently adequate in dealing with the effects of other geometry variables on K.

5.1.3 Investigation of geometry dependence

Let normalized shear, $V^N =$ V/bh . This variable provides a means to compare this work with that of other researchers and to show sensitivity of V^N to geometry changes. The geometry factors identified in the left-most two columns of Table 5.2 were fixed for each row. The remaining geometry factor (with subheadings A, B, C and D) was changed to one value from a base; the corresponding change in V^N is noted as a ratio to the base V^N. For example, as M/V changed from 10.0 in. to 1.0 in. (subheading A), with h fixed at 3.5 in. and ϕ at 0.50, the mean experimental V^N for SYP beams increased by 2.90 times. As R changed from 0.50 in. to 0.25 in. (subheading D), h fixed at 9.0 in. and M/V at 10.0 in., the mean experimental V^N for YP beams increased 1.05 times. It should be noted that these experimental multiplication

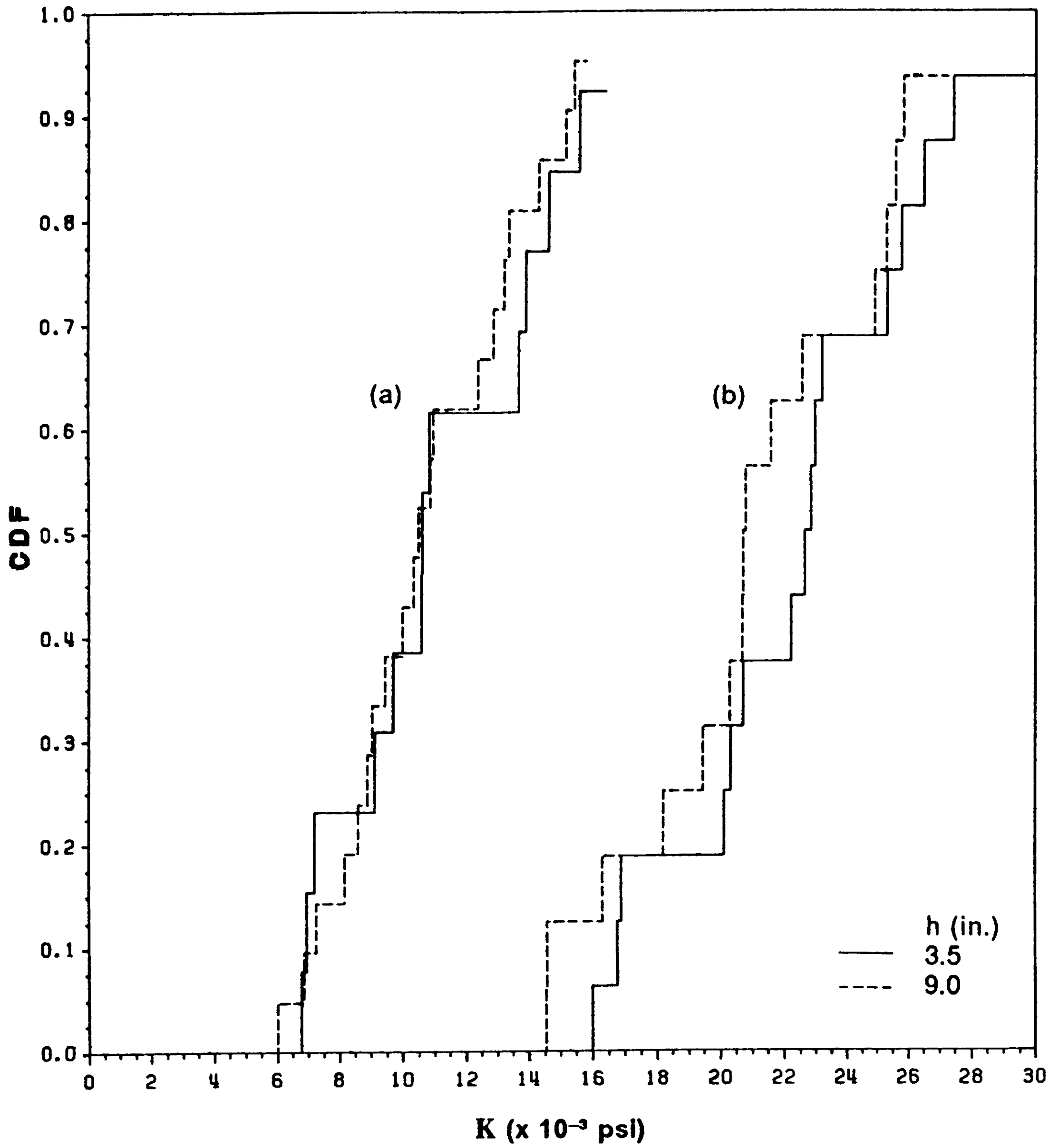

Figure 5.3. Cumulative frequency distributions of K_{MAJ} for YP, classified by M/V and beam height,h: (a) M/V = 1.0 in., (b) M/V = 10.0 in.

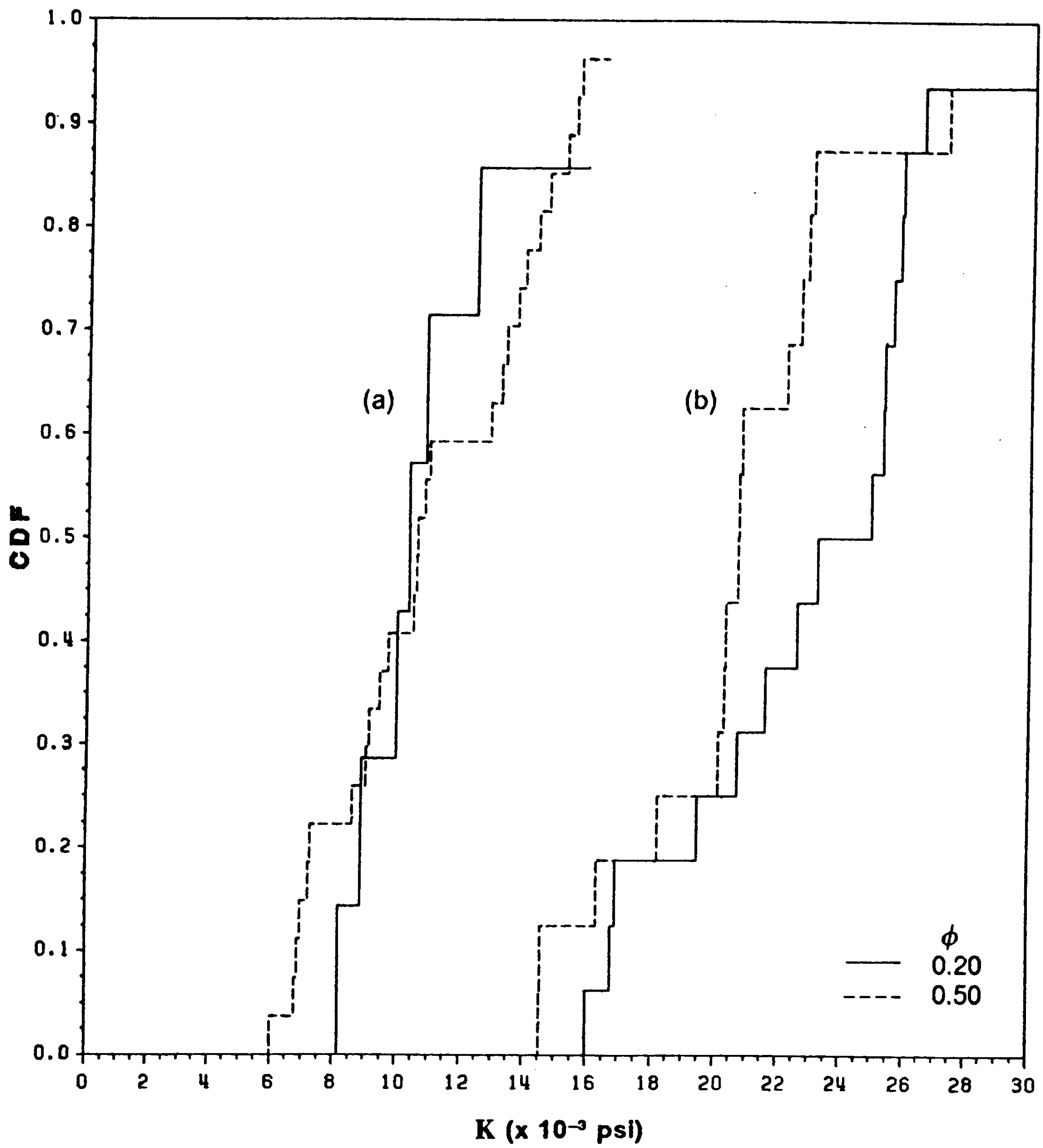

Figure 5.4. Cumulative frequency distributions of K_{MAJ} for YP, classified by M/V and fractional notch depth, ϕ: (a) M/V = 1.0 in., (b) M/V = 10.0 in.

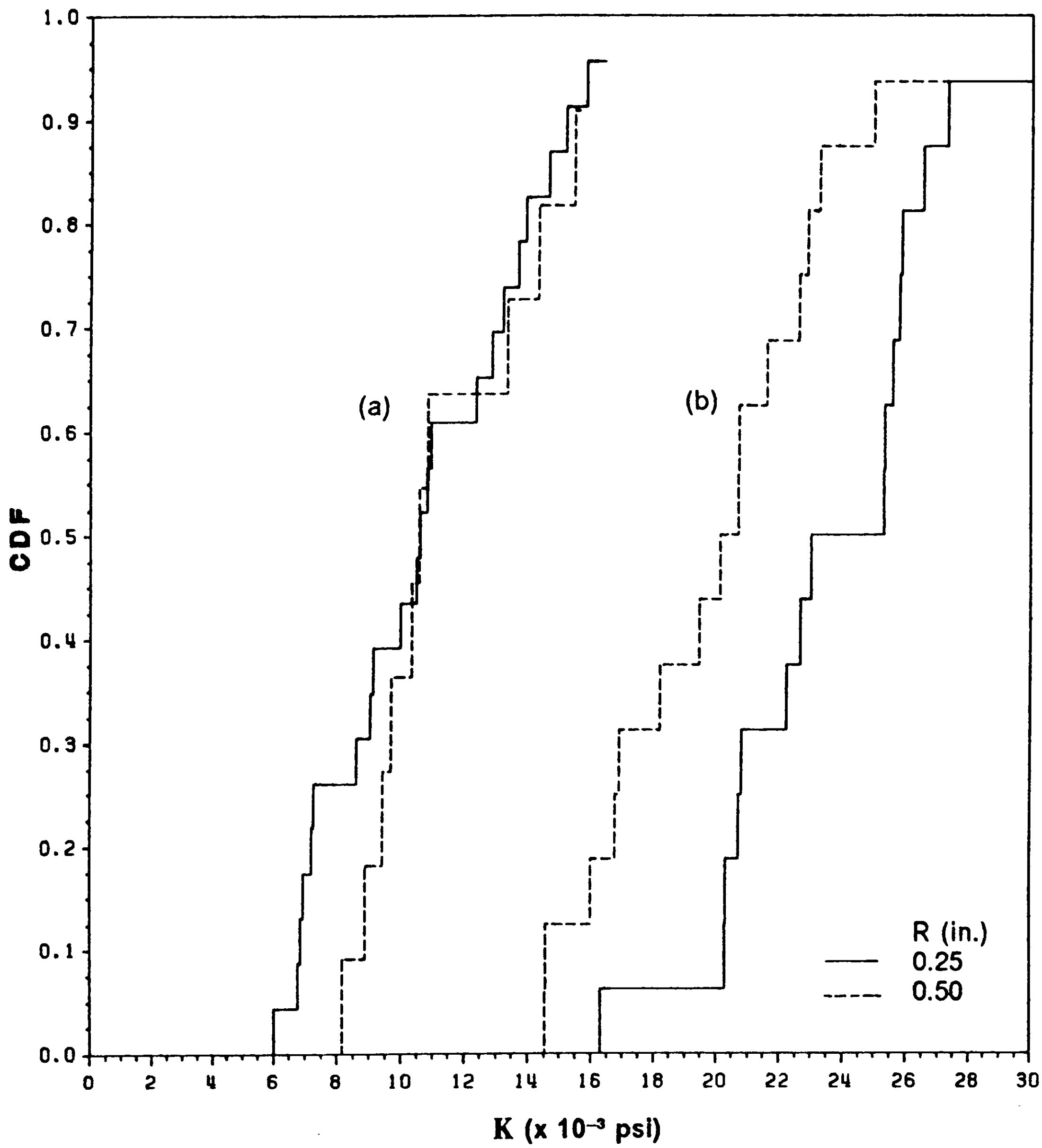

Figure 5.5. Cumulative frequency distributions of K_{MAJ} for YP, classified by M/V and radius, R: (a) M/V = 1.0 in., (b) M/V = 10.0 in.

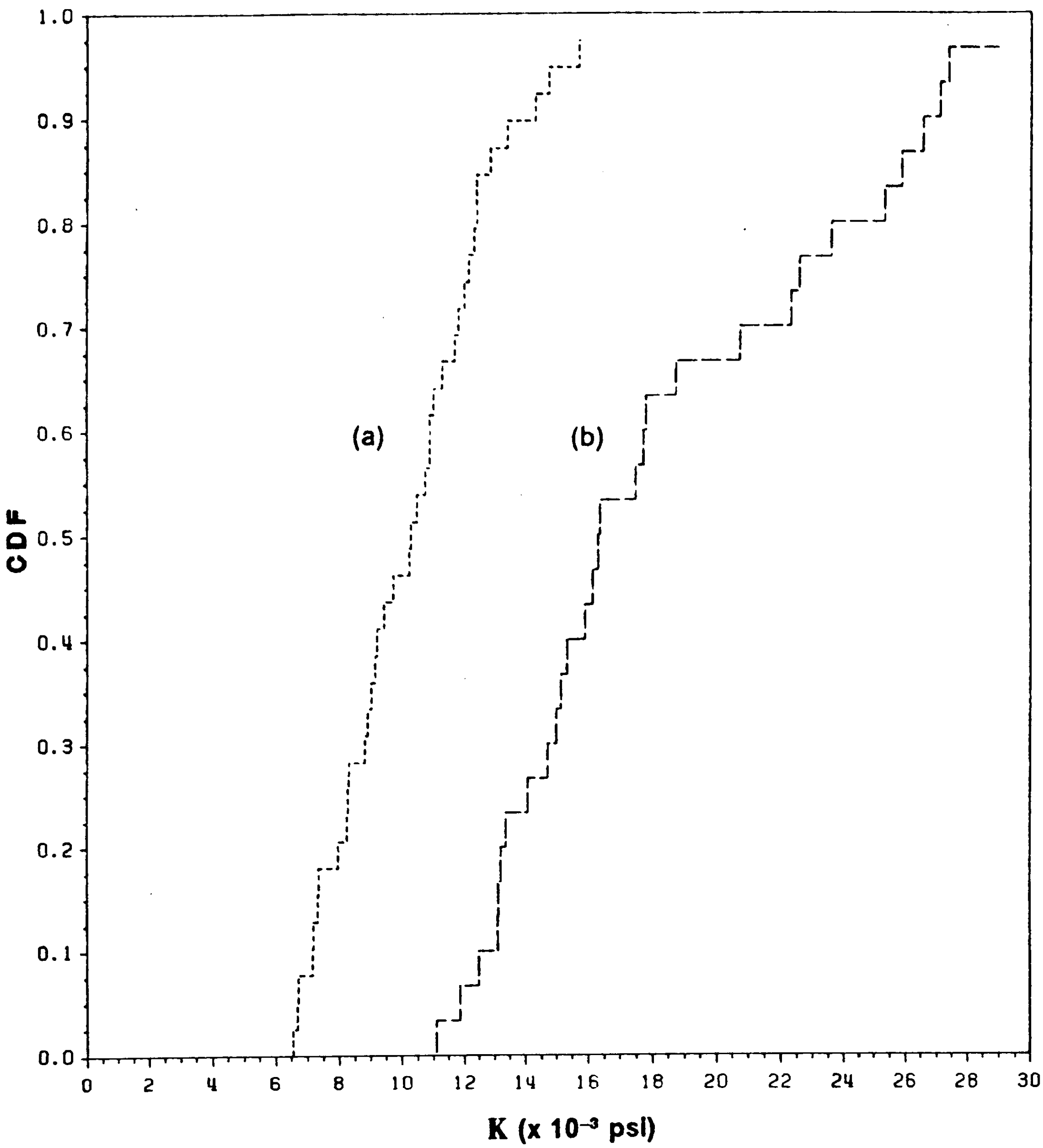

Figure 5.6. Cumulative frequency distributions of K_{MAJ} for SYP, classified by M/V: (a) M/V = 1.0 in., (b) M/V = 10.0 in.

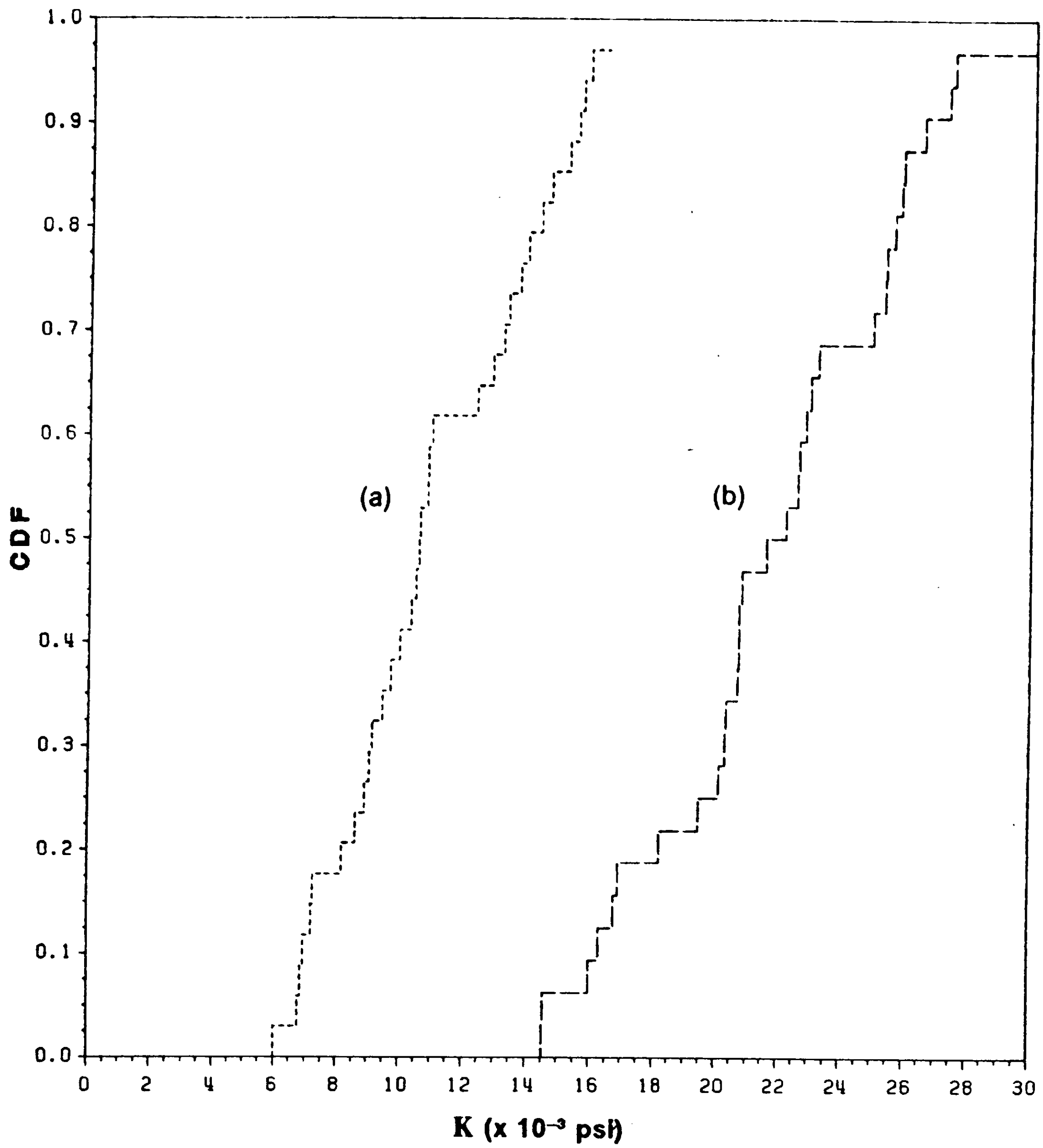

Figure 5.7. Cumulative frequency distributions of K_{MAJ} for YP, classified by M/V: (a) M/V = 1.0 in., (b) M/V = 10.0 in.

factors (or sample mean V^N ratios) are just estimates of the true (or population) mean V^N ratios of the material. Accuracy of the estimates is dependent on sample sizes and variance. These sample mean ratios, however, provide a basis for comparison with those predicted by theoretical models.

In a similar manner, the theoretical sensitivity of V^N to geometry changes was calculated from several models. Using the CFHS theory, K and κ were fixed for both TEN and Zalph (1989) equations and V^N's calculated for the selected geometry changes. This was also done with LEFM-based models, Gustafsson (1988) and Australian code (1988) equations.

Table 5.2 shows that for a change in M/V (subheading A), ratios from theoretical models varied substantially from the experimental ratios, with the exception of those from the Australian equation. For other geometry changes (subheading B for h, subheading C for ϕ, and subheading D for R), the ratios from most theoretical models were reasonably close to those from the experimental results. The TEN equation, in particular, gave ratios similar to those from experiment, thus, supporting the observations made on plots by cumulative frequency distribution in Figs. 5.3 to 5.5 regarding the TEN equation's treatment of the effects of ϕ, h and R.

Consistent differences between expectation and reality were associated with the variable M/V. It is interesting to note that the increase in V^N resulting from a change of M/V from 10.0 in. (away from the support) to 1.0 in. (very close to the support) was overestimated by both CFHS-based models and the LEFM model based on strain energy release rate criterion (i.e. Gustafsson equation). In other words, the actual change in V^N of a TEN wood beam when the notch is varied from a location far from the support to one very close to the support is considerably less than what most

Table 5.2. **Sensitivity of normalized shear capacity to single geometry changes (at MAJ)**

Fixed Geometry		V^N multiplication factor (at MAJ) as one geometry variable is changed ...					
		Experiment		CFHS Theory		LEFM Theory[1]	
		SYP	YP	TEN	Zalph	Gus	Aus
h (in.)	**ϕ**	**(A) from M/V=10.0 in. to M/V=1.0 in.**					
3.5	0.20	-	-	4.54	5.41	3.70	2.13
	0.50	2.90	2.67	5.00	6.06	4.35	2.13
9.0	0.20	1.23	1.06	2.25	2.06	2.27	1.47
	0.50	1.61	1.57	2.70	2.25	2.63	1.47
M/V (in.)		**(B) from h=3.5 in. to h=9.0 in.**					
1.0		0.64	0.81	0.73	0.49	0.78	0.71
10.0		1.28	1.37	1.41	1.30	1.27	1.02
h (in.)	**M/V (in.)**	**(C) from ϕ=0.20 to ϕ=0.50**					
3.5	1.00	-	-	0.52	0.48	0.45	0.62
	10.00	0.42	0.46	0.44	0.44	0.39	0.62
9.0	1.00	0.46	0.65	0.61	0.53	0.48	0.62
	10.00	0.36	0.41	0.50	0.48	0.41	0.62
h (in.)	**M/V (in.)**	**(D) from R=0.50 in. to R=0.25 in.**					
3.5	1.00	0.98	1.44	1.34	1.36	-	-
	10.00	0.88	1.14	1.35	1.30	-	-
9.0	1.00	1.14	1.34	1.30	1.40	-	-
	10.00	1.26	1.05	1.22	1.26	-	-

[1] Gus - Gustafsson (1988) ; Aus - Australian Standard (1988)

theoretical equations would predict. The Australian equation, based on LEFM stress intensity factor criterion, seemed to have accounted for this M/V effect fairly well.

For notches very close to the support, the stress field due to combined shear and bending interacts with the stress field due to compression over the support. Apparently, theory based on transverse orthotropic linear elastic assumptions does not accurately model this situation. When these complex stress interactions occur very near the support, the deviation between assumed simplified boundary conditions and the actual support condition may further compound modeling errors. Other than these thoughts, the systematic difference between experimental and theoretical results for the case of TEN beams with M/V = 1.0 in. (when the results for the M/V = 10.0 in. case agree) is baffling.

5.1.4 Adjustment of prediction equation

The prediction equation in its original form seems to be valid at this point for notch roots located where the moment to shear ratio, M/V, is greater than or equal to 10.0 in.. For the case of TEN at the support (modeled here as having M/V = 1.0 in.), K's are distributed as shown in Figs. 5.3 to 5.7. Similar distributions for M/V = 10.0 in. are found to the right of those for M/V = 1.0 in.. One way to use the prediction equation for notches at the support is to apply an adjustment factor which, in effect, shifts the strength distribution. This would keep prediction simplicity and the need for only one material strength parameter, K, for TEN wood beams.

Figure 5.8 graphically shows how two separate strength distributions are combined. Probability density functions PDF1 and PDF2 are shown for the two cumulative distribution functions CDF1 and CDF2, respectively. The means are separated by a distance K_A. For consistency with Zalph (1989), whose κ is equivalent to the TEN strength data at M/V = 10.0 in. (i.e. $\kappa \simeq K_2$), any adjustment should be applied to the strength data at M/V = 1.0 in. (K_1). To shift the entire distribution of CDF1 (or PDF1) without increasing the variance, K_A is simply added to all values in this distribution. Thus, adjusted $K = K_2 = K_1 + K_A$. This can be applied by shifting at the mean K or at the lower 5% exclusion limit (L5EL) of K.

From unadjusted experimental results for SYP and YP materials (CDF's are shown in Figs. 5.5 and 5.6), K_A at PL was computed from mean experimental K's to be 8011 and 7345 psi, respectively. A fixed value of 7700 psi was used to adjust all K_{PL}'s for M/V = 1.0 in. case. Similarly, K_A at MAJ was computed and found to be 7974 and 10795 psi for SYP and YP, respectively. A fixed value of 9400 psi was added to all K_{MAJ}'s for M/V = 1.0 in. case. The adjusted set of strength distribution for YP at MAJ is shown in Fig. 5.9 with a fitted 3-parameter Weibull distribution. The probability (p-value) that the observed Chi-square test statistic would result if the distribution were not, in fact, a 3-parameter Weibull was 0.16. The p-value arising from fitting a 3-parameter lognormal distribution was 0.55. With SYP materials, however, p-values arising from Chi-square tests were greater than 0.85 for both distributions. The reason for the seemingly poor fits for either Weibull or lognormal distribution is the slightly bimodal nature of the adjusted K_{MAJ} which shows in Fig. 5.9. This is essentially the result of averaging the adjustment factor K_A for the two different species and using this average value to adjust both strength sets. This is a possible indication of one of two things: (1) K_A is different for hardwood and softwood species groups, or (2) K_A is different for every species. This cannot be experimentally tested, however, from

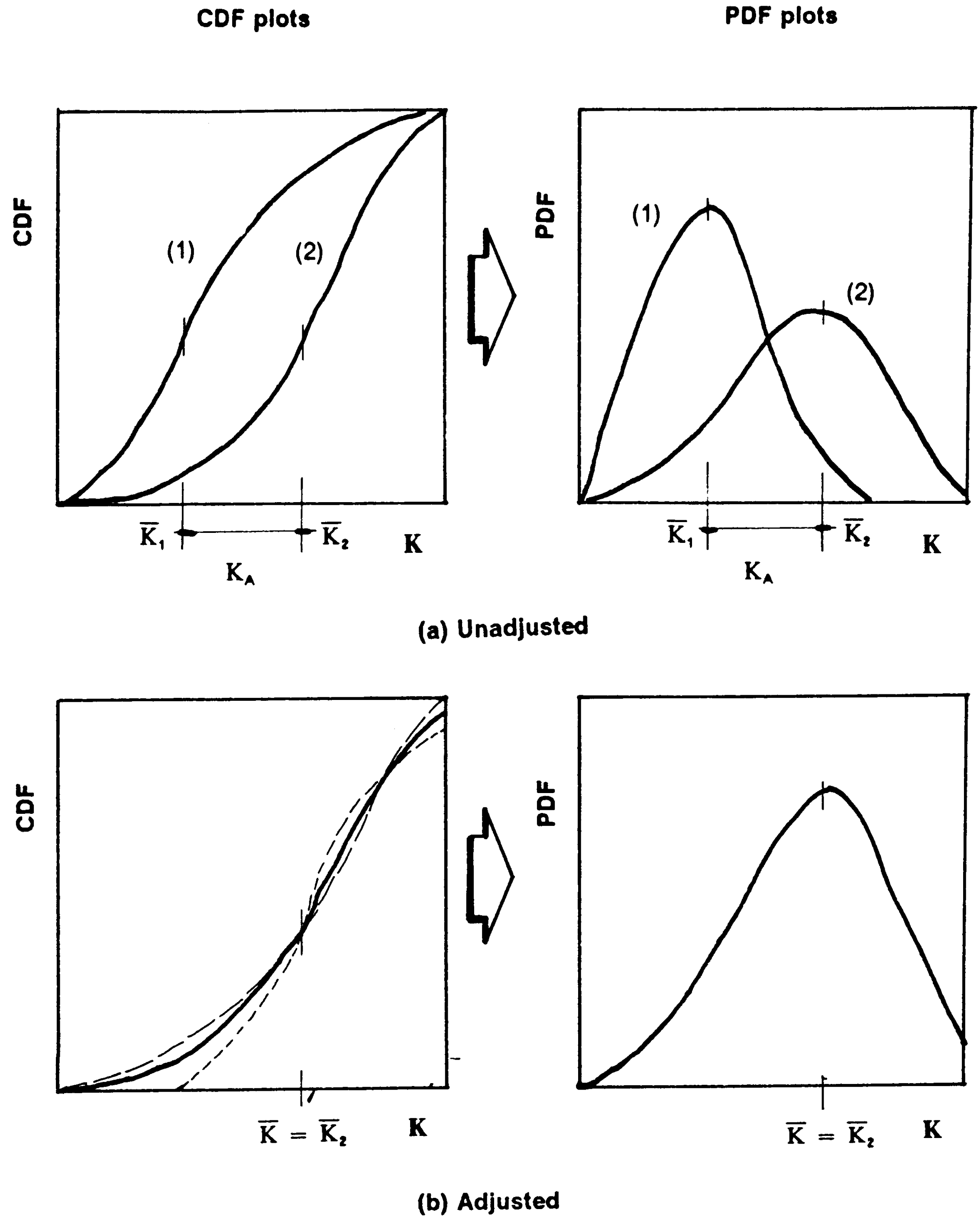

Figure 5.8. Adjustment process to shift distribution

this work. Pending further verification of K_A for other species, the fixed value of 9400 psi is retained for adjusting K_{MAJ}'s of TEN beams with M/V = 1.0 in..

5.2 Determination of Effective Radius

This sub-study was limited to the case where M/V = 1.0 in. and $\phi = 0.50$. Most beams (whether sharp-cornered, R = 0, or filleted, R = 0.25 in., notches) failed in the manner represented by P-Δ curve 1 shown in Fig. 5.1, i.e. major load drop coinciding with the maximum load. Normalized shear (V^N) values calculated from experimental results for sharp-cornered and filleted notches were compared via a one-way t-test with Ho: $\overline{V}^N_{(R=0.25)} = \overline{V}^N_{(R=0)}$. The results are presented in Table 5.3. With $\alpha = 5\%$, the null hypothesis is rejected for most cases. One exception is for SYP with h = 9.0 in.. This rejection is due to the high variance in V^N, despite seemingly dissimilar mean values. This means that a bigger sample size is necessary for this particular case to increase the chance of reaching a correct decision.

An effective radius to model sharp-cornered TEN cases was computed using the adjusted TEN prediction equation. The equation was simplified as follows

$$\overline{V}^N = \frac{\overline{V}}{bh} = \frac{\frac{\overline{K}_1}{6}}{\left[F_1 \left(\frac{M}{V} \right) \frac{1}{h} + \mu F_2 \right]} \qquad [5.4]$$

where $\overline{K}_1 = \overline{K} - K_A$; all other terms are defined in equation [5.1].

Let

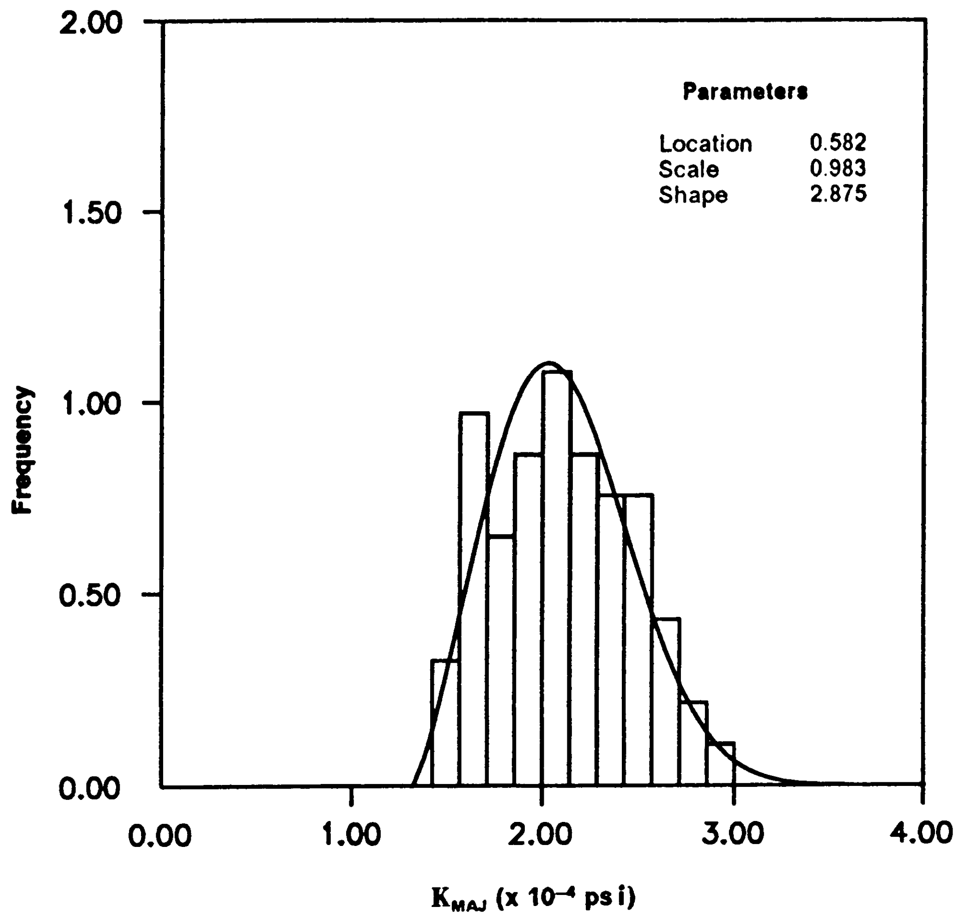

Figure 5.9. Frequency distribution of K_{MAJ} for YP fitted with a 3-parameter Weibull distribution

Table 5.3. Results of one-way t-test for normalized shear, R=0 vs R=0.25 in., M/V=1.0 in. and ϕ=0.50

Species	h (in.)	Level	R (in.)	n	V^N Mean (psi)	V^N Std. Dev.	t-obs	p[1]
SYP	3.50	PL	0.00	18	110	26	2.250	0.0164
			0.25	11	129	16		
		MAJ	0.00	18	183	41	5.415	0.0000
			0.25	12	259	32		
	9.00	PL	0.00	15	91	43	1.195	0.1216
			0.25	12	108	25		
		MAJ	0.00	15	132	50	1.282	0.1058
			0.25	12	153	30		
YP	3.50	PL	0.00	16	123	24	2.184	0.0195
			0.25	10	141	11		
		MAJ	0.00	16	163	45	2.876	0.0042
			0.25	10	230	74		
	9.00	PL	0.00	9	105	23	2.447	0.0128
			0.25	10	147	46		
		MAJ	0.00	9	132	30	1.889	0.0381
			0.25	10	169	51		

[1] p - probability that the observed t-test statistic would result if the means were not, in fact, the same; (Ho : $\overline{V}^N_{(R=0.25)} = \overline{V}^N_{(R=0)}$)

$$g = \frac{1}{\left[F_1 \left(\frac{M}{V} \right) \frac{1}{h} + \mu F_2 \right]} \qquad [5.5]$$

and substitute to equation [5.4],

$$\overline{V}^N = \frac{\overline{K}_1}{6} \; g \qquad [5.6]$$

The normalized shear ratios of filleted and sharp-cornered notches were computed as

$$\frac{\overline{V}^N_{(R=0)}}{\overline{V}^N_{(R=0.25)}} = \frac{\frac{\overline{K}_1}{6} \; g_{Re}}{\frac{\overline{K}_1}{6} \; g_{(R=0.25)}} \qquad [5.7]$$

Rearranging,

$$g_{Re} = \left[\frac{\overline{V}^N_{(R=0)}}{\overline{V}^N_{(R=0.25)}} \right] g_{(R=0.25)} \qquad [5.8]$$

Everything on the right hand side of equation [5.8] is known : the bracketed term is a ratio of experimental results and $g_{(R=0.25)}$ is computed using equation [5.5], with nominal values of h, ϕ and D with R = 0.25 in.. The computed value of g_{Re} was equated with equation [5.5] (value for μ and forms of F_1 and F_2 were substituted)

$$\frac{1}{\dfrac{(M/V)\,(1/h)}{0.159 - 0.213\phi + 0.187(\frac{R}{D})} + 1.64\,\phi^{0.712}\,R^{-0.418}\,h^{(0.847-0.316\phi)}} = g_{Re}\;. \qquad [5.9]$$

All variables are known except R. The calculated radius becomes R_e which is the theoretical effective ratio to model sharp-cornered notches. Results of iterative calculation of equation [5.9] are summarized in Table 5.4. Minimum calculated R_e was 0.091 in. for both species. In all cases, $0.091 \leq R_e \leq 0.173$. It may be sufficient to use $R_e = 0.080$ in. to model sharp-cornered notches for all species because R_e does not indicate any species dependence and this proposed value is thought to provide enough margin for possible R_e variation caused by mean V^N variation.

Zalph (1989) conducted a preliminary study determining R_e for tension interior notches. His limited results suggest a value of 0.175 in. for dry SYP and 0.004 in. for green YP beams with $\phi = 0.51$, $M/V = 10.0$ in. and $h = 3.5$ in.. R_e for dry SYP compares closely with present results (0.16 in. at PL, and 0.09 in. at MAJ) but that for green YP was anomalously low. He qualified that these results are "equivocal due to small sample sizes (6 for SYP and 4 for YP) and high variability".

Zalph (1989) hinted at a possible linear dependence of R_e on h when he investigated the condition of equivalence of his model with that of Gustafsson (1988). He was not able to verify this experimentally because his tests were limited to a single level of h. Results of the present sub-study (Table 5.4) do not indicate any organized dependence of R_e on h.

5.3 Comparisons With Other Models

The normalized shear, V^N, predicted by the TEN equation was compared with that predicted by other models. These predictions are overlaid with experimental results. V^N was calculated using a general equation

Table 5.4. Effective radius, R_e, to model sharp-cornered end notches, derived for M/V = 1.0 in. and $\phi = 0.50$ by equation [5.9]

Species	h (in.)	Level	R = 0		R = 0.25 in.		R_e (in.)
			$\bar{V}^N$ (psi)	g	$\bar{V}^N$ (psi)	g	
SYP	3.50	PL	110	0.1084	129	0.1275	0.159
		MAJ	183	0.0903	259	0.1275	0.091
	9.00	PL	91	0.0855	108	0.1012	0.159
		MAJ	132	0.0872	153	0.1012	0.168
YP	3.50	PL	123	0.1115	141	0.1275	0.173
		MAJ	163	0.0904	230	0.1275	0.091
	9.00	PL	105	0.0723	147	0.1012	0.101
		MAJ	132	0.0790	169	0.1012	0.128

$$V^N = \frac{V}{bh} = \frac{\mathbf{MATL}}{\left[\mathbf{A} \left(\frac{M}{V} \right) \frac{1}{h} + \mathbf{B} \right]} \qquad [5.10]$$

where **MATL, A** and **B** are defined as shown in Table 5.5. In effect all of the different models have been cast into a single form to facilitate comparison. Note that they degenerate to their original form described in Chapter 2.

5.3.1. *Filleted Notches*

Equations by Gerhardt (1984a) and Zalph (1989) have been proposed for predicting the strength of filleted notches. Both are based on CFHS theory and derived for the case of tension interior notches. Zalph (l989) showed that his model is consistent with Gerhardt's but also deals with additional variables R and h. He also confirmed the applicability of his equation on eight materials, in contrast to one material for Gerhardt. Consequently, Zalph's equation was chosen for comparison with the TEN equation. The intended applications for the Zalph (1989) and the TEN equation are different but both share the same underlying assumptions in derivation. The formulation was based on the linear relationship between M/V (or V/M for Zalph) and normalized hoop stress ShCF (or MCF for Zalph). Another is the separation of the material effects, μ_1 and μ_2 , from the geometric functions F_1 and F_2, respectively. Zalph (1989) formulated κ as $\frac{\sigma_{h,max}}{\mu_1}$, which is also the material strength in the present work (i.e. $K = \kappa$).

The filleted notch equation can be generally stated as

Table 5.5. Comparative forms of the terms MATL, A and B in equation [5.10]

Basis	Source	MATL	A	B	Note[a]
•Notch Factor	NDS (1986)	$\frac{2}{3}\, F_v$	0	$\frac{1}{(1-\phi)^2}$	SN
•LEFM Theory	Australian Standard (1988)	$(g_{40}\, F_{sj})^{b}$	$\frac{1}{(1-\phi)^2}$	$\frac{1}{(1-\phi)}$	SN
	Gustafsson (1988)	$\sqrt{\frac{G_c\, E_x}{6h}}$	$\sqrt{\frac{1}{(1-\phi)^3}-1}$	$\sqrt{\frac{\phi}{10(1-\phi)}\ \frac{E_x}{G_{xy}}}^{\,c}$	SN
•CFHS Theory	Gerhardt (1984a)	$\frac{K_{crit}}{6}$	$\frac{1}{(1-1.26\phi)}$	$1.13\,\phi + 0.30$	FN
	Zalph (1989)	$\frac{\kappa}{6}$	$\frac{1}{0.165-0.217\phi+0.145(\frac{R}{D})}$	$1.246\,\phi^{0.664}(\frac{R}{h})^{-0.539}(\frac{h}{3.5\text{in.}})^{0.164}$	FN
	TEN (present work)	$\frac{(K-K_A)}{6}$	$\frac{1}{0.159-0.213\phi+0.187(\frac{R}{D})}$	$1.64\,\phi^{0.712}\, R^{-0.418}\, h^{(0.847-0.316\phi)}$	FN
			$\frac{1}{0.159-0.213\phi+\frac{0.015}{D}}$	$4.71\,\phi^{0.712}\, h^{(0.847-0.316\phi)}$	SN

Note: [a]SN - for sharp-cornered notches ; FN - for filleted notches

[b]See Table 2.1 for g_{40} ; $F_{sj} = F_v$

[c]Assuming $\frac{E_x}{G_{xy}} = 17$, this expression becomes $\sqrt{\frac{1.7\phi}{(1-\phi)}}$

$$K_{MAJ} = \left(\frac{6M}{bh^2}\right) F_1 + \left(\frac{6V}{bh}\right) \mu F_2 + K_A \qquad [5.11]$$

where K_A = 0 for all cases in Zalph equation

= 0 for notches with $M/V \geq 10.0$ in. in TEN equation

= 9400 psi for notches with $M/V < 10.0$ in. in TEN equation

Both the TEN and the Zalph equations essentially predict the same notched beam material strength parameter. A basic difference is that Zalph derived F_1 and F_2 from theoretical cases where moment always dominated ($M >> V$). In the TEN work, F_1 and F_2 were theoretically derived from notch cases where moment dominated in 66% of the cases and shear dominated in 34%. This explains why the F_1's from both studies are almost the same while the F_2's are slightly different. Another difference is the treatment of μ. Zalph (1989) fixed μ as unity for all materials while a conservative $\mu = 1.12$ was fixed for the TEN. Figure 5.10 shows that the two models predict essentially similar trends for $M/V = 10.0$ in.. (The ordinate scale was maintained the same with that in Fig 5.11 for easy graphical comparison.) Agreement with the plotted SYP experimental quantities is excellent. But the theoretical linear relationship between M/V and normalized hoop stress is at odds with experimental results. Consequently, there are substantial differences betweeen the adjusted TEN equation and Zalph equation for $M/V = 1.0$ in. as seen clearly in Figure 5.11. Plotted SYP experimental quantities were predicted accurately by the adjusted TEN equation. Similar results are found with YP material.

In summary, the Zalph and TEN equations can be used interchangeably for filleted TEN's with M/V ratio of 10.0 in. or greater. The adjusted TEN equation provides ac-

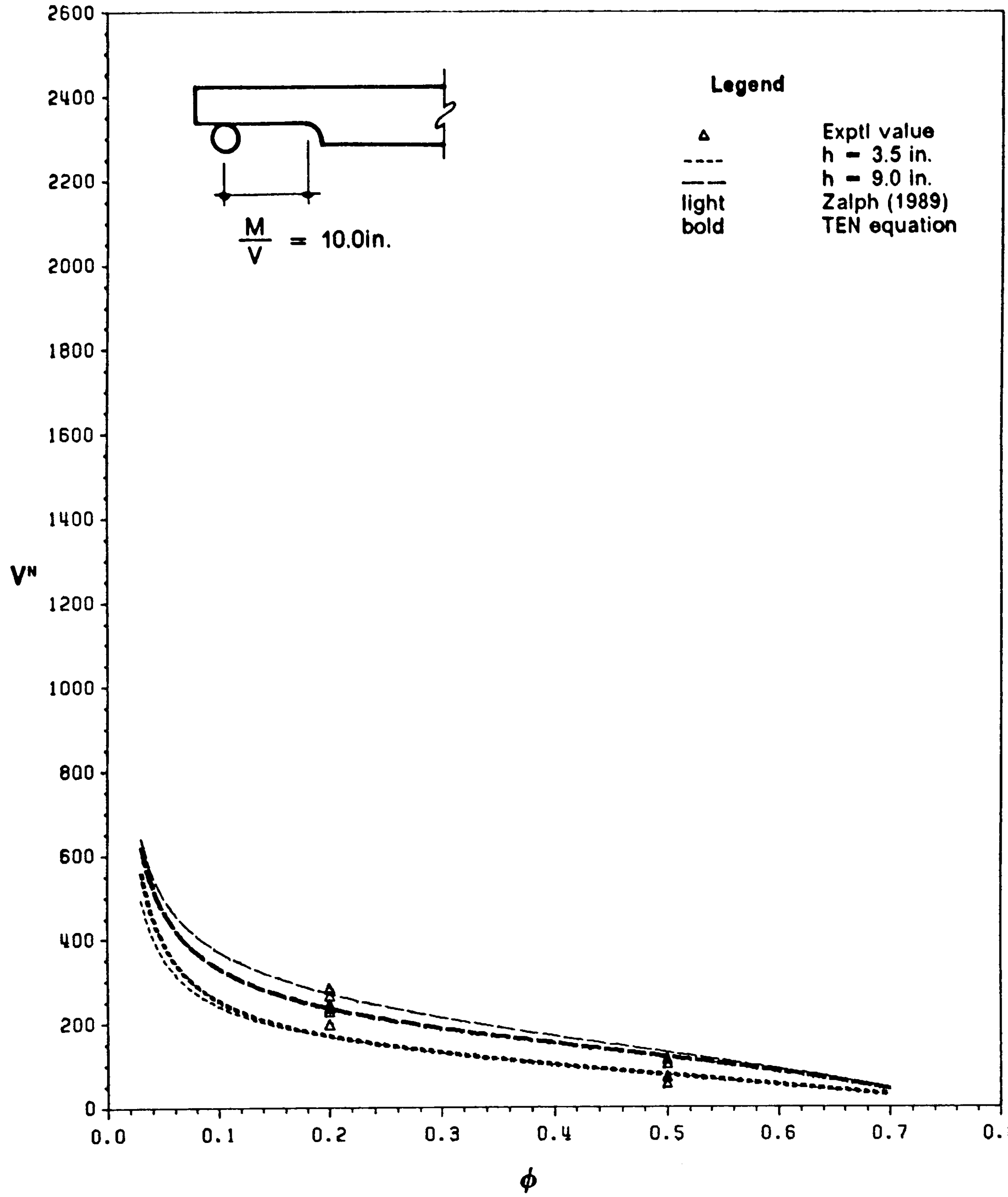

Figure 5.10. **Normalized shear capacity (at MAJ) against fractional notch depth for SYP beam with filleted notch:** $K_{MAJ} = 18300$ psi, $R = 0.25$ in., $M/V = 10.0$ in.
(NOTE : Ordinate scale is the same as that in Fig. 5.11 for easy graphical comparison.)

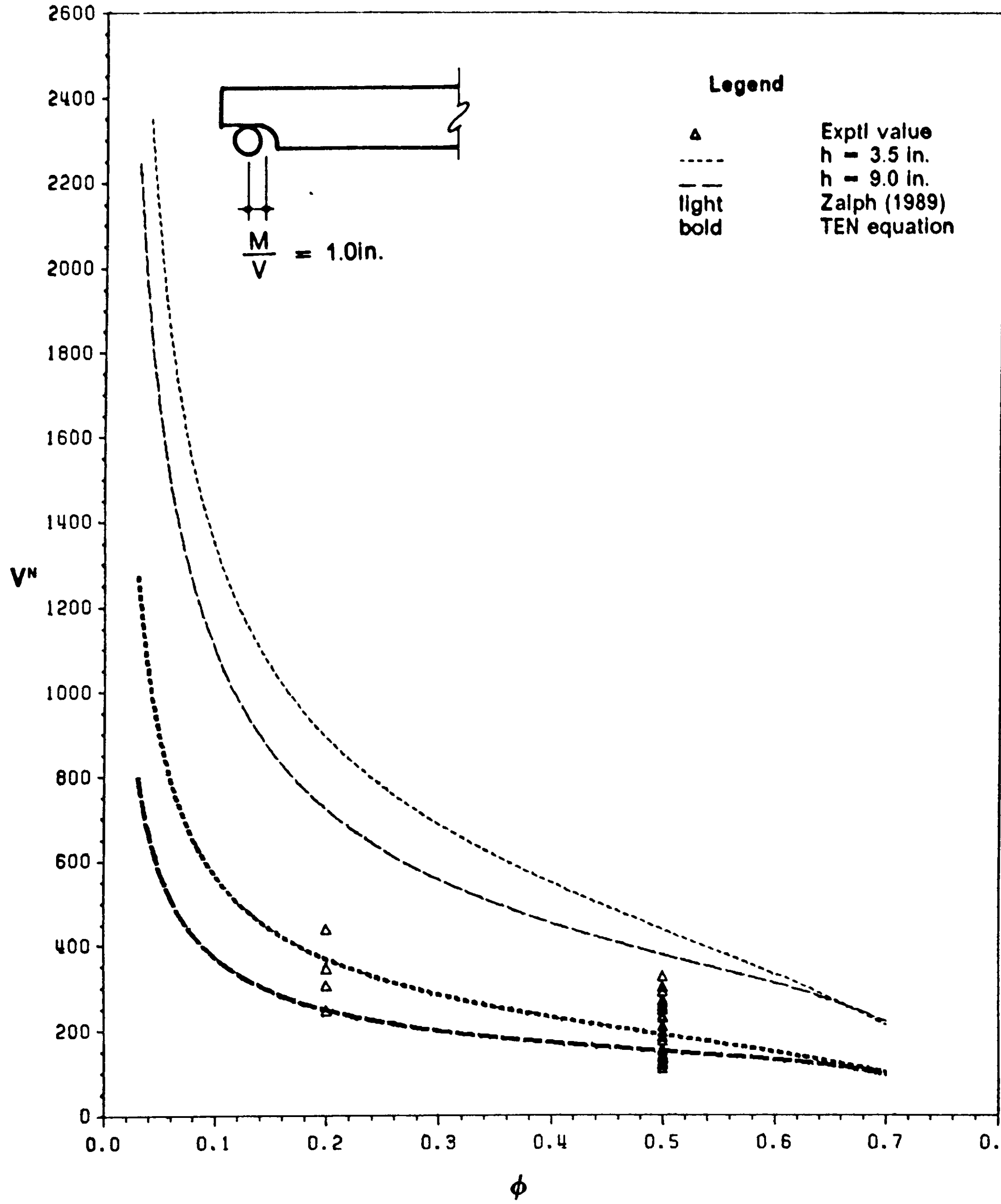

Figure 5.11. **Normalized shear capacity (at MAJ) against fractional notch depth for SYP beam with filleted notch:** $K_{MAJ} = 18300$ psi, $R = 0.25$ in., $M/V = 1.0$ in.

curate prediction for M/V < 10.0 in.. The Zalph equation seriously overestimates the normalized shear (V^N) capacity of these cases.

5.3.2 *Sharp-cornered notches*

Two basic approaches are used in the strength prediction of sharp-cornered notches : (1) notch factor, and (2) LEFM theory. The notch factor approach is the most used by current codes and deals solely with the effect of ϕ. The use of LEFM theory, on the other hand, allows consideration of other variables, such as h and notch location, L_n (L_n = M/V for center-point loaded, simply supported beam). Equation comparisons are shown in Table 5.5.

The Australian equation (SAA 1988) given in section 2.3 was chosen to represent stress intensity factor, K-criterion, approach in LEFM analysis. Gustafsson (1988) used a strain energy release rate, G-criterion, approach based on the same LEFM assumptions.

Figure 5.12 graphically compares the influence of ϕ with the different models for notched beams with h = 9.0 in. and M/V = 1.0 in.. For the TEN equation, effective radius, R_e, was set at 0.08 in.. All experimental values for sharp-cornered notches (R = 0) were for ϕ = 0.50. The experimenal values plotted for ϕ = 0.20 were for R = 0.25 in.. These points for filleted notches were plotted to get a feel of the experimental trend for TEN cases with ϕ < 0.50. Actual V^N values for sharp-cornered notches with ϕ = 0.20 should be slightly less than those plotted for filleted notches in Fig. 5.12. For the NDS and the Australian equations, shear stress Fv for dry SYP was set as 1380 psi (Wood Handbook 1987). The NDS (NFPA 1986) equation is recommended for short deep beams. Figure 5.12 is a plot for TEN beams with span-to-depth (L/h) ratio of 4.67. It is clear from Fig. 5.12 that the NDS, Australian and Gustafsson equations overpredict the normalized shear capacity of TEN's at the support (i.e. M/V = 1.0 in.). Only the adjusted TEN equation provided good prediction as it shows a conservative fit with SYP results. This may be attributed to R_e which was conservatively fixed at 0.08 in.. Similar observations were made for h = 3.50 in. and in all equivalent plots for the YP material.

To investigate what happens at M/V = 10.0 in., theoretical prediction curves were plotted as shown in Fig. 5.13. The NDS equation was unchanged because it does not account for any effect of notch location. Prediction curves for the Australian, Gustafsson and TEN equations are shifted downwards relative to Fig. 5.12. The TEN equation provided the most conservative prediction. Experimental trend is unknown because no tests were made for sharp-cornered notches at M/V = 10.0 in.. Considering the good prediction exhibited by the TEN equation for filleted notches at M/V = 10.0 in. (e.g. Fig. 5.10), however, its reliability for the sharp-cornered case may also be justified.

Note that although the Australian equation seemed to have accounted for the M/V effect as shown in Table 5.2 and discussed in section 5.1.3, Figs. 5.12 and 5.13 show that its V^N prediction is an overestimate of actual value.

5.4 Relationship Between K and Other Material Properties

To relate K with other material properties (SG, block shear strength (S) and perpendicular-to-grain tensile strength (T)), several linear and nonlinear models

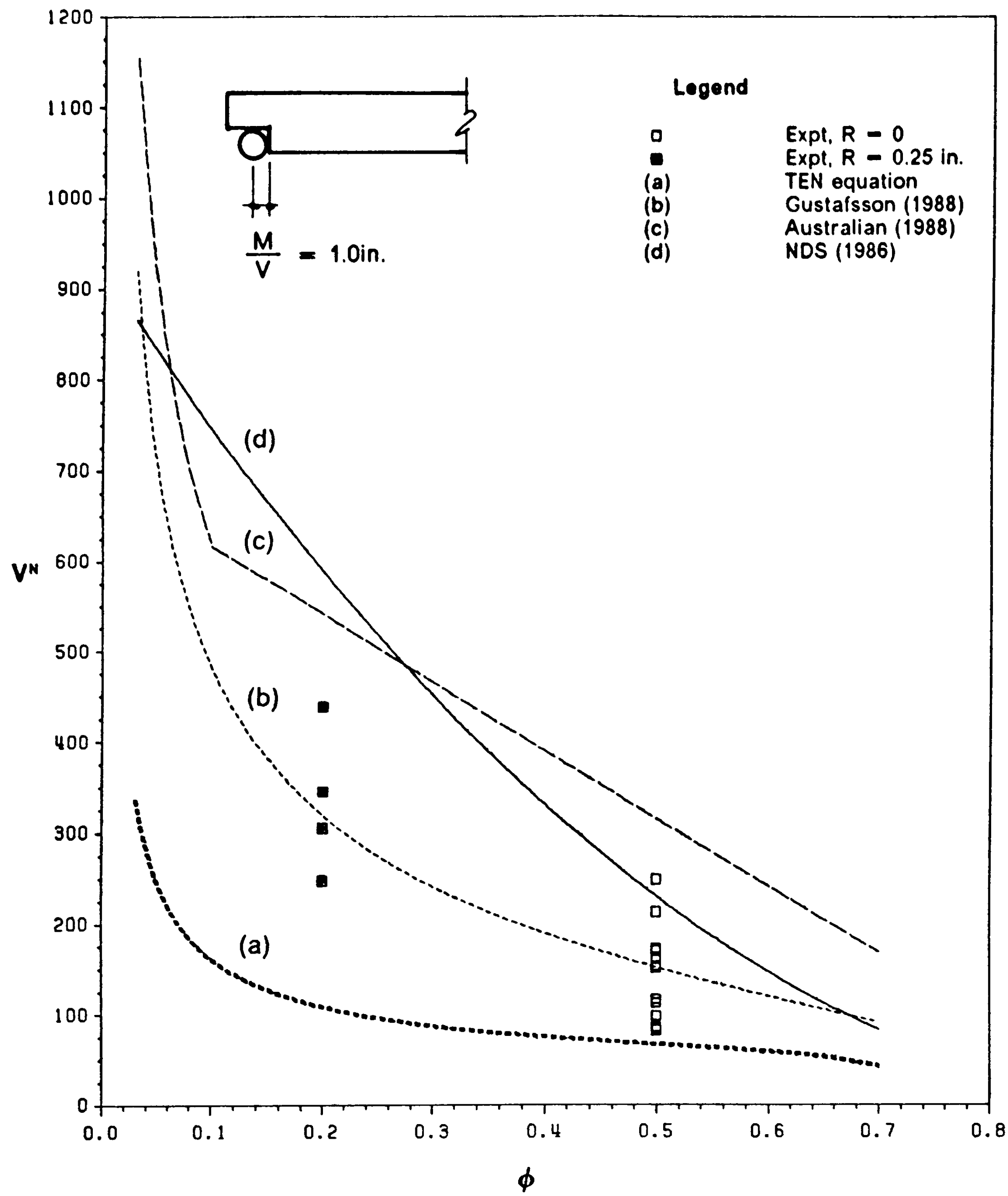

Figure 5.12. **Normalized shear capacity (at MAJ) against fractional notch depth for SYP beam with sharp-cornered notch:** R = 0, M/V = 1.0 in., h = 9.0 in.

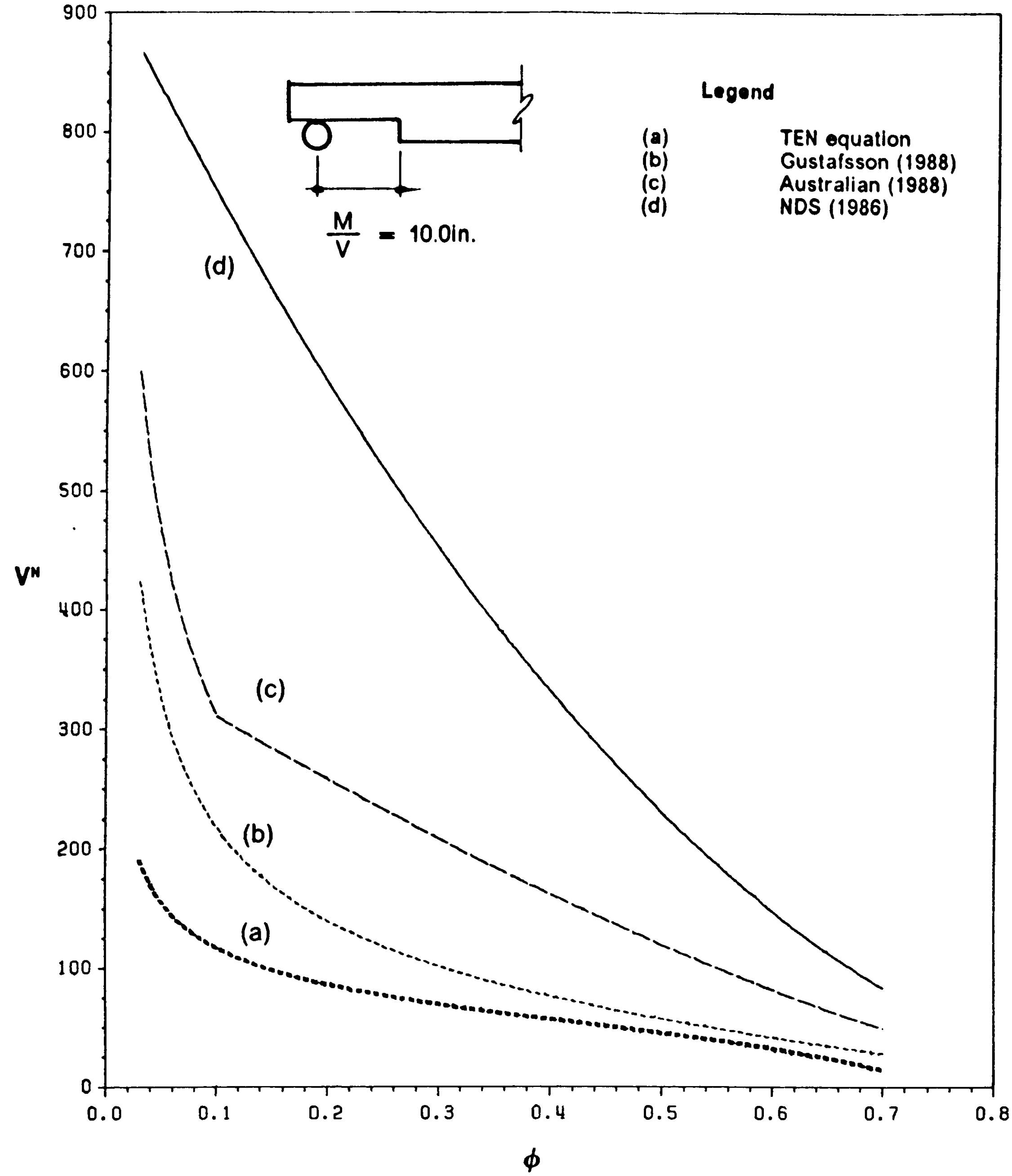

Figure 5.13. Normalized shear capacity (at MAJ) against fractional notch depth for SYP beam with sharp-cornered notch: R = 0, M/V = 10.0 in., h = 9.0 in.

were investigated. The nonlinear models were confined to those that are linearizable by transformation of either response or predictor variables. The models had the form similar to those investigated in the FE study shown in Table 3.4. A full model, containing all three material properties as predictor variables, and its subsets were fitted to a separate data of SYP and YP using individual specimen values. Since the objective is to predict K from readily known material properties, the evaluation of the models followed the procedure described in the derivation of the theoretical closed-form equation (section 3.7). The relative prediction error was computed as KPERR = (actual - predicted) / (actual) x 100%.

Difficulty was encountered in selecting the best prediction equation because none of the equation forms investigated stood out in prediction accuracy. The best model among the selection has the form

$$K_{MAJ} = C_0 \, X_1^{C_1} \, X_2^{C_2} \tag{5.12}$$

where X_1 and X_2 are predictor variables and C_0 , C_1 and C_2 are coefficients given in Table 5.6. The table also gives statistics of KPERR. The mean KPERR in most models is close to zero but the range of maximum overprediction and underprediction percent error is large in the two species, especially in SYP. Addition of either S or T in a model already containing SG did not provide any substantial prediction improvement of K_{MAJ}. The coefficient estimate of additional predictors was non-significant. The simplest form practical for adoption is that containing only one variable. The model involving SG only has a maximum overprediction error of 69% and maximum underprediction error of 33% for SYP, and maximum overprediction of 39% and maximum underprediction of 19% for YP. The strength prediction errors that were not accounted by SG may be attributed to differing ring orientation and grain angle characteristics of the notched beams.

The range of prediction errors for the model involving either S or T only was similar to that for the model with SG only. The wide margin of prediction error for these strength property models can be explained by the nature of standard ASTM clear specimen tests (American Society of Testing and Materials 1988). In block shear test, eccentric loading of the specimen causes failure due to a complex combination of shear and normal stresses and not due to pure shear stress (Bodig and Jayne 1982). In tension perpendicular-to-grain test, the specimen is subjected to a nonuniform stress distribution which is considered to be uniform in strength calculation of T (Bodig and Jayne 1982). Because the calculated experimental S and T values were not the accurate shear strength and tensile strength perpendicular-to-grain of the material, respectively, the prediction accuracy for K using either one of the strength variables as predictor was not as expected.

The form of the prediction equation for K involving SG only is consistent with that used for predicting the other strength properties of wood (Armstrong et al. 1984) and is, therefore, the one proposed in predicting K. This allows a simple and practical way of designing wood beams with TEN.

5.5 Influence of TEN on Beam Stiffness

From the flatwise stiffness (P/Δ) measurements of unnotched boards described in section 4.6, the true modulus of elasticity, $E_{t,flat}$, for each board was calculated as

Table 5.6. **Coefficient estimates and relative prediction error of equation [5.12] using different predictor variables**

Indep. Var. (X_i)	Species	n	Coefficient Estimates			Relative Prediction Error, KPERR (%)			
			C_0	C_1	C_2	Mean[1]	Std. Dev.	Max. Overprediction	Max. Underprediction
SG	SYP	52	34822	1.04	-	-1.99	21.21	69.18	32.96
	YP	53	43827	1.01	-	-0.92	14.30	38.84	19.35
S	SYP	47	98	0.69	-	-2.15	21.74	61.49	28.27
	YP	45	168	0.66	-	-0.90	14.04	45.80	23.79
T	SYP	47	4684	0.23	-	-2.52	23.63	63.19	34.60
	YP	41	6130	0.21	-	-1.24	16.60	52.01	24.01
SG, S	SYP	47	11114	1.05	0.15	-1.74	20.12	70.94	24.24
	YP	45	1109	0.46	0.44	-0.86	13.76	40.14	21.56
SG, T	SYP	47	31634	1.16	0.03	-1.76	20.28	70.98	25.00
	YP	41	22622	1.08	0.12	-0.82	13.47	32.71	20.68

Note: [1] Negative sign means on the side of overprediction

$$E_{t,flat} = \left(\frac{P}{\Delta}\right)\left(\frac{L^3}{48\,(I)}\right)\left[\,1 + 1.2\left(\frac{h}{L}\right)^2 \frac{E}{G}\,\right] \qquad [5.13]$$

where I = moment of inertia, $\frac{bh^3}{12}$

$\frac{E}{G}$ = assumed orthotropic ratio

= 13 for SYP (from Bodig and Goodman 1973)

= 14 for YP (from Wood Handbook 1987).

The true modulus of elasticity for edgewise test is

$$E_{t,edge} = \omega\ E_{t,flat} \qquad [5.14]$$

where ω is an empirically determined adjustment factor, which is dependent on a number of factors, e.g. species, MC, grade, size. Because of lack of reliable empirical data on SYP and YP materials, ω was assumed as unity. The equivalent stiffness for edgewise test of the unnotched board was then calculated as

$$\left(\frac{P}{\Delta}\right)_{un} = \frac{48\,(E_{t,edge})\,(I)}{L^3\left[\,1 + 1.2\left(\frac{h}{L}\right)^2 \frac{E}{G}\,\right]} \qquad [5.15]$$

When the boards were notched and destructively tested, stiffness values were measured and recorded as $(P/\Delta)_n$. To determine the change in stiffness of a board before and after notching, the ratio of edgewise stiffness after notching, $(P/\Delta)_n$, and adjusted edgewise stiffness before notching, $(P/\Delta)_{un}$, was calculated. Using the formula for calculating apparent modulus of elasticity (E_a) (which is the form used in engineering design) the ratio is written as

$$\frac{\left(\frac{P}{\Delta}\right)_n}{\left(\frac{P}{\Delta}\right)_{un}} = \frac{\frac{48\,(E_a)\,(I_{eff})}{L^3}}{\frac{48\,(E_a)\,(I)}{L^3}} \qquad [5.16]$$

which simplifies to

$$\frac{\left(\frac{P}{\Delta}\right)_n}{\left(\frac{P}{\Delta}\right)_{un}} = \left(\frac{I_{eff}}{I}\right) \qquad [5.17]$$

where I_{eff} is the effective moment of inertia for the TEN beam of the geometry from which $(P/\Delta)_n$ was measured (not necessarily equivalent to that corresponding to net section).

Table 5.7 presents the calculated stiffness ratios for SYP and YP materials using equation [5.17]. Practically, $(\frac{I_{eff}}{I}) \leq 1.0$. A ratio of 1.0 means that notching did not affect the stiffness of the beam. A ratio greater than 1.0 is anomalous because the moment of inertia of a board is not logically increased by notching. The ratios for the 9 in.-deep SYP beams in Table 5.7 are therefore questionable. (This set of data also exhibited high variability of V^N during the determination of R_e.) The possible cause of this anomaly could be one or a combination of some or all of the following: (1) incorrect assumption for the value of ω in equation [5.14], (2) incorrect assumption of E/G for SYP, (3) inaccuracy of the equation for calculating E_t (the form of equation [5.13]), which was derived from a strain energy analysis of an orthotropic material. The other stiffness ratios for both SYP and YP materials show a definite influence of TEN on beam stiffness which seemed to be largely caused by fractional notch depth, ϕ, and notch location M/V. Any specific relationship of these factors can be established by testing notched beams with additional levels of ϕ and M/V variables. This was not attempted because of very limited data.

5.6 Practical Implications of Results

5.6.1 Commentary on code recommendations

At this point, it would be helpful to evaluate the current code recommendations directly related to the results of the present work. The review of current design guidance in section 2.3 provides the background in this evaluation.

5.6.1.1 "Notch factor" equation

All 3.5 in.-deep TEN beams with $\phi = 0.20.$, $L/h = 12$ and $M/V = 1.0$ in. did not fail at the notch; the 9.0 in.-deep beams with $\phi = 0.20$, $L/h = 4.67$ and $M/V = 1.0$ in. failed at the notch. TCM (AITC 1986) recommends equation [2.1] for TEN's with $\phi \leq 0.10$ and only for "smaller wood members". The NDS (NFPA 1986) recommends equation [2.1] for TEN's with $\phi \leq 0.25$ and especially for beams with low L/h although no specific guidance on this is provided. The new Canadian code (CSA 1989) advises the same limitation on ϕ as that given in NDS. The Japanese code (Architecture Institute of Japan 1974) allows the use of equation [2.1] for cases where $\phi < 0.50$. The British timber code (Ozelton and Baird 1976; Mettem 1986) permits no special calculations for a beam under uniform loading with $h < 10.0$ in. , $(M/V) < L/4$ and $\phi < 0.125$. For other notch cases, equation [2.1] is used. EUROCODE 5 (Crubile et al. 1988) does not put limitation on ϕ for the use of a similar equation.

Table 5.7. Approximate stiffness ratios between a notched and an unnotched beam, (I_{eff}/I)

ϕ	M/V (in.)	Species	h (in.) 3.50	h (in.) 9.00
0.20	1.00	SYP	0.99	1.33
		YP	0.94	1.01
	10.00	SYP	0.90	1.12
		YP	0.88	0.93
0.50	1.00	SYP	0.95	1.24
		YP	0.90	0.87
	10.00	SYP	0.54	0.62
		YP	0.53	0.53

Fig. 5.12 shows that the "notch factor" equation seriously overestimates normalized shear, V^N, for beams with $\phi = 0.20$ (and $\phi = 0.50$), L/h = 4.67 and M/V = 1.0 in.. This equation has been in North American codes for more than 3 decades and has been adopted by other countries probably because of the absence of any catastrophic failure arising from its use. Considering the safety factor of 4.1 when designing for shear and the very conservative limitations imposed by TCM on the use of equation [2.1], safety of previous uses of the equation can now be understood. Experimental results show that flexure rather than notch failure governs for cases with $\phi \leq 0.20$, M/V = 1.0 in. and L/h $\geq$ 12. The NDS recommendation also allows the use of equation [2.1] for most cases where notch failure does not actually govern. The absence of a specific guidance on limitations based on L/h makes this scenario possible. For all other cases where notch failure actually governs, the use of equation [2.1] becomes very risky (e.g. Japanese code and British code recommendations) as seen in Fig. 5.12.

It is difficult to comment on the exclusion recommendations of the British code because of the different loading conditions between the case given in the code and the experimental range in this work.

For TEN locations away from the support, e.g. M/V = 10 in., Fig. 5.13 shows that the "notch factor" equation is nonconservative in predicting V^N-capacity of a notched beam. Thus, code recommendations limiting its use for "notches at the ends of the beams" (interpreted as M/V = 1.0 in. case) are a good way to avoid misapplication of the equation.

5.6.1.2 LEFM equation

The Australian code (SAA 1988) is the only code that has formally adopted an LEFM equation in the design of notched beams. Table 2.1, providing values for angle factor g_{40} in equation [2.8], shows that the effects of h and D do not interact in the equation but are applied separately depending on the ϕ-value, i.e. only D is applied for cases with ϕ values < 0.10 in. and only h is applied for cases with $\phi > 0.10$. Figure 5.12 shows how this specification changes the prediction curve of equation [2.8]. It also shows that given a fixed material shear strength for TEN beams with h=9.0 in., L/h=4.67 and M/V=1.0 in., its prediction curve is more conservative than that of the "notch factor" equation only in the range $0.05 < \phi < 0.30$. V^N capacity was consistently overestimated for a practical range of ϕ-values. The Australian and "notch factor" equations gave different prediction curves, however, for M/V=10.0 in. as shown in Fig. 5.13. It is also noticeable in this figure that the shape of the curve for equation [2.8] looks like a combination of the curves for "notch factor" equation and Gustafsson or TEN equation.

5.6.1.3 Stiffness

Commenting on the effect of notching on beam stiffness, Ozelton and Baird (1976) stated in their timber design manual based on the British code that, "Deflection will hardly be affected, as it is a function of the summation of EI". Design codes and standards do not specifically address the effect of notching on beam stiffness. Theoretical results of FE study by Abou-Ghaida and Gopu (1984) on the effect of end notching on beam stiffness corroborated the statement of Ozelton and Baird. The former reasoned out that "the loss of section at the end region does not, for all practical purposes, alter the angle change (M/EI) diagram for the member" (Abou-Ghaida and Gopu 1984). Experimental results given in Table 5.6, however, suggest that some consideration should be given to deflection of TEN beams with high values of ϕ and M/V.

5.6.2 *Application of TEN equation for design*

The analyses of results and comparisons with other models show that the TEN equation provides the best prediction accuracy of normalized shear capacity of SYP and YP materials with TEN. The equation is applicable to sharp-cornered and filleted end notches. It accurately handles the effects of beam height, h, fractional notch depth, ϕ, notch location (equivalent to M/V for center-point loaded, simply supported beam) and radius, R, for filleted notches on notched beam strength. The effect of L/h is implicitly accounted for in the derived expression. Considering the wide range of elastic ratios included in the theoretical derivation of the equation, the TEN equation may extend to all wood materials. Its applicability has been confirmed with two anatomically different materials. (Comments on current limitations are discussed in the next section.)

It is suggested that TEN's located to fit the support condition be treated to have an M/V-value at least equal to 1.0 in. With the current formulation, the equation is conservative for cases 1.0 in. $<$ M/V $<$ 10.0 in. because of the fixed recommended value of K_A for M/V $<$ 10.0 in.. (The most conservative case would be that with M/V at around 9.9 in..)

Successful application of this equation hinges on the availability of allowable values of K for the most important commercial species. Tabulated values would be most helpful to engineers and designers. One method of establishing these values is by collecting a random sample of notched beams from a given population, e.g. species. K is determined by destructive testing of a beam with the notch located at $M/V \geq 10.0$ in. because this was the basis of K defined in this work. All other notch and beam geometry variables can be arbitrarily selected but should be varied for wide applicability and smoothing of any minor effects. With adequate sample size, appropriate statistical properties of the K distribution can be determined. An allowable value can be established for each species by modifying the lower 5% exclusion limit (L5EL), similar to current practice for deriving allowable unit stresses of visually graded structural lumber (Bodig and Jayne 1982). Alternatively, the designer can select a tabulated SG-value for his material and directly calculate K from equation [5.1]. The accuracy of the K estimate depends on the accuracy of the SG-value. A more reliable estimate of K is obtained from a measure of the SG of an individual piece of lumber or the component in question. This approach is similar to the concept of nondestructive testing, assigning strength values to individual pieces of lumber to enhance the efficient use of materials.

Finally, simple and practical enhancement to the basic TEN equation, as verified by research, should increase the reliability of its use in many applications, i.e. by quantifying the effects of load duration, service environment and the associated changes in it and other relevant design factors.

5.6.3 Limitations

The adjusted TEN equation was derived without considering any effect of beam width (or thickness), b, on strength. The CFHS theory was based on planar FE formulation and a constant beam width of 1.5 in. was maintained in the experiment. Its accuracy for TEN beams with h > 9.0 in. was not experimentally verified.

The adjustment factor, K_A, used to calibrate TEN cases with M/V = 1.0 in. was derived for two species. This factor may, however, be species-dependent. Pending verification for other species, the recommended K_A only applies for the two materials tested in this work. Actual K_A for notch roots with 1.0 in. < M/V < 10.0 in. is unknown. The relationship between K_A and M/V was not investigated but is a critical next step.

The TEN equation should apply to a wide variety of load types, requiring only accurate calculations of the moment, M, and shear, V, at the notch root. It is limited, however, to statically applied loads (normal load duration). The effects of high-rate and long-duration loads were not addressed.

Other support conditions different than the simply supported case that was theoretically analyzed and experimentally tested in this work may cause varied stress interactions especially when the notch is located close to the support. The adjustment factor may also change.

Applicability of present results is limited to dry SYP and YP TEN beams in a constant temperature environment. The influence of different material and environmental conditions on K is unquantified. Also, K is a measure of the strength of beams with notches located in a defect-free region of the material. How this measure of notched beam strength changes in the presence of serious anatomical deviations such as knots and compression wood is unknown.

5.6.4 *Future research*

A natural way to determine potential topics for future work is to look at present limitations of what has been done. The limitations of the TEN model, discussed in the previous section, provide wide areas of possible research. Selection of a specific topic for further investigation is just a matter of prioritizing needs.

It is felt that the most urgent need is the establishment of allowable K-values, along with a verification of K_A, for commercially important species in the construction industry. The relationship of K_A with M/V should be established for the efficient use of the proposed equation for notch cases with 1.0 in. $<$ M/V $<$ 10.0 in.. This exercise is mostly experimental in nature and is relatively straightforward. Another experimental activity is the evaluation of the TEN equation for applicability to large glulam beams (i.e. h $>$ 9.0 in.). Other topics of practical importance include designing a simple method to determine the effect of end notching on beam stiffness and quantifying the effect of notch tapering on beam strength.

Additional theoretical work is needed to understand the interaction of stresses at notches located very near to or at the support. Knowing the sensitivity of these stresses to different support conditions might possibly shed light on the real cause of deviation of experimental results from theoretical predictions made by orthotropic linear elastic models.

6. Summary and Conclusions

An equation for predicting the strength of wood beams with tension end notches (TEN) has been developed based on Gerhardt's (1984a,b) critical fillet hoop stress (CFHS) theory. The equation is a simplified description of the results of hundreds of finite element (FE) analyses of TEN beams with varied geometries (total of 690 configurations). It accounts for the effects of loading type and beam and notch geometry variables, such as beam height, fractional notch depth, radius and notch location. The effect of span-to-depth ratio is implicitly incorporated in the formulation of the model. Notched beam strength is represented by a material parameter, K, which was found to be related to specific gravity. A simple equation for predicting K from specific gravity was derived from experimental results.

The notched beam expression is applicable to both filleted and sharp-cornered notches. An effective radius, R_e, is used to model a sharp-cornered notch ($R \simeq 0$); R_e was determined and confirmed for two materials. A method of determining R_e for other materials was established.

The FE model used in this study was inadequate when modeling the complex interaction of stresses at notch roots at or very near the support. The CFHS theory and the linear elastic fracture mechanics (LEFM) approach based on strain energy release rate criterion showed consistently similar strength prediction trends for many cases, including notches at or very near the support. The TEN equation was adjusted to correct the inadequacy of the FE model by an experimentally determined additive factor K_A. With this adjustment, the TEN equation provided accurate predictions of the normalized shear capacity of TEN beams over a wide range of geometry. The TEN equation was compared with other models and notch equations currently recommended in design codes and significant differences were noted. Chief among them is the sensitivity of notched beam strength to notch location (or the ratio M/V). This is not currently considered by "notch factor"-based design equations.

Stiffness of TEN wood beams was reduced by end notching in some cases. The magnitude of reduction was heavily influenced by notch geometry variables ϕ and M/V. No relationship was established because of limited data. This experimental finding is important because the effect of end notching on beam stiffness has not been seriously addressed before and theoretical analysis does not predict the reduction.

Bibliography

1. Abou-Ghaida, S. and V.K.A. Gopu. 1984. Shear strength in notched timber beams. Proc. Pacific Timber Engineering Conf., Auckland, New Zealand. May 1984. pp. 579-586.

2. American Institute of Timber Construction. 1985. Timber Construction Manual. 3rd ed. John Wiley and Sons, New York. 836 pp.

3. American Society for Testing and Materials. 1988. Annual Book of ASTM Standards, Vol. 4.09, Wood. ASTM, Philadelphia, PA. 758 pp.

4. Architectural Institute of Japan. 1974. Timber Structure Design Specifications and Commentary. Maruzen Co., Tokyo, Japan. 416 pp.

5. Armstrong, J.P., C. Skaar and C. de Zeeuw. 1984. The effect of specific gravity on several mechanical properties of some world woods. Wood Science and Technology 18:137-146.

6. Barrett, J.D. 1974. Effect of size on tension perpendicular-to-grain strength of Douglas-fir. Wood and Fiber 6(2):126-143.

7. Barrett, J.D. 1981. Fracture mechanics and the design of wood structures. Philosophical Trans. Royal Society London A299: 217-226.

8. Barrett, J.D., R.O. Foschi and S.P. Fox. 1975. Perpendicular-to-grain strength of Douglas-fir. Can J. Civil Engineering 2(1):50-57

9. Bendtsen, B.A. and S. Porter. 1978. Comparison of results from standard 2-inch with 1-1/2-inch shear block tests. For. Prods. J. 28(7): 54-56.

10. Bodig, J. and B.A. Jayne. 1982. Mechanics of Wood and Wood Composites. Van Nostrand Rheinhold Co., New York. 711 pp.

11. Breyer, D.E. 1988. Design of Wood Structures. 2nd ed. McGraw-Hill, New York, NY. 680 pp.

12. Canadian Standards Association. 1989. Engineering design in wood (limit states design). CAN3-086.1-M89, CSA.

13. Crubile, P., J, Ehlbeck, H. Bruninghoff, H.J. Larsen and J. Sunley. 1985. Eurocode 5: Common Unified Rules for Timber Structures. Drafting Panel EC5, Commission of the European Communities. 126 pp.

14. Crubile, P., J, Ehlbeck, H. Bruninghoff, H.J. Larsen and J. Sunley. 1988. Eurocode 5: Common Unified Rules for Timber Structures. Commission of the European Communities, Luxembourg, Belgium. 137 pp.

15. Draper, N.R. and H. Smith. 1981. Applied Regression Analysis. Second edition. John Wiley and Sons Inc., New York. 709 pp.

16. Gerhardt, T.D. 1983. Plane stress analysis of wood members using isoparametric finite elements: a computer program. US Forest Service General Technical Report FPL 35. Madison, WI.

17. Gerhardt, T.D. 1984a. Strength and stiffness analysis of notched green oak pallet stringers. US Forest Service Research Paper FPL 452. Madison, WI. 25 pp.

18. Gerhardt, T.D. 1984b. A hybrid/finite element approach for stress analysis of notched anisotropic materials. J. Applied Mechanics Vol. 51(Dec.): 804-810.

19. Goodman, J.R. and J. Bodig. 1970. Orthotropic elastic properties of wood. J. Struct. Div., ASCE 96(11): 2301-2319.

20. Green, A.E. and G.I. Taylor. 1939. Stress systems in aeolotropic plates, I. Proc. Royal Soc. London A173: 162-172.

21. Green, A.E. and G.I. Taylor. 1942. Stress systems in aeolotropic plates, IV. Proc. Royal Soc. London A180: 173-208.

22. Green, A.E. and G.I. Taylor. 1945a. Stress systems in aeolotropic plates, III. Proc. Royal Soc. London A184: 181-195.

23. Green, A.E. and G.I. Taylor. 1945b. Stress systems in aeolotropic plates, V. Proc. Royal Soc. London A184: 231-252.

24. Gustafsson, P.J. 1988. A study of strength of notched beams. Paper CIB-W18A/21-10-1. Intl. Council for Bldg. Research Studies and Documentation, Vancouver, B.C., Canada. 25 pp.

25. Hirai, T. and M. Sawada. 1979. Stiffness and load carrying capacity of square-notched beams, 1: On the estimation of the effective stiffness. Research Bulletins of the College Experiment Forests, College of Agriculture, Hokkaido University XXXVI(2): 387-420. Sapporo, Japan.

26. Hirai, T. and M. Sawada. 1980. Stiffness and load carrying capacity of square-notched beams, 3: On the maximum faiure moments. Research Bulletins of the College Experiment Forests, College of Agriculture, Hokkaido University XXXVII(3): 759-788. Sapporo, Japan.

27. Hooley, R.F. and P.D. Hibbert 1967. Stress concentrations in timber beams. J. Struct. Div., ASCE Vol. 93, St2, pp. 126-139.

28. Huddleston, E. Undated. Wood as a structural material. Introduction to Selected Topics in Timber Engineering. Univ. of Sydney, Australia. pp. 1-26.

29. Krebs, H.J., P. Hoffmeyer and L.G. Nielsen. 1984. Duration of load tests with notched Spruce beams at two moisture levels. Proc. IUFRO Timber Engineering Meeting, 1984, Xalapa, Mexico. IUFRO, Vienna, Austria.

30. Larsen, H.J. 1975. The design of timber beams R101. Paper Prepared for CIB-W18, Int'l. Council for Bldg. Research Studies and Documentation, Timber Structures, Karlsruhe, Germany. 29 pp.

31. Leicester, R.H. 1969. The size effect of notches. Proc. Second Australasian Conf. Mechanics of Structures and Materials, Adelaide, S.A. 4: 1-20.

32. Leicester, R.H. 1974. Fracture strength of wood. Proc. First Australian Conf. Engineering Materials. Univ. of New South Wales, Sydney, Australia. 26-28 August 1974.

33. Leicester, R.H. 1985. The fracture strength of wood. Lecture No. 11, pp. 3-26 in Timber Engineering for Developing Countries, Part 4. UNIDO/IO.609.

34. Leicester, R.H. and W.G. Poynter. 1979. On the design strength of notched beams. Proc. 19th For Prods. Res. Conf., Melbourne, Australia. 12-16 November 1979.

35. Lum, C. and R.O. Foschi. 1988. Arbitrary V-notches in orthotropic plates. J. Engineering Mechanics 114(4): 638-655.

36. Madsen,B. 1975. Duration of load tests for wood in tension perpendicular to grain. Forest Products J. 25(8):48-53.

37. Mall, S., J.F. Murphy and J.E. Shottafer. 1983. Criterion for the mixed mode fracture in wood. ASCE J. Engineering Mechanics 109(3): 680-690.

38. Masuda, M. 1988. Theoretical consideration on fracture criteria of wood-proposal of finite small area theory. Proc. 1988 Intl. Timber Engineering, Seattle, WA, 1988. For. Prods. Research Soc., Madison, WI. pp. 584-595.

39. McLain, T.E. 1988. Extending the critical hoop stress criterion for notched wood beams. Proposal to USDA Competitive Grants Program for Forest and Rangeland Renewable Resources. VPISU, Blacksburg, VA. April 1988. 20 pp.

40. McLain, T.E. 1989. Evaluation of current NDS criteria for notched wood beams. Personal communication. Professor, Dept. of Wood Science and Forest Products, VPISU, Blacksburg, VA.

41. Mettem, C.J. 1986. Structural Timber Design and Technology. Longman Scientific and Technical, Essex, England. 343 pp.

42. Mohler, K. 1978. Beams notched at the ends (concerning section 5.1.1.4 of CIB Timber Code). CIB-W18/9-10-2, Perth, Scotland. June 1978.

43. Murphy, J.F. 1978. Using fracture mechanics to predict failure in notched wood beams. Proc. First Intl. Conf. Wood Fracture. Banft, Alberta, Canada. Aug. 1978. pp. 159-173.

44. Murphy, J.F. 1986. Strength and stiffness reduction of large notched beams. J. Structural Engineering 2(9): 1989-2000.

45. Myers, R.H. 1976. Response Surface Methodology. VPISU, Blacksburg, VA. 246 pp.

46. NFPA. 1986. National Design Specification for Wood Construction. National Forest Products Association. Washington, DC. 87 pp.

47. Norris, C.B. 1962. Strength of orthotropic materials subjected to combined stresses. US Forest Products Lab. Report No. 1816. Madison, WI.

48. Ozelton, E.C. and J.A. Baird. 1976. Timber Designers' Manual. Granada Publishing Limited, London, England. 518 pp.

49. Palettas, P.N. 1989. Statistical test procedure for evaluation of notched beam strength. Personal communication. Assistant Professor, Dept. of Statistics, VPISU, Blacksburg, VA.

50. Palka, L.C. and B. Holmes. 1973. Tangential failure of small wood cantilevered beams with square notches. Wood Science 5(3): 172-180.

51. Panshin,A.J. and C. de Zeeuw. 1980. Textbook of Wood Technology. 4th ed. McGraw-Hill, New York, NY. 687 pp.

52. Patton-Mallory, M. and S.M. Cramer. 1987. Fracture mechanics: a tool for predicting wood component strength. For. Prods. J. 37(718): 39-47.

53. Peterson, R.M. 1983. Keynote Address. Proc. Workshop Structural Wood Research: State-of-the-Art and Research Needs. Edited by R.Y. Itani and K.F. Faherty. ASCE. 210 pp.

54. Porter, A.W. 1964. On the mechanics of fracture in wood. For. Prods. J. 14(8): 325-331.

55. Reeves, J.R. 1973. The effect of stringer design and leading-edge design on the strength characteristics of wooden pallets. M.Arch. thesis, VPISU, Blacksburg, VA.

56. Richards, D.B. 1974. Strength of wood beams with shallow curved notches. Wood Science 7(1): 77-84.

57. Rizzo, F.J. and D.J. Shippy. 1970. A method for stress determination in plane anisotropic elastic bodies. J. Composite materials 4(1): 36-61.

58. SAS Institute. 1985. SAS User's guide: statistics. Version 5 edition. SAS Institute Inc., Cary, NC. 956 pp.

59. Scholten, J.A. 1935. Rounding notches makes stronger joists. American Lumberman. March 1935.

60. Sih, G.C., P.C. Paris, and G.R. Irwin. 1965. On cracks in rectilinearly anisotropic bodies. Intl. J. of Fracture 1(3):189-192.

61. Standards Association of Australia. 1988. Australian standard 1720.1-1988: SAA timber structures code, Part 1- design methods. SAA, Sydney, Australia. 85 pp.

62. Stieda, C.K.A. 1964. Stress concentrations in notched timber beams. Trans. Engineering Inst. Canada Vol. 7, No. A-5. October 1964. 8 pp.

63. Stieda, C.K.A. 1966. Stress concentrations around holes and notches and their effect on the strength of wood beams. J. Materials 1(3): 560-582.

64. Taylor, R.L. 1977. Computer procedures for finite element analysis, Chap. 24, pp. 677-757 in The Finite Element Method, 3rd ed., O.C. Zienkiewicz, editor. McGraw-Hill, London. 757 pp.

65. USDA. 1955. Wood Handbook: Wood as an Engineering Material. USDA Ag. Handbook No. 72. US Forest Prods. Lab. Madison, WI.

66. USDA. 1974. Wood Handbook: Wood as an Engineering Material. USDA Ag. Handbook No. 72. US Forest Prods. Lab. Madison, WI.

67. USDA. 1987. Wood Handbook: Wood as an Engineering Material. USDA Ag. Handbook No. 72. US Forest Products Laboratory, Madison, WI. 466 pp.

68. Walsh, P.F. 1972. Linear fracture mechanics in orthotropic materials. Engineering Fracture Mechanics 4: 533-541.

69. Woeste, F.E. 1972. Stress Concentrations Around Holes and Notches in Laminated Wood Beams. Master's Thesis, Univ. of Kentucky, Lexington, KY. 64 pp.

70. Wood, L.W. 1951. Relation of strength of wood to duration of load. Report No. R1916, US Forest Prods. Lab., Madison, WI.

71. Wu, E.M. 1967. Application of fracture mechanics to anisotropic plates. J. Applied Mechanics, Trans. ASME 34(4) Series E. pp. 967-974.

72. Zahn, J. 1988. Telephone conversation with T.E. McLain. March 25, 1988. US For. Prods. Lab., Madison, WI.

73. Zalph, B.L. 1989. Predicting the strength of notched wood beams. PhD dissertation. Dept. of Wood Science and Forest Prods., VPISU, Blacksburg, VA.

Appendix A. Equation [2.2] coefficients

Sample computation of coefficients A and B using equation [2.2] for Douglas fir, notch case where $\phi = (D/h) =$ 0.33. From Zahn (1988).

Equation [2.2] may be expressed as

$$6A\left(\frac{M}{bh^{3/2}}\right) + \frac{3B}{2}\left(\frac{V}{bh^{1/2}}\right) = 1\,. \qquad \text{[A.1]}$$

Using Murphy's (1988) combined transformed SIF failure criterion,

$$\frac{\overline{\overline{K}}_{I}}{K_{Ic}} + \frac{\overline{\overline{K}}_{II}}{K_{IIc}} = 1 \qquad \text{[A.2]}$$

where $\overline{\overline{K}}_{I}$, $\overline{\overline{K}}_{II}$ = effective SIF's on the imminent fracture plane

$\overline{\overline{K}}_{I} = 0.12\ K_{I} + 0.82\ K_{II}$

$\overline{\overline{K}}_{II} = 0.24\ K_{I} + 0.47\ K_{II}$

K_{Ic}, K_{IIc} = critical mode I, II SIF's

$K_{Ic} = 170 \text{ psi} \sqrt{\text{in.}}$

$K_{IIc} = 1140 \text{ psi} \sqrt{\text{in.}}$ from lower 5% exclusion limit for D. fir.

After substitution and simplification,

$$\frac{K_I}{1091} + \frac{K_{II}}{191} = 1 \qquad [A.3]$$

but $K_I = \frac{7M}{bh^{3/2}}$ and $K_{II} = \frac{1.03V}{bh^{1/2}}$.

Further substitution and simplification gives

$$\frac{7}{1091}\left(\frac{M}{bh^{3/2}}\right) + \frac{1.03}{191}\left(\frac{V}{bh^{1/2}}\right) = 1 . \qquad [A.4]$$

Equating equations [A.1] and [A.4], one gets

$A = 0.0010693$, and $B = 0.003595$.

Appendix B. Expressions for M/V for common loading types

B.1 Center-point loading

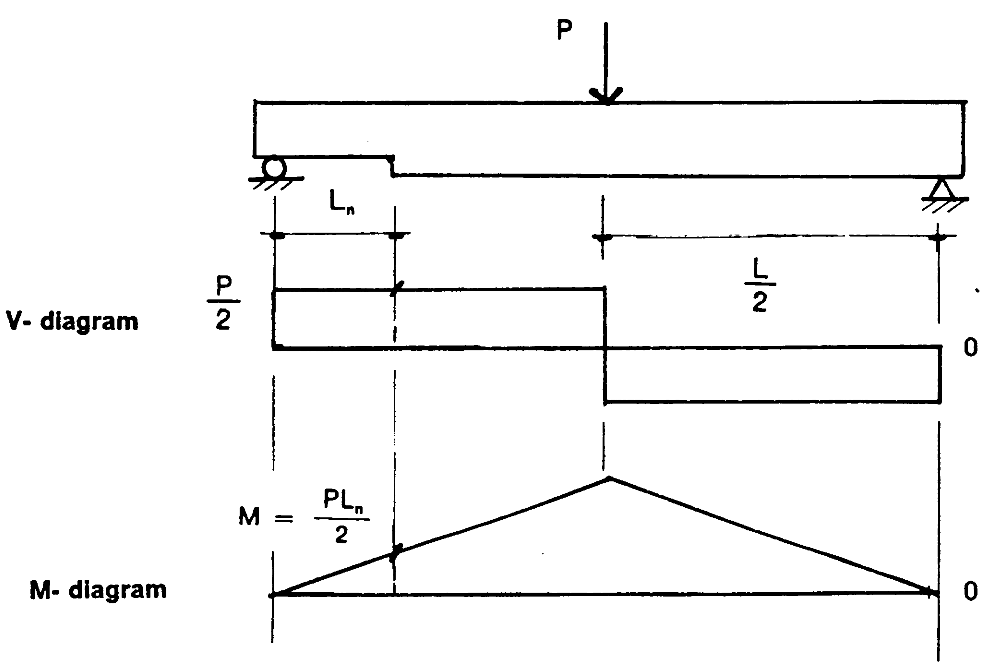

$$\boxed{\frac{M}{V} = L_n}$$

B.2 Two-point loading

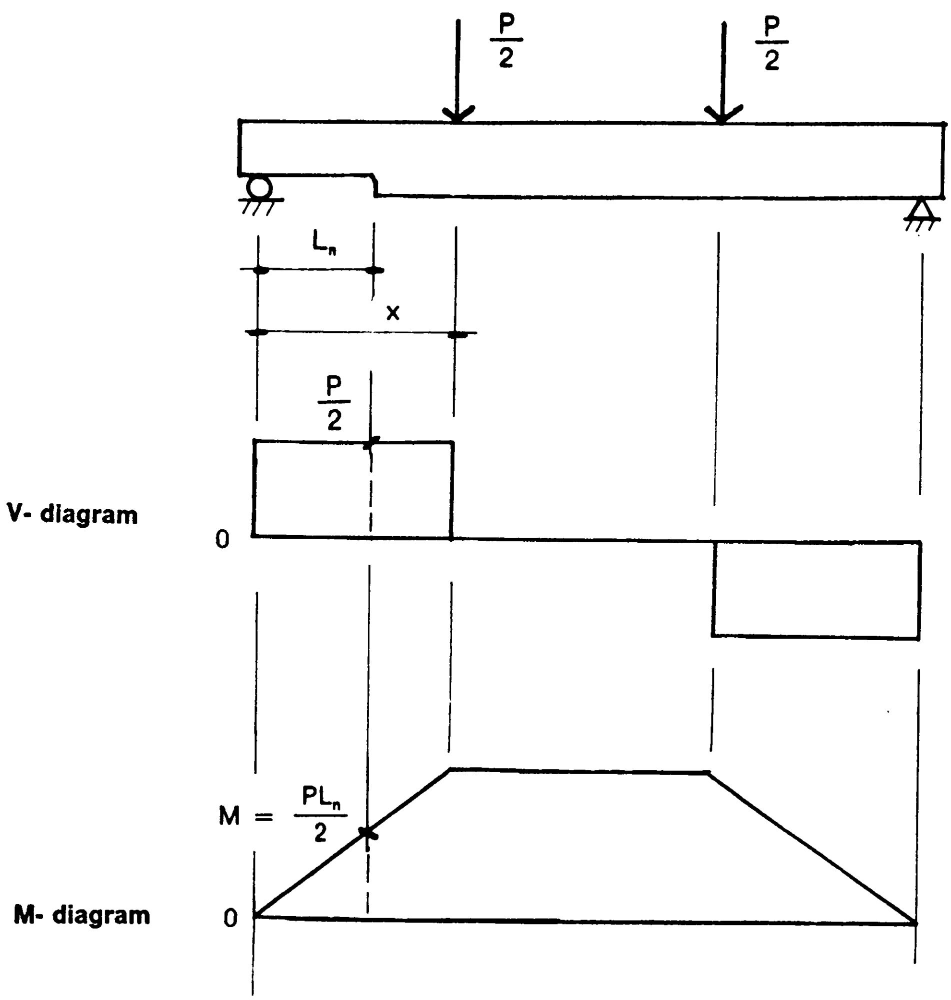

$$\boxed{\frac{M}{V} = L_n}$$

B.3 Multiple concentrated loading

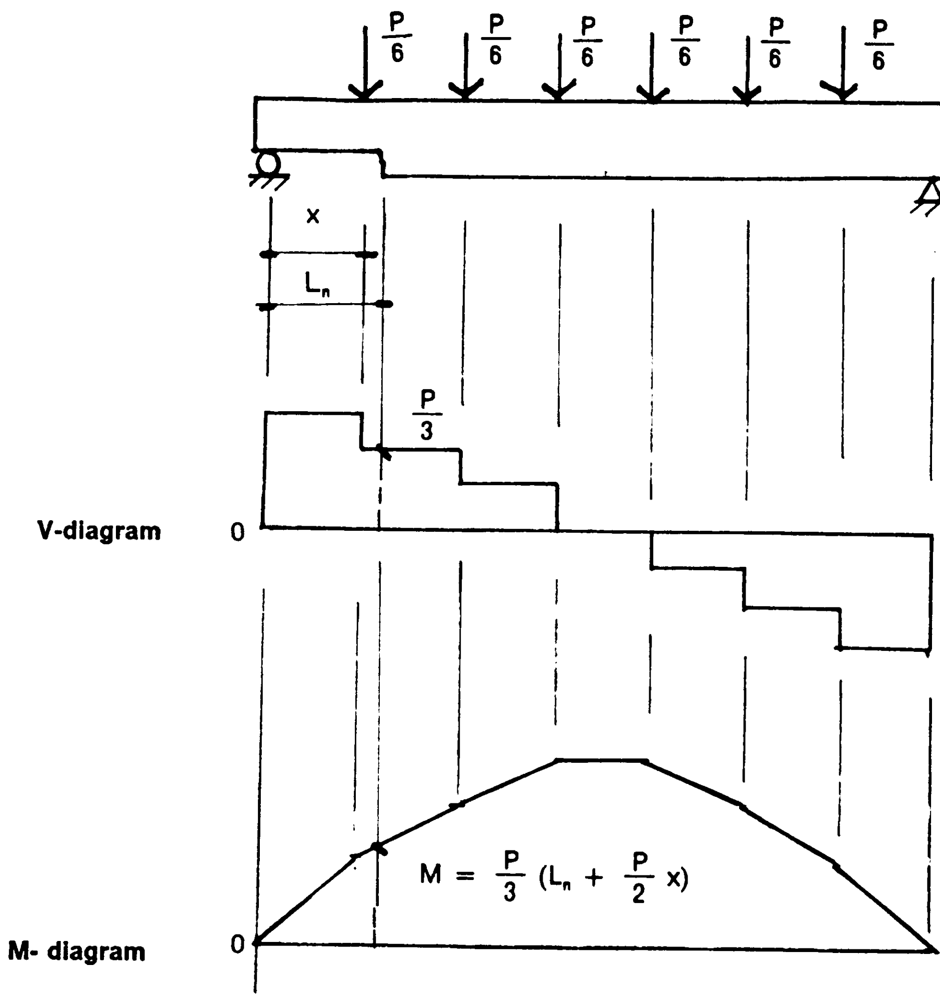

$$\boxed{\frac{M}{V} = L_n + \frac{P}{2} x}$$

B.4 Uniform loading

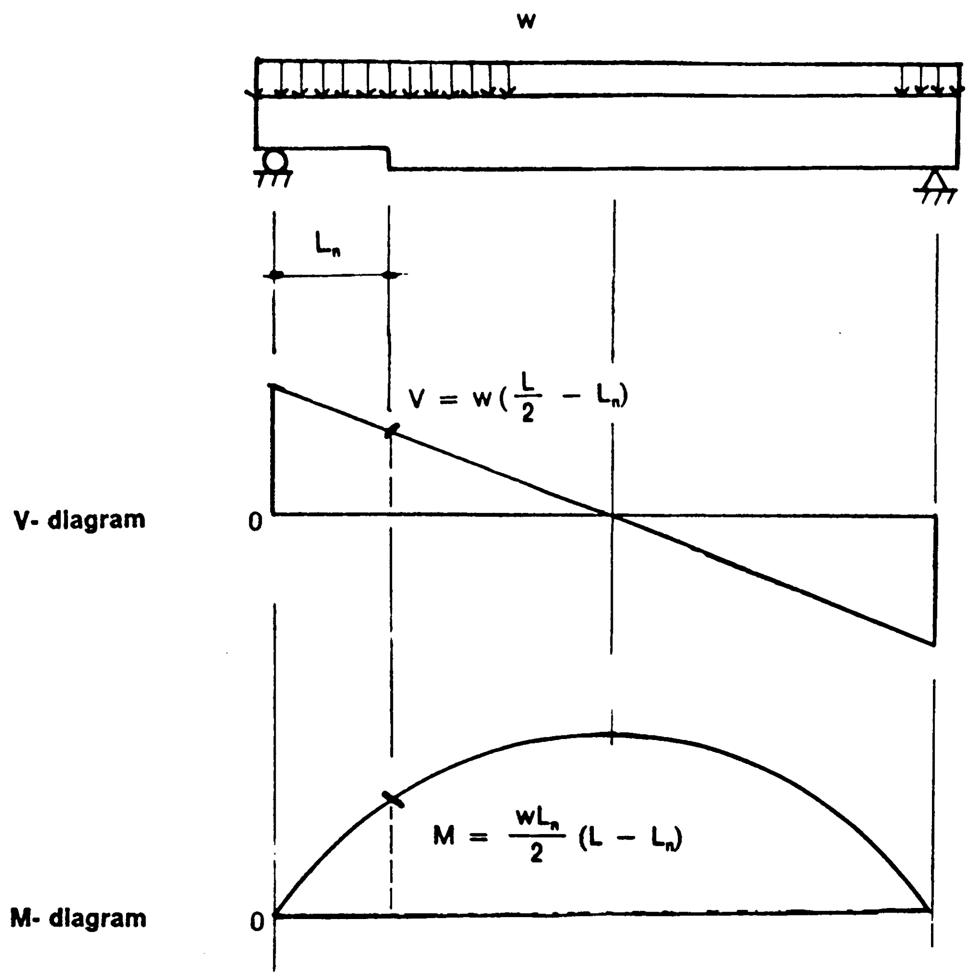

$$\boxed{\frac{M}{V} = L_n\left(\frac{L - L_n}{L - 2L_n}\right)}$$

Appendix C. Results of preliminary substudies

C.1 Loading Effect

Material EP set A : G11-E13 (see Table 3.1 for details of material properties)
Beam height, h : 3.5 in.
Fractional notch depth, ϕ : 0.314 (or D=1.10 in.)

R (in.)	M/V (in.)	ShCF	θ[1] (deg.)
0.1875	0.5	4.44	81.0
	1.0	4.97	82.0
	2.0	7.06	83.0
	4.0	11.10	84.0
	6.0	15.44	84.0
	10.0	24.20	84.0
	11.0	26.40	84.0
0.500	0.5	3.93	86.0
	1.0	3.48	82.0
	2.0	4.77	83.0
	4.0	7.78	84.0
	6.0	10.89	84.0
	10.0	17.10	85.0
	11.0	18.68	85.0

[1] angle from the horizontal where $\sigma_{h,max}$ (or max ShCF) occured

C.2 Beam Height Effect

Material EP set A : G11-E13
Notch location, M/V : 0.50 in.
Radius, R : 0.163 in.

ϕ	h (in.)	ShCF	λ
0.10	2.0	1.99	0.532
	9.5	4.56	
0.314	2.0	4.17	0.393
	9.5	7.69	
0.50	2.0	5.97	0.321
	9.5	9.84	

Appendix D. Evaluation of NDS design criteria

NDS design criteria for center-point loaded, simply supported TEN beams (NFPA 1986) :

- bending

$$f_b = \frac{6\left(\frac{wL^2}{8}\right)}{bh^2} \leq (LDF)\,F_v \qquad [D.1]$$

- shear

$$f_v = \frac{3\left(\frac{wL}{2}\right)}{2\,bh} \; \frac{1}{(1-\phi)^2} \leq (LDF)\,F_v \qquad [D.2]$$

- deflection

$$\Delta = 5\,\frac{wL^4}{384\,EI} \leq \frac{L}{k} \qquad [D.3]$$

Using recommended values for lumber and glulam materials from NDS and solving for $\frac{w}{b}$, McLain (1989) obtained the following maximum $\frac{L}{h}$ ratios where shear, eq. [D.2], governs:

wood material	k in [D.3]	ϕ 0.0[1]	0.10	0.20	0.30	0.40	0.50
So. pine lumber S-19, No. 2 J & P	240	15	19	21	25	> 26	> 26
	360	15	17	19	21	25	> 26
SPF lumber S-19, No. 2 J & P	240	14	17	22	25	> 26	> 26
	360	14	17	19	22	> 26	> 26
So. pine glulam SP22F-V5 dry	180	10	12	16	19	23	26
	240	10	12	14	16	19	23
	360	10	12	15	18	21	25

[1] unnotched beam

Appendix E. Calculated ShCF's from FE analysis

The following ShCF values for the listed notch geometries were computed using Gerhardt's (1984b) FE program. Material EP sets are represented as follows :

Matl	**EP set**
1	A : G11-E13
2	B : G17-E17
3	C : G27-E21
4	D : G11-E17
5	E : G27-E17

The columns in the tabulation are identified in this heading:

Matl	Obs.	Cell No.	M/V (in.)	R (in.)	h (in.)	ϕ	ShCF

1	1	1	1	0.1875	3.5	0.1	2.4567
1	2	1	6.5	0.1875	3.5	0.1	8.4143
1	3	1	12	0.1875	3.5	0.1	14.7715
1	4	2	1	0.344	3.5	0.1	2.1162
1	5	2	6.5	0.344	3.5	0.1	6.9464
1	6	2	12	0.344	3.5	0.1	12.2212
1	7	4	1	0.1875	3.5	0.35	5.3733
1	8	4	6.5	0.1875	3.5	0.35	18.1561
1	9	4	12	0.1875	3.5	0.35	31.4493
1	10	5	1	0.344	3.5	0.35	4.3277
1	11	5	6.5	0.344	3.5	0.35	14.5299
1	12	5	12	0.344	3.5	0.35	25.2641
1	13	6	1	0.5	3.5	0.35	3.7435
1	14	6	6.5	0.5	3.5	0.35	12.7998
1	15	6	12	0.5	3.5	0.35	22.2326
1	16	7	1	0.1875	3.5	0.52	7.6052
1	17	7	6.5	0.1875	3.5	0.52	29.1083
1	18	7	12	0.1875	3.5	0.52	51.0687
1	19	8	1	0.344	3.5	0.52	6.0498
1	20	8	6.5	0.344	3.5	0.52	23.2851
1	21	8	12	0.344	3.5	0.52	41.0093
1	22	9	1	0.5	3.5	0.52	5.2437
1	23	9	6.5	0.5	3.5	0.52	20.5015
1	24	9	12	0.5	3.5	0.52	36.1762
1	25	10	1	0.1875	3.5	0.6	9.3077
1	26	10	6.5	0.1875	3.5	0.6	38.8358
1	27	10	12	0.1875	3.5	0.6	68.7501
1	28	11	1	0.344	3.5	0.6	7.4091
1	29	11	6.5	0.344	3.5	0.6	31.1965
1	30	11	12	0.344	3.5	0.6	55.4679
1	31	12	1	0.5	3.5	0.6	6.4571
1	32	12	6.5	0.5	3.5	0.6	27.6005
1	33	12	12	0.5	3.5	0.6	49.0651
1	34	13	1	0.1875	4.71	0.1	2.5022
1	35	13	6.5	0.1875	4.71	0.1	7.2153
1	36	13	12	0.1875	4.71	0.1	12.459
1	37	14	1	0.344	4.71	0.1	2.1535
1	38	14	6.5	0.344	4.71	0.1	5.8925
1	39	14	12	0.344	4.71	0.1	10.211
1	40	16	1	0.1875	4.71	0.35	5.559
1	41	16	6.5	0.1875	4.71	0.35	15.8463
1	42	16	12	0.1875	4.71	0.35	26.9245
1	43	17	1	0.344	4.71	0.35	4.4682
1	44	17	6.5	0.344	4.71	0.35	12.592
1	45	17	12	0.344	4.71	0.35	21.4995
1	46	18	1	0.5	4.71	0.35	3.8387
1	47	18	6.5	0.5	4.71	0.35	11.0471
1	48	18	12	0.5	4.71	0.35	18.8331
1	49	19	1	0.1875	4.71	0.52	7.7044
1	50	19	6.5	0.1875	4.71	0.52	25.1857

1	51	19	12	0.1875	4.71	0.52	43.4338
1	52	20	1	0.344	4.71	0.52	6.101
1	53	20	6.5	0.344	4.71	0.52	19.9587
1	54	20	12	0.344	4.71	0.52	34.5981
1	55	21	1	0.5	4.71	0.52	5.2449
1	56	21	6.5	0.5	4.71	0.52	17.5023
1	57	21	12	0.5	4.71	0.52	30.3661
1	58	22	1	0.1875	4.71	0.6	9.2409
1	59	22	6.5	0.1875	4.71	0.6	33.3348
1	60	22	12	0.1875	4.71	0.6	58.1327
1	61	23	1	0.344	4.71	0.6	7.3044
1	62	23	6.5	0.344	4.71	0.6	26.513
1	63	23	12	0.344	4.71	0.6	46.4551
1	64	24	1	0.5	4.71	0.6	6.2853
1	65	24	6.5	0.5	4.71	0.6	23.2611
1	66	24	12	0.5	4.71	0.6	40.8019
1	67	25	1	0.1875	7.125	0.1	2.884
1	68	25	6.5	0.1875	7.125	0.1	6.1869
1	69	25	12	0.1875	7.125	0.1	10.2118
1	70	26	1	0.344	7.125	0.1	2.4715
1	71	26	6.5	0.344	7.125	0.1	4.9898
1	72	26	12	0.344	7.125	0.1	8.2924
1	73	27	1	0.5	7.125	0.1	2.1201
1	74	27	6.5	0.5	7.125	0.1	4.5249
1	75	27	12	0.5	7.125	0.1	7.3317
1	76	28	1	0.1875	7.125	0.35	6.1624
1	77	28	6.5	0.1875	7.125	0.35	13.7103
1	78	28	12	0.1875	7.125	0.35	22.1872
1	79	29	1	0.344	7.125	0.35	4.9412
1	80	29	6.5	0.344	7.125	0.35	10.7625
1	81	29	12	0.344	7.125	0.35	17.5446
1	82	30	1	0.5	7.125	0.35	4.2137
1	83	30	6.5	0.5	7.125	0.35	9.4215
1	84	30	12	0.5	7.125	0.35	15.2474
1	85	31	1	0.1875	7.125	0.52	8.308
1	86	31	6.5	0.1875	7.125	0.52	21.2855
1	87	31	12	0.1875	7.125	0.52	35.3469
1	88	32	1	0.344	7.125	0.52	6.5477
1	89	32	6.5	0.344	7.125	0.52	16.6517
1	90	32	12	0.344	7.125	0.52	27.8943
1	91	33	1	0.5	7.125	0.52	5.5651
1	92	33	6.5	0.5	7.125	0.52	14.4838
1	93	33	12	0.5	7.125	0.52	24.2748
1	94	34	1	0.1875	7.125	0.6	9.725
1	95	34	6.5	0.1875	7.125	0.6	27.7145
1	96	34	12	0.1875	7.125	0.6	46.8834
1	97	35	1	0.344	7.125	0.6	7.6342
1	98	35	6.5	0.344	7.125	0.6	21.7335
1	99	35	12	0.344	7.125	0.6	37.0785
1	100	36	1	0.5	7.125	0.6	6.4985

1	101	36	6.5	0.5	7.125	0.6	18.9307
1	102	36	12	0.5	7.125	0.6	32.3555
1	103	37	1	0.1875	10.75	0.1	3.8768
1	104	37	6.5	0.1875	10.75	0.1	6.0829
1	105	37	12	0.1875	10.75	0.1	8.7507
1	106	38	1	0.344	10.75	0.1	3.3404
1	107	38	6.5	0.344	10.75	0.1	4.8533
1	108	38	12	0.344	10.75	0.1	7.0405
1	109	39	1	0.5	10.75	0.1	2.853
1	110	39	6.5	0.5	10.75	0.1	4.4235
1	111	39	12	0.5	10.75	0.1	6.1957
1	112	40	1	0.1875	10.75	0.35	7.4851
1	113	40	6.5	0.1875	10.75	0.35	12.7955
1	114	40	12	0.1875	10.75	0.35	18.0609
1	115	41	1	0.344	10.75	0.35	6.0013
1	116	41	6.5	0.344	10.75	0.35	9.9247
1	117	41	12	0.344	10.75	0.35	14.1942
1	118	42	1	0.5	10.75	0.35	5.0608
1	119	42	6.5	0.5	10.75	0.35	8.6946
1	120	42	12	0.5	10.75	0.35	12.1502
1	121	43	1	0.1875	10.75	0.52	9.6149
1	122	43	6.5	0.1875	10.75	0.52	19.0308
1	123	43	12	0.1875	10.75	0.52	28.9104
1	124	44	1	0.344	10.75	0.52	7.5638
1	125	44	6.5	0.344	10.75	0.52	14.7049
1	126	44	12	0.344	10.75	0.52	22.665
1	127	45	1	0.5	10.75	0.52	6.3653
1	128	45	6.5	0.5	10.75	0.52	12.7643
1	129	45	12	0.5	10.75	0.52	19.5574
1	130	46	1	0.1875	10.75	0.6	10.9215
1	131	46	6.5	0.1875	10.75	0.6	24.1786
1	132	46	12	0.1875	10.75	0.6	38.4225
1	133	47	1	0.344	10.75	0.6	8.5554
1	134	47	6.5	0.344	10.75	0.6	18.7424
1	135	47	12	0.344	10.75	0.6	30.1802
1	136	48	1	0.5	10.75	0.6	7.2131
1	137	48	6.5	0.5	10.75	0.6	16.2304
1	138	48	12	0.5	10.75	0.6	26.1312
2	1	1	1	0.1875	3.5	0.1	2.8321
2	2	1	6.5	0.1875	3.5	0.1	9.447
2	3	1	12	0.1875	3.5	0.1	16.4364
2	4	2	1	0.344	3.5	0.1	2.4034
2	5	2	6.5	0.344	3.5	0.1	7.7365
2	6	2	12	0.344	3.5	0.1	13.5065
2	7	4	1	0.1875	3.5	0.35	6.332
2	8	4	6.5	0.1875	3.5	0.35	20.4932
2	9	4	12	0.1875	3.5	0.35	35.1191
2	10	5	1	0.344	3.5	0.35	5.0799
2	11	5	6.5	0.344	3.5	0.35	16.4022

2	12	5	12	0.344	3.5	0.35	28.2473
2	13	6	1	0.5	3.5	0.35	4.3516
2	14	6	6.5	0.5	3.5	0.35	14.4578
2	15	6	12	0.5	3.5	0.35	24.8464
2	16	7	1	0.1875	3.5	0.52	8.9009
2	17	7	6.5	0.1875	3.5	0.52	32.635
2	18	7	12	0.1875	3.5	0.52	56.7798
2	19	8	1	0.344	3.5	0.52	7.0536
2	20	8	6.5	0.344	3.5	0.52	26.128
2	21	8	12	0.344	3.5	0.52	45.6838
2	22	9	1	0.5	3.5	0.52	6.0485
2	23	9	6.5	0.5	3.5	0.52	23.0404
2	24	9	12	0.5	3.5	0.52	40.3089
2	25	10	1	0.1875	3.5	0.6	10.8148
2	26	10	6.5	0.1875	3.5	0.6	43.3717
2	27	10	12	0.1875	3.5	0.6	76.2672
2	28	11	1	0.344	3.5	0.6	8.5766
2	29	11	6.5	0.344	3.5	0.6	34.8886
2	30	11	12	0.344	3.5	0.6	61.6179
2	31	12	1	0.5	3.5	0.6	7.4098
2	32	12	6.5	0.5	3.5	0.6	30.8732
2	33	12	12	0.5	3.5	0.6	54.5062
2	34	13	1	0.1875	4.71	0.1	2.8965
2	35	13	6.5	0.1875	4.71	0.1	8.1662
2	36	13	12	0.1875	4.71	0.1	13.948
2	37	14	1	0.344	4.71	0.1	2.4766
2	38	14	6.5	0.344	4.71	0.1	6.6532
2	39	14	12	0.344	4.71	0.1	11.4086
2	40	16	1	0.1875	4.71	0.35	6.5835
2	41	16	6.5	0.1875	4.71	0.35	18.0192
2	42	16	12	0.1875	4.71	0.35	30.1278
2	43	17	1	0.344	4.71	0.35	5.2697
2	44	17	6.5	0.344	4.71	0.35	14.3196
2	45	17	12	0.344	4.71	0.35	24.0863
2	46	18	1	0.5	4.71	0.35	4.4716
2	47	18	6.5	0.5	4.71	0.35	12.5721
2	48	18	12	0.5	4.71	0.35	21.1265
2	49	19	1	0.1875	4.71	0.52	9.0693
2	50	19	6.5	0.1875	4.71	0.52	28.3991
2	51	19	12	0.1875	4.71	0.52	48.3846
2	52	20	1	0.344	4.71	0.52	7.1494
2	53	20	6.5	0.344	4.71	0.52	22.5098
2	54	20	12	0.344	4.71	0.52	38.6025
2	55	21	1	0.5	4.71	0.52	6.0804
2	56	21	6.5	0.5	4.71	0.52	19.7562
2	57	21	12	0.5	4.71	0.52	33.9397
2	58	22	1	0.1875	4.71	0.6	10.8084
2	59	22	6.5	0.1875	4.71	0.6	37.3901
2	60	22	12	0.1875	4.71	0.6	64.5979
2	61	23	1	0.344	4.71	0.6	8.5049

2	62	23	6.5	0.344	4.71	0.6	29.7574
2	63	23	12	0.344	4.71	0.6	51.7212
2	64	24	1	0.5	4.71	0.6	7.2322
2	65	24	6.5	0.5	4.71	0.6	26.146
2	66	24	12	0.5	4.71	0.6	45.5065
2	67	25	1	0.1875	7.125	0.1	3.3361
2	68	25	6.5	0.1875	7.125	0.1	7.0943
2	69	25	12	0.1875	7.125	0.1	11.5446
2	70	26	1	0.344	7.125	0.1	2.8798
2	71	26	6.5	0.344	7.125	0.1	5.7147
2	72	26	12	0.344	7.125	0.1	9.3609
2	73	27	1	0.5	7.125	0.1	2.4163
2	74	27	6.5	0.5	7.125	0.1	5.1793
2	75	27	12	0.5	7.125	0.1	8.2585
2	76	28	1	0.1875	7.125	0.35	7.3236
2	77	28	6.5	0.1875	7.125	0.35	15.7529
2	78	28	12	0.1875	7.125	0.35	24.6753
2	79	29	1	0.344	7.125	0.35	5.8432
2	80	29	6.5	0.344	7.125	0.35	12.3685
2	81	29	12	0.344	7.125	0.35	19.5338
2	82	30	1	0.5	7.125	0.35	4.9194
2	83	30	6.5	0.5	7.125	0.35	10.8429
2	84	30	12	0.5	7.125	0.35	17.0262
2	85	31	1	0.1875	7.125	0.52	9.8229
2	86	31	6.5	0.1875	7.125	0.52	24.2195
2	87	31	12	0.1875	7.125	0.52	39.2794
2	88	32	1	0.344	7.125	0.52	7.7065
2	89	32	6.5	0.344	7.125	0.52	18.9511
2	90	32	12	0.344	7.125	0.52	31.0609
2	91	33	1	0.5	7.125	0.52	6.4742
2	92	33	6.5	0.5	7.125	0.52	16.5042
2	93	33	12	0.5	7.125	0.52	27.0796
2	94	34	1	0.1875	7.125	0.6	11.4333
2	95	34	6.5	0.1875	7.125	0.6	31.3367
2	96	34	12	0.1875	7.125	0.6	52.1288
2	97	35	1	0.344	7.125	0.6	8.9356
2	98	35	6.5	0.344	7.125	0.6	24.5806
2	99	35	12	0.344	7.125	0.6	41.314
2	100	36	1	0.5	7.125	0.6	7.5228
2	101	36	6.5	0.5	7.125	0.6	21.4403
2	102	36	12	0.5	7.125	0.6	36.1078
2	103	37	1	0.1875	10.75	0.1	4.5814
2	104	37	6.5	0.1875	10.75	0.1	7.0691
2	105	37	12	0.1875	10.75	0.1	10.037
2	106	38	1	0.344	10.75	0.1	3.934
2	107	38	6.5	0.344	10.75	0.1	5.6356
2	108	38	12	0.344	10.75	0.1	8.0763
2	109	39	1	0.5	10.75	0.1	3.2839
2	110	39	6.5	0.5	10.75	0.1	5.1505
2	111	39	12	0.5	10.75	0.1	7.0987

2	112	40	1	0.1875	10.75	0.35	8.8457
2	113	40	6.5	0.1875	10.75	0.35	14.6762
2	114	40	12	0.1875	10.75	0.35	19.9168
2	115	41	1	0.344	10.75	0.35	7.0673
2	116	41	6.5	0.344	10.75	0.35	11.382
2	117	41	12	0.344	10.75	0.35	15.6829
2	118	42	1	0.5	10.75	0.35	5.866
2	119	42	6.5	0.5	10.75	0.35	9.9879
2	120	42	12	0.5	10.75	0.35	13.4889
2	121	43	1	0.1875	10.75	0.52	11.3369
2	122	43	6.5	0.1875	10.75	0.52	21.7138
2	123	43	12	0.1875	10.75	0.52	31.8345
2	124	44	1	0.344	10.75	0.52	8.8879
2	125	44	6.5	0.344	10.75	0.52	16.7885
2	126	44	12	0.344	10.75	0.52	25.0352
2	127	45	1	0.5	10.75	0.52	7.3818
2	128	45	6.5	0.5	10.75	0.52	14.6026
2	129	45	12	0.5	10.75	0.52	21.6733
2	130	46	1	0.1875	10.75	0.6	12.8495
2	131	46	6.5	0.1875	10.75	0.6	27.5184
2	132	46	12	0.1875	10.75	0.6	42.4453
2	133	47	1	0.344	10.75	0.6	10.0252
2	134	47	6.5	0.344	10.75	0.6	21.3501
2	135	47	12	0.344	10.75	0.6	33.4349
2	136	48	1	0.5	10.75	0.6	8.3507
2	137	48	6.5	0.5	10.75	0.6	18.5173
2	138	48	12	0.5	10.75	0.6	29.0323
3	1	1	1	0.1875	3.5	0.1	3.2744
3	2	1	6.5	0.1875	3.5	0.1	10.7924
3	3	1	12	0.1875	3.5	0.1	18.5895
3	4	2	1	0.344	3.5	0.1	2.7303
3	5	2	6.5	0.344	3.5	0.1	8.7883
3	6	2	12	0.344	3.5	0.1	15.211
3	7	4	1	0.1875	3.5	0.35	7.6456
3	8	4	6.5	0.1875	3.5	0.35	23.6734
3	9	4	12	0.1875	3.5	0.35	39.9105
3	10	5	1	0.344	3.5	0.35	6.1184
3	11	5	6.5	0.344	3.5	0.35	19.0089
3	12	5	12	0.344	3.5	0.35	32.2208
3	13	6	1	0.5	3.5	0.35	5.1877
3	14	6	6.5	0.5	3.5	0.35	16.7676
3	15	6	12	0.5	3.5	0.35	28.3556
3	16	7	1	0.1875	3.5	0.52	10.6982
3	17	7	6.5	0.1875	3.5	0.52	37.3915
3	18	7	12	0.1875	3.5	0.52	64.2236
3	19	8	1	0.344	3.5	0.52	8.465
3	20	8	6.5	0.344	3.5	0.52	30.0551
3	21	8	12	0.344	3.5	0.52	51.8976
3	22	9	1	0.5	3.5	0.52	7.1694

3	23	9	6.5	0.5	3.5	0.52	26.5087
3	24	9	12	0.5	3.5	0.52	45.855
3	25	10	1	0.1875	3.5	0.6	12.9155
3	26	10	6.5	0.1875	3.5	0.6	49.4195
3	27	10	12	0.1875	3.5	0.6	86.0088
3	28	11	1	0.344	3.5	0.6	10.2319
3	29	11	6.5	0.344	3.5	0.6	39.922
3	30	11	12	0.344	3.5	0.6	69.8243
3	31	12	1	0.5	3.5	0.6	8.7515
3	32	12	6.5	0.5	3.5	0.6	35.3199
3	33	12	12	0.5	3.5	0.6	61.935
3	34	13	1	0.1875	4.71	0.1	3.3704
3	35	13	6.5	0.1875	4.71	0.1	9.3975
3	36	13	12	0.1875	4.71	0.1	15.8689
3	37	14	1	0.344	4.71	0.1	2.8637
3	38	14	6.5	0.344	4.71	0.1	7.6744
3	39	14	12	0.344	4.71	0.1	13.0401
3	40	16	1	0.1875	4.71	0.35	7.9669
3	41	16	6.5	0.1875	4.71	0.35	20.9997
3	42	16	12	0.1875	4.71	0.35	34.2468
3	43	17	1	0.344	4.71	0.35	6.3551
3	44	17	6.5	0.344	4.71	0.35	16.7437
3	45	17	12	0.344	4.71	0.35	27.4858
3	46	18	1	0.5	4.71	0.35	5.3281
3	47	18	6.5	0.5	4.71	0.35	14.7142
3	48	18	12	0.5	4.71	0.35	24.1429
3	49	19	1	0.1875	4.71	0.52	10.9352
3	50	19	6.5	0.1875	4.71	0.52	32.7916
3	51	19	12	0.1875	4.71	0.52	54.811
3	52	20	1	0.344	4.71	0.52	8.6051
3	53	20	6.5	0.344	4.71	0.52	26.091
3	54	20	12	0.344	4.71	0.52	43.9324
3	55	21	1	0.5	4.71	0.52	7.2425
3	56	21	6.5	0.5	4.71	0.52	22.908
3	57	21	12	0.5	4.71	0.52	38.6687
3	58	22	1	0.1875	4.71	0.6	12.9564
3	59	22	6.5	0.1875	4.71	0.6	42.8849
3	60	22	12	0.1875	4.71	0.6	73.0243
3	61	23	1	0.344	4.71	0.6	10.1809
3	62	23	6.5	0.344	4.71	0.6	34.269
3	63	23	12	0.344	4.71	0.6	58.7415
3	64	24	1	0.5	4.71	0.6	8.54
3	65	24	6.5	0.5	4.71	0.6	30.1359
3	66	24	12	0.5	4.71	0.6	51.7414
3	67	25	1	0.1875	7.125	0.1	3.9151
3	68	25	6.5	0.1875	7.125	0.1	8.2517
3	69	25	12	0.1875	7.125	0.1	13.2838
3	70	26	1	0.344	7.125	0.1	3.3621
3	71	26	6.5	0.344	7.125	0.1	6.6654
3	72	26	12	0.344	7.125	0.1	10.8167

3	73	27	1	0.5	7.125	0.1	2.7257
3	74	27	6.5	0.5	7.125	0.1	6.0365
3	75	27	12	0.5	7.125	0.1	9.5321
3	76	28	1	0.1875	7.125	0.35	8.8565
3	77	28	6.5	0.1875	7.125	0.35	18.4759
3	78	28	12	0.1875	7.125	0.35	27.8165
3	79	29	1	0.344	7.125	0.35	7.0387
3	80	29	6.5	0.344	7.125	0.35	14.5745
3	81	29	12	0.344	7.125	0.35	22.1312
3	82	30	1	0.5	7.125	0.35	5.8241
3	83	30	6.5	0.5	7.125	0.35	12.7903
3	84	30	12	0.5	7.125	0.35	19.3414
3	85	31	1	0.1875	7.125	0.52	11.8569
3	86	31	6.5	0.1875	7.125	0.52	28.1714
3	87	31	12	0.1875	7.125	0.52	44.2812
3	88	32	1	0.344	7.125	0.52	9.2974
3	89	32	6.5	0.344	7.125	0.52	22.2013
3	90	32	12	0.344	7.125	0.52	35.2742
3	91	33	1	0.5	7.125	0.52	7.6852
3	92	33	6.5	0.5	7.125	0.52	19.3372
3	93	33	12	0.5	7.125	0.52	30.7615
3	94	34	1	0.1875	7.125	0.6	13.7407
3	95	34	6.5	0.1875	7.125	0.6	36.2603
3	96	34	12	0.1875	7.125	0.6	58.8755
3	97	35	1	0.344	7.125	0.6	10.7393
3	98	35	6.5	0.344	7.125	0.6	28.6521
3	99	35	12	0.344	7.125	0.6	47.0028
3	100	36	1	0.5	7.125	0.6	8.9052
3	101	36	6.5	0.5	7.125	0.6	24.9735
3	102	36	12	0.5	7.125	0.6	41.0697
3	103	37	1	0.1875	10.75	0.1	5.4457
3	104	37	6.5	0.1875	10.75	0.1	8.3524
3	105	37	12	0.1875	10.75	0.1	11.8345
3	106	38	1	0.344	10.75	0.1	4.6746
3	107	38	6.5	0.344	10.75	0.1	6.6983
3	108	38	12	0.344	10.75	0.1	9.597
3	109	39	1	0.5	10.75	0.1	3.7697
3	110	39	6.5	0.5	10.75	0.1	6.1313
3	111	39	12	0.5	10.75	0.1	8.3936
3	112	40	1	0.1875	10.75	0.35	10.5597
3	113	40	6.5	0.1875	10.75	0.35	17.0465
3	114	40	12	0.1875	10.75	0.35	22.4634
3	115	41	1	0.344	10.75	0.35	8.397
3	116	41	6.5	0.344	10.75	0.35	13.2781
3	117	41	12	0.344	10.75	0.35	17.7802
3	118	42	1	0.5	10.75	0.35	6.8235
3	119	42	6.5	0.5	10.75	0.35	11.6836
3	120	42	12	0.5	10.75	0.35	15.3728
3	121	43	1	0.1875	10.75	0.52	13.5462
3	122	43	6.5	0.1875	10.75	0.52	25.1494

3	123	43	12	0.1875	10.75	0.52	35.682
3	124	44	1	0.344	10.75	0.52	10.5788
3	125	44	6.5	0.344	10.75	0.52	19.5431
3	126	44	12	0.344	10.75	0.52	28.2147
3	127	45	1	0.5	10.75	0.52	8.6449
3	128	45	6.5	0.5	10.75	0.52	17.0637
3	129	45	12	0.5	10.75	0.52	24.5141
3	130	46	1	0.1875	10.75	0.6	15.3681
3	131	46	6.5	0.1875	10.75	0.6	31.882
3	132	46	12	0.1875	10.75	0.6	47.629
3	133	47	1	0.344	10.75	0.6	11.9713
3	134	47	6.5	0.344	10.75	0.6	24.9261
3	135	47	12	0.344	10.75	0.6	37.7929
3	136	48	1	0.5	10.75	0.6	9.8104
3	137	48	6.5	0.5	10.75	0.6	21.6486
3	138	48	12	0.5	10.75	0.6	32.8579
4	1	1	1	0.1875	3.5	0.1	2.7288
4	2	1	6.5	0.1875	3.5	0.1	8.6617
4	3	1	12	0.1875	3.5	0.1	15.1829
4	4	2	1	0.344	3.5	0.1	2.2998
4	5	2	6.5	0.344	3.5	0.1	7.1627
4	6	2	12	0.344	3.5	0.1	12.5747
4	7	4	1	0.1875	3.5	0.35	5.8542
4	8	4	6.5	0.1875	3.5	0.35	18.8145
4	9	4	12	0.1875	3.5	0.35	32.5359
4	10	5	1	0.344	3.5	0.35	4.6546
4	11	5	6.5	0.344	3.5	0.35	15.0125
4	12	5	12	0.344	3.5	0.35	26.057
4	13	6	1	0.5	3.5	0.35	4.0261
4	14	6	6.5	0.5	3.5	0.35	13.1817
4	15	6	12	0.5	3.5	0.35	22.8572
4	16	7	1	0.1875	3.5	0.52	8.2148
4	17	7	6.5	0.1875	3.5	0.52	30.1643
4	18	7	12	0.1875	3.5	0.52	52.8251
4	19	8	1	0.344	3.5	0.52	6.4707
4	20	8	6.5	0.344	3.5	0.52	24.0445
4	21	8	12	0.344	3.5	0.52	42.2719
4	22	9	1	0.5	3.5	0.52	5.5998
4	23	9	6.5	0.5	3.5	0.52	21.103
4	24	9	12	0.5	3.5	0.52	37.147
4	25	10	1	0.1875	3.5	0.6	9.9937
4	26	10	6.5	0.1875	3.5	0.6	40.2078
4	27	10	12	0.1875	3.5	0.6	71.0569
4	28	11	1	0.344	3.5	0.6	7.8804
4	29	11	6.5	0.344	3.5	0.6	32.1734
4	30	11	12	0.344	3.5	0.6	57.0552
4	31	12	1	0.5	3.5	0.6	6.8558
4	32	12	6.5	0.5	3.5	0.6	28.3404
4	33	12	12	0.5	3.5	0.6	50.3176

4	34	13	1	0.1875	4.71	0.1	2.8369
4	35	13	6.5	0.1875	4.71	0.1	7.469
4	36	13	12	0.1875	4.71	0.1	12.8657
4	37	14	1	0.344	4.71	0.1	2.3612
4	38	14	6.5	0.344	4.71	0.1	6.0883
4	39	14	12	0.344	4.71	0.1	10.5178
4	40	16	1	0.1875	4.71	0.35	6.1317
4	41	16	6.5	0.1875	4.71	0.35	16.4891
4	42	16	12	0.1875	4.71	0.35	27.9648
4	43	17	1	0.344	4.71	0.35	4.8553
4	44	17	6.5	0.344	4.71	0.35	13.0601
4	45	17	12	0.344	4.71	0.35	22.2618
4	46	18	1	0.5	4.71	0.35	4.1711
4	47	18	6.5	0.5	4.71	0.35	11.4126
4	48	18	12	0.5	4.71	0.35	19.4503
4	49	19	1	0.1875	4.71	0.52	8.4244
4	50	19	6.5	0.1875	4.71	0.52	26.2064
4	51	19	12	0.1875	4.71	0.52	45.0671
4	52	20	1	0.344	4.71	0.52	6.596
4	53	20	6.5	0.344	4.71	0.52	20.6788
4	54	20	12	0.344	4.71	0.52	35.7788
4	55	21	1	0.5	4.71	0.52	5.6648
4	56	21	6.5	0.5	4.71	0.52	18.0659
4	57	21	12	0.5	4.71	0.52	31.323
4	58	22	1	0.1875	4.71	0.6	10.0488
4	59	22	6.5	0.1875	4.71	0.6	34.6307
4	60	22	12	0.1875	4.71	0.6	60.2486
4	61	23	1	0.344	4.71	0.6	7.862
4	62	23	6.5	0.344	4.71	0.6	27.4331
4	63	23	12	0.344	4.71	0.6	47.9748
4	64	24	1	0.5	4.71	0.6	6.7528
4	65	24	6.5	0.5	4.71	0.6	23.9725
4	66	24	12	0.5	4.71	0.6	42.0112
4	67	25	1	0.1875	7.125	0.1	3.3599
4	68	25	6.5	0.1875	7.125	0.1	6.5382
4	69	25	12	0.1875	7.125	0.1	10.6468
4	70	26	1	0.344	7.125	0.1	2.7972
4	71	26	6.5	0.344	7.125	0.1	5.2665
4	72	26	12	0.344	7.125	0.1	8.6149
4	73	27	1	0.5	7.125	0.1	2.4094
4	74	27	6.5	0.5	7.125	0.1	4.7308
4	75	27	12	0.5	7.125	0.1	7.601
4	76	28	1	0.1875	7.125	0.35	6.9421
4	77	28	6.5	0.1875	7.125	0.35	14.4378
4	78	28	12	0.1875	7.125	0.35	23.1852
4	79	29	1	0.344	7.125	0.35	5.4618
4	80	29	6.5	0.344	7.125	0.35	11.3073
4	81	29	12	0.344	7.125	0.35	18.272
4	82	30	1	0.5	7.125	0.35	4.662
4	83	30	6.5	0.5	7.125	0.35	9.842

4	84	30	12	0.5	7.125	0.35	15.8239
4	85	31	1	0.1875	7.125	0.52	9.2412
4	86	31	6.5	0.1875	7.125	0.52	22.3178
4	87	31	12	0.1875	7.125	0.52	36.9058
4	88	32	1	0.344	7.125	0.52	7.1761
4	89	32	6.5	0.344	7.125	0.52	17.4031
4	90	32	12	0.344	7.125	0.52	28.9985
4	91	33	1	0.5	7.125	0.52	6.1048
4	92	33	6.5	0.5	7.125	0.52	15.0755
4	93	33	12	0.5	7.125	0.52	25.1741
4	94	34	1	0.1875	7.125	0.6	10.753
4	95	34	6.5	0.1875	7.125	0.6	28.9875
4	96	34	12	0.1875	7.125	0.6	48.862
4	97	35	1	0.344	7.125	0.6	8.3313
4	98	35	6.5	0.344	7.125	0.6	22.6519
4	99	35	12	0.344	7.125	0.6	38.482
4	100	36	1	0.5	7.125	0.6	7.0951
4	101	36	6.5	0.5	7.125	0.6	19.643
4	102	36	12	0.5	7.125	0.6	33.504
4	103	37	1	0.1875	10.75	0.1	4.7375
4	104	37	6.5	0.1875	10.75	0.1	6.6357
4	105	37	12	0.1875	10.75	0.1	9.1358
4	106	38	1	0.344	10.75	0.1	3.9076
4	107	38	6.5	0.344	10.75	0.1	5.2948
4	108	38	12	0.344	10.75	0.1	7.3345
4	109	39	1	0.5	10.75	0.1	3.3486
4	110	39	6.5	0.5	10.75	0.1	4.758
4	111	39	12	0.5	10.75	0.1	6.4387
4	112	40	1	0.1875	10.75	0.35	8.6746
4	113	40	6.5	0.1875	10.75	0.35	13.7093
4	114	40	12	0.1875	10.75	0.35	18.7452
4	115	41	1	0.344	10.75	0.35	6.8042
4	116	41	6.5	0.344	10.75	0.35	10.6219
4	117	41	12	0.344	10.75	0.35	14.7023
4	118	42	1	0.5	10.75	0.35	5.7513
4	119	42	6.5	0.5	10.75	0.35	9.2433
4	120	42	12	0.5	10.75	0.35	12.5398
4	121	43	1	0.1875	10.75	0.52	10.9343
4	122	43	6.5	0.1875	10.75	0.52	20.2002
4	123	43	12	0.1875	10.75	0.52	30.1314
4	124	44	1	0.344	10.75	0.52	8.4621
4	125	44	6.5	0.344	10.75	0.52	15.5782
4	126	44	12	0.344	10.75	0.52	23.5747
4	127	45	1	0.5	10.75	0.52	7.1295
4	128	45	6.5	0.5	10.75	0.52	13.4508
4	129	45	12	0.5	10.75	0.52	20.2678
4	130	46	1	0.1875	10.75	0.6	12.3152
4	131	46	6.5	0.1875	10.75	0.6	25.5448
4	132	46	12	0.1875	10.75	0.6	40.121
4	133	47	1	0.344	10.75	0.6	9.5013

4	134	47	6.5	0.344	10.75	0.6	19.7466
4	135	47	12	0.344	10.75	0.6	31.4209
4	136	48	1	0.5	10.75	0.6	8.0183
4	137	48	6.5	0.5	10.75	0.6	17.0208
4	138	48	12	0.5	10.75	0.6	27.1221
5	1	1	1	0.1875	3.5	0.1	3.0406
5	2	1	6.5	0.1875	3.5	0.1	10.7065
5	3	1	12	0.1875	3.5	0.1	18.4647
5	4	2	1	0.344	3.5	0.1	2.5614
5	5	2	6.5	0.344	3.5	0.1	8.6056
5	6	2	12	0.344	3.5	0.1	14.9335
5	7	4	1	0.1875	3.5	0.35	7.2796
5	8	4	6.5	0.1875	3.5	0.35	23.3645
5	9	4	12	0.1875	3.5	0.35	39.4145
5	10	5	1	0.344	3.5	0.35	5.8651
5	11	5	6.5	0.344	3.5	0.35	18.7139
5	12	5	12	0.344	3.5	0.35	31.7621
5	13	6	1	0.5	3.5	0.35	4.9933
5	14	6	6.5	0.5	3.5	0.35	16.5615
5	15	6	12	0.5	3.5	0.35	28.0056
5	16	7	1	0.1875	3.5	0.52	10.2644
5	17	7	6.5	0.1875	3.5	0.52	36.9089
5	18	7	12	0.1875	3.5	0.52	63.4406
5	19	8	1	0.344	3.5	0.52	8.161
5	20	8	6.5	0.344	3.5	0.52	29.6134
5	21	8	12	0.344	3.5	0.52	51.2224
5	22	9	1	0.5	3.5	0.52	6.9493
5	23	9	6.5	0.5	3.5	0.52	26.2149
5	24	9	12	0.5	3.5	0.52	45.3701
5	25	10	1	0.1875	3.5	0.6	12.4492
5	26	10	6.5	0.1875	3.5	0.6	48.807
5	27	10	12	0.1875	3.5	0.6	85.0014
5	28	11	1	0.344	3.5	0.6	9.9051
5	29	11	6.5	0.344	3.5	0.6	39.3704
5	30	11	12	0.344	3.5	0.6	69.0242
5	31	12	1	0.5	3.5	0.6	8.5141
5	32	12	6.5	0.5	3.5	0.6	34.9987
5	33	12	12	0.5	3.5	0.6	61.3216
5	34	13	1	0.1875	4.71	0.1	3.0711
5	35	13	6.5	0.1875	4.71	0.1	9.2807
5	36	13	12	0.1875	4.71	0.1	15.709
5	37	14	1	0.344	4.71	0.1	2.6675
5	38	14	6.5	0.344	4.71	0.1	7.5217
5	39	14	12	0.344	4.71	0.1	12.8307
5	40	16	1	0.1875	4.71	0.35	7.5095
5	41	16	6.5	0.1875	4.71	0.35	20.6793
5	42	16	12	0.1875	4.71	0.35	33.7575
5	43	17	1	0.344	4.71	0.35	6.0457
5	44	17	6.5	0.344	4.71	0.35	16.4375

5	45	17	12	0.344	4.71	0.35	27.0358
5	46	18	1	0.5	4.71	0.35	5.0978
5	47	18	6.5	0.5	4.71	0.35	14.5167
5	48	18	12	0.5	4.71	0.35	23.7869
5	49	19	1	0.1875	4.71	0.52	10.3908
5	50	19	6.5	0.1875	4.71	0.52	32.3044
5	51	19	12	0.1875	4.71	0.52	54.0502
5	52	20	1	0.344	4.71	0.52	8.2297
5	53	20	6.5	0.344	4.71	0.52	25.6455
5	54	20	12	0.344	4.71	0.52	43.2484
5	55	21	1	0.5	4.71	0.52	6.9602
5	56	21	6.5	0.5	4.71	0.52	22.6101
5	57	21	12	0.5	4.71	0.52	38.1404
5	58	22	1	0.1875	4.71	0.6	12.3673
5	59	22	6.5	0.1875	4.71	0.6	42.273
5	60	22	12	0.1875	4.71	0.6	72.0501
5	61	23	1	0.344	4.71	0.6	9.772
5	62	23	6.5	0.344	4.71	0.6	33.7182
5	63	23	12	0.344	4.71	0.6	57.8723
5	64	24	1	0.5	4.71	0.6	8.2472
5	65	24	6.5	0.5	4.71	0.6	29.7748
5	66	24	12	0.5	4.71	0.6	51.1287
5	67	25	1	0.1875	7.125	0.1	3.4456
5	68	25	6.5	0.1875	7.125	0.1	8.0478
5	69	25	12	0.1875	7.125	0.1	13.0595
5	70	26	1	0.344	7.125	0.1	3.0651
5	71	26	6.5	0.344	7.125	0.1	6.4514
5	72	26	12	0.344	7.125	0.1	10.6019
5	73	27	1	0.5	7.125	0.1	2.5087
5	74	27	6.5	0.5	7.125	0.1	5.9336
5	75	27	12	0.5	7.125	0.1	9.3728
5	76	28	1	0.1875	7.125	0.35	8.2081
5	77	28	6.5	0.1875	7.125	0.35	18.086
5	78	28	12	0.1875	7.125	0.35	27.3572
5	79	29	1	0.344	7.125	0.35	6.5977
5	80	29	6.5	0.344	7.125	0.35	14.1825
5	81	29	12	0.344	7.125	0.35	21.676
5	82	30	1	0.5	7.125	0.35	5.4993
5	83	30	6.5	0.5	7.125	0.35	12.5578
5	84	30	12	0.5	7.125	0.35	19.0167
5	85	31	1	0.1875	7.125	0.52	11.1086
5	86	31	6.5	0.1875	7.125	0.52	27.6403
5	87	31	12	0.1875	7.125	0.52	43.5664
5	88	32	1	0.344	7.125	0.52	8.7742
5	89	32	6.5	0.344	7.125	0.52	21.6694
5	90	32	12	0.344	7.125	0.52	34.5613
5	91	33	1	0.5	7.125	0.52	7.3059
5	92	33	6.5	0.5	7.125	0.52	19.0224
5	93	33	12	0.5	7.125	0.52	30.2526
5	94	34	1	0.1875	7.125	0.6	12.9352

5	95	34	6.5	0.1875	7.125	0.6	35.6196
5	96	34	12	0.1875	7.125	0.6	57.9485
5	97	35	1	0.344	7.125	0.6	10.1685
5	98	35	6.5	0.344	7.125	0.6	28.0124
5	99	35	12	0.344	7.125	0.6	46.0805
5	100	36	1	0.5	7.125	0.6	8.497
5	101	36	6.5	0.5	7.125	0.6	24.5936
5	102	36	12	0.5	7.125	0.6	40.414
5	103	37	1	0.1875	10.75	0.1	4.6341
5	104	37	6.5	0.1875	10.75	0.1	7.9296
5	105	37	12	0.1875	10.75	0.1	11.5525
5	106	38	1	0.344	10.75	0.1	4.0874
5	107	38	6.5	0.344	10.75	0.1	6.2448
5	108	38	12	0.344	10.75	0.1	9.2531
5	109	39	1	0.5	10.75	0.1	3.3703
5	110	39	6.5	0.5	10.75	0.1	5.8887
5	111	39	12	0.5	10.75	0.1	8.1854
5	112	40	1	0.1875	10.75	0.35	9.5686
5	113	40	6.5	0.1875	10.75	0.35	16.5203
5	114	40	12	0.1875	10.75	0.35	22.1293
5	115	41	1	0.344	10.75	0.35	7.7312
5	116	41	6.5	0.344	10.75	0.35	12.7703
5	117	41	12	0.344	10.75	0.35	17.424
5	118	42	1	0.5	10.75	0.35	6.3285
5	119	42	6.5	0.5	10.75	0.35	11.3773
5	120	42	12	0.5	10.75	0.35	15.1361
5	121	43	1	0.1875	10.75	0.52	12.4703
5	122	43	6.5	0.1875	10.75	0.52	24.5134
5	123	43	12	0.1875	10.75	0.52	35.1078
5	124	44	1	0.344	10.75	0.52	9.8679
5	125	44	6.5	0.344	10.75	0.52	18.9678
5	126	44	12	0.344	10.75	0.52	26.678
5	127	45	1	0.5	10.75	0.52	8.0995
5	128	45	6.5	0.5	10.75	0.52	16.6893
5	129	45	12	0.5	10.75	0.52	24.0987
5	130	46	1	0.1875	10.75	0.6	14.2391
5	131	46	6.5	0.1875	10.75	0.6	31.1467
5	132	46	12	0.1875	10.75	0.6	46.8305
5	133	47	1	0.344	10.75	0.6	11.1921
5	134	47	6.5	0.344	10.75	0.6	24.2086
5	135	47	12	0.344	10.75	0.6	36.9898
5	136	48	1	0.5	10.75	0.6	9.2323
5	137	48	6.5	0.5	10.75	0.6	21.2156
5	138	48	12	0.5	10.75	0.6	32.2826

Appendix F. Calculated K's from experiment

F.1 Southern yellow pine (SYP) : Load, P, and calculated strength parameter, K, at MAJ using equation [3.17]

M/V (in.)	R (in.)	h (in.)	D (in.)	ϕ	P (lb)	K (psi)
10.0	0.25	3.51	0.672	0.191	2576	25316.88
10.0	0.25	3.52	0.673	0.191	2780	27367.45
10.0	0.25	3.52	0.667	0.190	2960	28985.11
10.0	0.25	3.5	0.636	0.182	2392	22592.58
1.0	0.25	3.5	1.716	0.490	2844	12407.43
1.0	0.25	3.53	1.751	0.496	3060	13403.55
1.0	0.25	3.5	1.727	0.493	2456	10713.8
1.0	0.25	3.53	1.815	0.514	3164	14306.5
1.0	0.25	3.51	1.788	0.509	2616	11694.07
1.0	0.25	3.52	1.799	0.511	2604	11805.47
1.0	0.25	3.52	1.818	0.516	2416	11008.43
1.0	0.25	3.5	1.801	0.514	2208	10207.55
1.0	0.25	3.52	1.815	0.515	3428	15694.02
1.0	0.25	3.51	1.78	0.507	2700	12011.03
1.0	0.25	3.48	1.783	0.512	2820	12873.29
1.0	0.25	3.51	1.804	0.514	2784	12405.36
10.0	0.25	3.52	1.762	0.501	1200	27086.37
10.0	0.25	3.54	1.717	0.485	764	16302.09
10.0	0.25	3.53	1.746	0.495	1180	25865.4
10.0	0.25	3.49	1.749	0.501	588	13382.46
10.0	0.5	3.52	0.713	0.203	1960	15005.83
10.0	0.5	3.52	0.721	0.205	2160	16124.82
10.0	0.5	3.53	0.711	0.201	1776	13141.53
10.0	0.5	3.52	0.688	0.195	1792	13120.11
1.0	0.5	3.5	1.759	0.503	3008	10273.26
1.0	0.5	3.52	1.749	0.497	2776	9145.683
1.0	0.5	3.52	1.745	0.496	2704	8830.436

1.0	0.5	3.53	1.731	0.490	2288	7377.113
10.0	0.5	3.53	1.718	0.487	1024	16362.34
10.0	0.5	3.52	1.749	0.497	792	13240.95
10.0	0.5	3.52	1.777	0.505	824	14087.93
10.0	0.5	3.53	1.751	0.496	1240	20738.18
1.0	0.25	8.97	1.814	0.202	8240	10904.57
1.0	0.25	9.00	1.824	0.203	9320	12331.18
1.0	0.25	9.02	1.825	0.202	11840	15739.49
1.0	0.25	9.00	1.826	0.203	6680	8902.225
10.0	0.25	8.95	1.797	0.201	7660	22341.19
10.0	0.25	8.97	1.8	0.201	5340	15324.85
10.0	0.25	9.00	1.822	0.202	6400	18748.73
1.0	0.25	8.97	4.468	0.498	4730	10457.24
1.0	0.25	8.97	4.468	0.498	4990	10885.93
1.0	0.25	9.01	4.5	0.499	4220	9197.865
1.0	0.25	9.00	4.507	0.501	3800	8247.152
1.0	0.25	9.02	4.485	0.497	5300	11287.91
1.0	0.25	9.02	4.522	0.501	3000	6550.112
1.0	0.25	8.99	4.508	0.501	3395	7330.975
1.0	0.25	9.00	4.522	0.502	3620	7978.061
1.0	0.25	9.03	4.51	0.499	4145	9022.757
1.0	0.25	9.01	4.518	0.501	5632	12145.59
1.0	0.25	8.97	4.515	0.503	3250	7184.861
1.0	0.25	9.04	4.516	0.500	3730	8279.804
10.0	0.25	8.99	4.469	0.497	3070	17479.34
10.0	0.25	9.01	4.512	0.501	2790	15893.03
10.0	0.25	8.97	4.479	0.499	1930	11089.71
1.0	0.5	9.02	1.83	0.203	6580	6713.309
1.0	0.5	9.00	1.82	0.202	14560	14743.27
1.0	0.5	9.01	1.833	0.203	9220	9426.039
10.0	0.5	8.99	1.808	0.201	11480	26547
10.0	0.5	9.00	1.801	0.200	10240	23582.7
10.0	0.5	8.98	1.806	0.201	7560	17737.91
10.0	0.5	8.99	1.803	0.201	7620	17827.87
1.0	0.5	9.01	4.515	0.501	5740	9693.764
1.0	0.5	9.01	4.484	0.498	4000	6681.098
1.0	0.5	9.00	4.514	0.502	4940	8297.648
1.0	0.5	9.02	4.511	0.500	4290	7183.121
10.0	0.5	9.00	4.479	0.498	2680	12487.83
10.0	0.5	9.02	4.477	0.496	3200	14717.59
10.0	0.5	9.00	4.506	0.501	2510	11868.79
10.0	0.5	8.98	4.485	0.499	3200	15125.99

F.2 Yellow poplar (YP) : Load, P, and calculated strength parameter, K, at MAJ using equation [3.17]

M/V (in.)	R (in.)	h (in.)	D (in.)	ϕ	P (lb)	K (psi)
10.0	0.25	3.51	0.711	0.202	2536	25780.37
10.0	0.25	3.5	0.719	0.205	2412	25327.86
10.0	0.25	3.51	0.708	0.202	2580	26507.31
10.0	0.25	3.51	0.727	0.207	2872	29984.59
1.0	0.25	3.5	1.782	0.509	3268	14639.73
1.0	0.25	3.52	1.753	0.498	3200	13927.34
1.0	0.25	3.51	1.78	0.507	3688	16406.17
1.0	0.25	3.47	1.778	0.512	1560	7188.619
1.0	0.25	3.5	1.734	0.495	2436	10813.18
1.0	0.25	3.5	1.822	0.521	1456	6774.43
1.0	0.25	3.52	1.803	0.512	2004	9107.492
1.0	0.25	3.47	1.74	0.501	2352	10587.61
1.0	0.25	3.5	1.813	0.518	2936	13674.51
1.0	0.25	3.52	1.793	0.509	1536	6938.243
10.0	0.25	3.48	1.78	0.512	860	20313.94
10.0	0.25	3.49	1.78	0.510	968	22658.78
10.0	0.25	3.46	1.761	0.509	940	22217.87
10.0	0.25	3.49	1.778	0.510	978	23001.28
10.0	0.5	3.47	0.711	0.205	2076	15998.96
10.0	0.5	3.46	0.76	0.220	2064	16766.6
10.0	0.5	3.49	0.729	0.209	2996	23228.44
10.0	0.5	3.48	0.703	0.202	2224	16907.61
1.0	0.5	3.5	1.792	0.512	4600	15581.98
1.0	0.5	3.49	1.789	0.513	3104	10553.04
1.0	0.5	3.5	1.781	0.509	2896	9685.778
10.0	0.5	3.48	1.781	0.512	1144	20132.55
10.0	0.5	3.48	1.797	0.516	1116	20713.71
10.0	0.5	3.48	1.772	0.509	1300	22858.74
10.0	0.5	3.48	1.758	0.505	1578	27431.44
1.0	0.25	8.98	1.799	0.200	-	-
1.0	0.25	9.00	1.79	0.199	12080	15815.1
1.0	0.25	8.91	1.813	0.204	9300	12385.39
1.0	0.25	9.01	1.816	0.202	7660	9967.708
10.0	0.25	8.99	1.825	0.203	8840	25288.95
10.0	0.25	8.96	1.81	0.202	9080	25842.61
10.0	0.25	8.97	1.81	0.202	7200	20722.26
10.0	0.25	8.97	1.829	0.204	8900	25586.33
1.0	0.25	8.95	4.501	0.503	6090	13209.27
1.0	0.25	8.97	4.49	0.501	5040	10956.64

1.0	0.25	9.00	4.497	0.500	7050	15179.3
1.0	0.25	8.92	4.477	0.502	5930	12871.26
1.0	0.25	8.97	4.475	0.499	4190	9030.116
1.0	0.25	8.99	4.517	0.502	3360	7264.607
1.0	0.25	8.98	4.476	0.498	4860	10461.39
1.0	0.25	8.98	4.489	0.500	3990	8604.412
1.0	0.25	8.99	4.479	0.498	2790	6000.05
1.0	0.25	8.99	4.512	0.502	3170	6848.982
10.0	0.25	8.99	4.491	0.500	2900	16297.45
10.0	0.25	8.99	4.49	0.499	3680	20810.54
10.0	0.25	8.99	4.477	0.498	4840	27261.15
10.0	0.25	8.97	4.504	0.502	3550	20286.72
1.0	0.5	8.95	1.801	0.201	8120	8164.773
1.0	0.5	8.99	1.806	0.201	10380	10339.14
1.0	0.5	8.98	1.824	0.203	8900	8867.279
1.0	0.5	9.00	1.793	0.199	10940	10839.96
10.0	0.5	8.99	1.804	0.201	10800	24943.21
10.0	0.5	8.94	1.815	0.203	9720	22594.10
10.0	0.5	8.98	1.81	0.202	9380	21603.7
10.0	0.5	8.93	1.814	0.203	8360	19464.06
1.0	0.5	8.98	4.499	0.501	8050	13352.88
1.0	0.5	9.00	4.53	0.503	8610	14305.56
1.0	0.5	8.98	4.5	0.501	9310	15445.09
1.0	0.5	8.98	4.509	0.502	5630	9413.576
10.0	0.5	8.97	4.487	0.500	4450	20695.72
10.0	0.5	8.98	4.524	0.504	3100	14535.59
10.0	0.5	8.99	4.531	0.504	3890	18223.92
10.0	0.5	8.98	4.51	0.502	3120	14567.61

The vita has been removed from the scanned document